

Controlling an Angiogenic Switch: Dissecting out the Role and Molecular Mechanism of *FRG1* in Tumorigenesis

By
ANKIT TIWARI
LIFE11201004013

National Institute of Science Education and Research, Bhubaneswar

A thesis submitted to the
Board of Studies in Life Sciences
In partial fulfillment of requirements
for the Degree of
DOCTOR OF PHILOSOPHY
of
HOMI BHABHA NATIONAL INSTITUTE

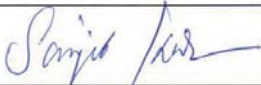


May 2018

Homi Bhabha National Institute¹

Recommendations of the Viva Voce Committee

As members of the Viva Voce Committee, we certify that we have read the dissertation prepared by ANKIT TIWARI entitled "Controlling an Angiogenic Switch: Dissecting out the Role and Molecular Mechanism of *FRGI* in Tumorigenesis" and recommend that it may be accepted as fulfilling the thesis requirement for the award of Degree of Doctor of Philosophy.

Chairman - Dr. Sanjib Kar		Date: 19-05-2018
Guide / Convener Dr. Manjusha Dixit		Date: 14-05-2018
Examiner - Dr. Gopal C. Kundu		Date: 14-05-2018
Member 1- Dr. Asima Bhattacharyya		Date: 14-5-18
Member 2- Dr. Subhasis Chattopadhyay		Date: 14/05/18
Member 3- Dr. Rajeeb Swain		Date: 14/05/18

Final approval and acceptance of this thesis is contingent upon the candidate's submission of the final copies of the thesis to HBNI.

I/We hereby certify that I/we have read this thesis prepared under my/our direction and recommend that it may be accepted as fulfilling the thesis requirement.

Date: 14-05-18

Place: NISER, Jatni

<Signature>

Co-guide (if applicable)



<Signature>

Guide

¹ This page is to be included only for final submission after successful completion of viva voce.

STATEMENT BY AUTHOR

This dissertation has been submitted in partial fulfillment of requirements for an advanced degree at Homi Bhabha National Institute (HBNI) and is deposited in the Library to be made available to borrowers under rules of the HBNI.

Brief quotations from this dissertation are allowable without special permission, provided that accurate acknowledgement of source is made. Requests for permission for extended quotation from or reproduction of this manuscript in whole or in part may be granted by the Competent Authority of HBNI when in his or her judgment the proposed use of the material is in the interests of scholarship. In all other instances, however, permission must be obtained from the author.

Ankit Tiwari

ANKIT TIWARI

DECLARATION

I, hereby declare that the investigation presented in the thesis has been carried out by me. The work is original and has not been submitted earlier as a whole or in part for a degree / diploma at this or any other Institution / University.

Ankit Tiwari

ANKIT TIWARI

List of Publications arising from the thesis

a. Published:

1. **Ankit Tiwari**, Niharika Pattanaik, Archita Mohanty Jaiswal, Manjusha Dixit; Increased FRG1 expression reduces in vitro cell migration, invasion and angiogenesis, ex vivo supported by reduced expression in tumors. Bioscience Reports, 2017, 37 (5). doi: 10.1042/BSR20171062 (Cover article)
2. **Ankit Tiwari**, Bratati Mukherjee, Manjusha Dixit; MicroRNA Key to Angiogenesis Regulation: miRNA Biology and Therapy. Current Cancer Drug Targets, 2017 Jun 30, doi: 10.2174/1568009617666170630142725.
3. Arman K Hansda*, **Ankit Tiwari***, Manjusha Dixit; Current Status and Future Prospect on FSHD Region Gene 1. Journal of Biosciences, 2017, 42(2), 345-353.

b. Communicated:

1. **Ankit Tiwari**, Bratati Mukherjee, Md Khurshidul Hassan, Niharika Pattanaik, Archita Mohanty Jaiswal, Manjusha Dixit. Reduced FRG1 expression promotes prostate cancer progression and affects prostate cancer cell migration and invasion (Under Revision/ Minor Revision)

Conferences

1. **Ankit Tiwari**, S.P. Singh, Manjusha Dixit; Finding out role of FRG1 expression in angiogenesis and cancer, Indian Cancer Genetics Conference, 2013, Mumbai, India.
2. **Ankit Tiwari**, Manjusha Dixit; Association of FRG1 with DAB2, a tumor suppressor gene in cancer cells, IACR 2014, Kollam, Kerala, India.
3. **Ankit Tiwari**, Manjusha Dixit; Reduced FRG1 expression promotes prostate cancer progression and affects prostate cancer cell migration and invasion, BIOSYM2017, Ootacamund, Tamil Nadu, India.

Ankit Tiwari

ANKIT TIWARI

DEDICATED TO

My Mother and my Grand Father

ACKNOWLEDGEMENTS

This thesis has been the summary of the great journey in my life. During these years of my thesis work I had learned a lot and every time, there were individuals to help me through this path. Therefore I feel glad writing this acknowledgment as it provides the picture of how my work is just more than me.

Firstly I would like to thank Dr. Manjusha Dixit for believing in me and providing support for this work. I would also like to thank her for providing freedom and self-belief which definitely helped me developed into a better student of science.

I would also extend this opportunity to acknowledge faculties at School of Biological Sciences and NISER administration, for providing me with the opportunity to carry out research work at this institute.

As a Ph.D. student, I was privileged to have wonderful scientists as my doctoral committee members. I would like to thank chairperson of my Doctoral committee Dr. Sanjib Kar. I would also like to appreciate the suggestions from my DC members Dr. Asima Bhattacharya and Dr. Subhashis Chattopadhyay which helped me immensely in my research work. I would like to extend special thanks to the external member of my DC committee Dr. Rajeeb Swain from Institute of Life Sciences for his valuable suggestions, inputs and resources.

I am very grateful to the team at SRL Diagnostics Bhubaneswar for their help in patient sample study. I would like to forward special thanks to Dr. Sambit K Mohanty for installing, rather reinstalled my belief in cancer research. I would like to thank Dr. Archita Mohanty Jaiswal for providing the facilities at SRL. Above all, I would like to acknowledge Dr. Niharika Pattanaik for all the effort and time she provided me with patient sample study and data analysis which has been the backbone of this study. Doctors at SRL had provided me with all help along their busy schedule but the technical staff of histopathology and cytopathology lab deserves similar acknowledgment. Hence I would like to thank Mr. Dinesh Kumar Behera for all the input provided by him. During my struggle with IHC set up in our lab, Sumanta Bhai from Apollo Hospitals provided with crucial suggestions for which I will always be indebted.

When I look back at SBS while writing this thesis, I felt few people deserved special mention. Dr. KVS Badireenath helped me with HEK93Tcells during a very crucial period of my Ph.D. career. Among faculties, I would like to make special mention of Dr. Chandan Goswami regarding his help in providing microscopy facility. Further, I would also like to mention his moral boasting pep talks and funny stories during the time when we shared lab space at IOP campus. Lab operators and lab assistant were also the essential part during my work period at IOP campus, thus I am thankful to all the lab operators and lab assistants for their support. I would also like to extend my gratitude towards Dr. Nagendra Kumar Sharma, School of Chemical Sciences and his lab members as I had pleasant work experience during my initial days of Ph.D. at NISER.

On more of a personal note, I would like to thank all my lab mates Subhranshu, Deepa, Rishi, Khurshid, Arman, Nirmala, Dinesh, Pratush, Monali, Bratati, Vinay, Kirti and Neha for helping me accomplish my task. I would like to extend special thanks to Subhranshu, Khurshid, Nirmala and Bratati for helping me carry out my work smoothly as on road they shared responsibilities of the various task along with me. I would always cherish fun moments with all my lab mates but would have the special mention for Rishi, Pratush, and Monali as they always looked up to me as a big brother rather than just lab mate.

I am truly grateful to all the individuals working at Biolab 8 at old IOP campus, Biolab 8 was the common lab for four PIs and I extend special thanks to all individuals who ever worked at that wonderful lab where work always was fun. Lastly, I would like to name few most important people to whom I owe more than just thanks or acknowledgment. These were the people without whom my research would just be a degree but not a journey that I would cherish in the future whenever I look back at my past at NISER. First and Foremost I would like to thank my flat mates Asim and Milan during my stay at C block of government housing colony hostel. I especially thank Mitali for being with me at tough times and that I owe a lot to her. I thank my beloved seniors Ashutosh and Sanjima as they were the Ph.D. student I looked up to when in any trouble and they were the teacher to me in many sense. Lopamudra Dash had always been the elder sister to me at NISER for which I would always be grateful. Lastly, I would like to extend thanks to my friends who were always fun to hang out with may be at the party or any other scientific discussion; Subhrashu, Manoj, Tapas, Srikant, Uday, Anoop, Rakesh. These guys would always turn up for any help when I was in need.

Lastly, I am grateful to my Mom, Dad, Diptika, and Pratik for bearing with me all these years. I am highly indebted to all these individuals for what I am today.

CONTENTS

	Page No.
SYNOPSIS	vi
LIST OF ABBREVIATIONS	xviii
LIST OF FIGURES	xx
LIST OF TABLES	xxii
1 INTRODUCTION	1
2 HYPOTHESIS	7
3 REVIEW OF LITREATURE	9
3.1 Angiogenesis in Health and Disease	10
3.2 Angiogenesis and Cancer	14
3.3 Expectations and Challenges of Anti angiogenic Therapy in Cancer	18
3.4 Clinically Approved Anti Angiogenic Therapy	19
3.5 Challenges of VEGF (receptor) Based Therapies	21
3.6 Alternative Approach for Anti Angiogenic Therapy	24
3.7 FSHD Region Gene 1 (FRG1)	26
3.8 FRG1 Associated Diseases and Molecular Function	29
3.9 FRG1`s Association with Angiogenesis and Tumorigenesis	31
4 MATERIALS AND METHODS	35
4.1 Oncomine Analysis	36
4.2 Kaplan Meier Plotter Analysis	36
4.3 Immunohistochemistry	36
4.3.1 Reagents for Immunohistochemistry	36
4.3.2 Poly-L –Lysine Coating of Slides	37
4.3.3 Preparation of Control Cell Block	37
4.3.4 Immunohistochemistry Protocol	37
4.3.5 Immunohistochemistry Scoring	38
4.3.6 Micro-Vessel Density Analysis	38
4.4 Plasmid Preparation	39

4.4.1	Reagents for Plasmid Preparation	39
4.4.2	Plasmids	39
4.4.3	Preparation of <i>E. coli</i> (DH5a) Competent Cells	39
4.4.4	Transformation Protocol	40
4.4.5	Plasmid Purification Protocol	40
4.4.6	Preparation of Glycerol Stock	41
4.5	Cell Culture	41
4.5.1	Reagents for Cell Culture	41
4.5.2	Preparation of Media	41
4.5.3	Cell Culture Protocol	42
4.5.4	Revival of Cells	42
4.5.5	Subculture, Splitting and Trypsinization of Cells	42
4.5.6	Cell Freezing and Cryopreservation	43
4.5.7	Transient Transfection	43
4.5.8	Stable Transfection	43
4.6	Cell Proliferation Assay	44
4.6.1	Reagents for Cell Proliferation Assay	44
4.6.2.	Protocol for Cell Proliferation Assay in Transiently Transfected Cells	44
4.6.3	Protocol for Cell Proliferation Assay in Stable Cells	44
4.6.4	Protocol for Cell Proliferation Assay in HUVECs	45
4.7	Scratch Wound Healing Assay	45
4.7.1	Reagents for Scratch Wound Healing Assay	45
4.7.2	Protocol for Scratch Wound Healing Assay for Transiently Transfected Cells	45
4.7.3	Protocol for Scratch Wound Healing Assay of Stable Cells	45
4.8	Transwell Migration Assay	46
4.8.1	Reagents for Transwell Migration Assay	46
4.8.2	Transwell Migration Assay Protocol for Cell lines	46
4.8.3	Transwell Migration Assay Protocol for HUVECs	46
4.9	Matrigel Invasion Assay	47
4.9.1	Reagents for Matrigel Invasion Assay	47
4.9.2	Matrigel Invasion Assay Protocol	47
4.10	Matrigel Tubule Formation Assay	48

4.10.1	Reagents for Matrigel Tubule Formation Assay	48
4.10.2	Matrigel Tubule Formation Assay Protocol	48
4.11	Preparation of Cell Lysate	48
4.11.1	Reagents for Preparation of Cell Lysate	48
4.11.2	Protocol for Preparation of Cell Lysate	48
4.12	Estimation of Protein by BCA Method	49
4.12.1	Reagents for Protein Estimation by BCA Method	49
4.12.2	Protocol for Protein Estimation by BCA Method	49
4.13	SDS-PAGE Electrophoresis	49
4.13.1	Reagents for SDS-PAGE Electrophoresis	49
4.13.2	Protocol for SDS-PAGE Electrophoresis	50
4.14	Coomassie Staining	50
4.14.1	Reagents for Coomassie Staining	50
4.14.2	Protocol for Coomassie Staining	50
4.15	Western Blot	51
4.15.1	Reagents for Western Blot	51
4.15.2	Protocol for Western Blot	51
4.16	RNA Extraction and cDNA Synthesis	53
4.16.1	Reagents for RNA Extraction and cDNA Synthesis	53
4.16.2	Protocol for RNA Extraction and cDNA Synthesis	53
4.17	Quantitative –Real Time PCR	53
4.17.1	Reagents for Quantitative –Real Time PCR	53
4.17.2	Protocol for Quantitative –Real Time PCR	53
4.18	Statistical Analysis	56
5	RESULTS AND DISCUSSION	57
CHAPTER 1	To Investigate the Effect of FRG1 Expression in Angiogenesis	58
5.1.1	Introduction	59
5.1.2	Results	59
5.1.2.1	FRG1 Levels Affect Endothelial Cell Functions	59
5.1.2.2	FRG1 Levels in Tumor Samples do not Correlate with MVD Count	61
5.1.3	Discussion	62

CHAPTER 2	To Establish Tumorigenic Properties of FRG1 <i>In vivo</i> and <i>In vitro</i>	64
5.2.1	Introduction	65
5.2.2	Results	66
5.2.2.1	Altered FRG1 Levels do not Affect Cell Proliferation but it Affects Cell Migration	66
5.2.2.2	FRG1 Regulates Cell Invasion	67
5.2.2.3	FRG1 expression levels alter expression of GCSF and MMP10	71
5.2.2.4	<i>In silico</i> Analysis Shows Reduced FRG1 Expression in Tumors and Poor Prognosis	71
5.2.2.5	<i>In vivo</i> Analysis Shows Reduced FRG1 Protein Expression in Tumors	73
5.2.3	Discussion	75
CHAPTER 3	Identifying Role and Molecular Mechanism of FRG1 in Prostate Cancer	79
5.3.1	Introduction	80
5.3.2	Results	81
5.3.2.1	FRG1 Levels in Prostate Adenocarcinoma	81
5.3.2.2	Varying Effect of FRG1 on Proliferation of Prostate Cancer Cells	83
5.3.2.3	FRG1 Affects Prostate Cancer Cell Motility and Invasiveness	85
5.3.2.4	FRG1 Expression Level Dictates Expression of Various Cytokines and MMP1	86
5.3.2.5	FRG1 Silencing Enhances p38 MAPK Activation	88
5.3.3	Discussion	91
CHAPTER 4	To Determine Role and Molecular Mechanism of FRG1 in Breast cancer	96
5.4.1	Introduction	97
5.4.2	Results	98
5.4.2.1	FRG1 Levels Affect MCF7 Cell Proliferation	98
5.4.2.2	FRG1 Levels Regulate Cellular Migration of MCF7	99
5.4.2.3	FRG1 Levels Affect MCF7 Invasiveness	100
5.4.2.4	FRG1 Knockdown Up Regulates CXCL1, CXCL8, PDGFB, MMP2 and MMP13	103
5.4.2.5	FRG1 Knockdown Leads to Activation of ERK in MCF7	105

5.4.2.6	FRG1 Levels are Reduced in Breast Tumor Tissue Compared to Normal Breast Tissue	105
5.4.3	Discussion	106
6	SUMMARY	111
7	REFERENCES	114
8	APPENDIX	125

6. SUMMARY

6. SUMMARY:

FRG1 has been primarily associated with FSHD. Hence till date cell based studies involving FRG1 had focus on muscle function and physiology. Experiments carried out in this thesis work represent first set of data connecting FRG1 with epithelial and endothelial cell functions. One of the most significant contributions of this study in understanding fundamental aspect of FRG1 would be, to first-time report the tissue based distribution and expression of FRG1 apart from muscle. Similarly, we also report FRG1 expression and distribution in tumors. Our observation provides a pellucid information regarding loss of FRG1 expression in tumor tissue compared to uninvolved counterpart in breast, prostate, oral, gastric and colon cancers. This study proves to be highly significant towards understanding functional aspect of FRG1 and its importance in tumor development.

Angiogenesis is crucial for tumor progression, while *in vitro* data supports relation between FRG1 expression level and angiogenesis regulation but we could not draw support from patient data. Higher patient sample size and heterogeneity amongst the sample could make the picture much transparent.

FRG1 expression level affects various cell properties associated with tumor progression; moreover, we observed similarity in behavior of both tumorigenic and non-tumorigenic cells. Higher level of FRG1 reduced cellular migration and invasion, which was reversed when RNAi silencing of FRG1 was done in these cell lines. Cell proliferation was affected only in tumor cells, as non tumorigenic HEK293T cells showed no effect on cell proliferation in respect to ectopic expression and knockdown of FRG1.

Identification of mechanistic pathway of function is crucial to understand regulation of physiological processes. Therefore, we checked molecules that could connect FRG1 with one or more molecular pathways. The study was done in tumor cell lines of prostate (PC3 and DU145) and breast (MCF7). Signaling cascade activated by altered FRG1 levels may vary according to the cells. In prostate cancer cell lines p38 MAPK activation was observed, but in MCF7 ERK activation was observed but no p38 MAPK activation was visualized.

This difference in activation of MAPKs can be attributed to cytokines and MMPs affected by expression levels of FRG1. We did not observe any significant change in cytokines and MMPs with FRG1 over expression, except for HEK293T. In HEK293T cells, FRG1 over expression led to reduced G-CSF expression, but in all three tumor lines FRG1 over expression did not affect any molecule that we screened in our study. Various molecules were activated during FRG1 knockdown which are known to promote tumorigenesis and angiogenesis *viz.* PDGFB, CXCL8, CXCL1, PLGF, GM-CSF, PDGFA, MMP1, MMP2 and MMP13.

The significance of this study is, it has opened a new paradigm in the quest of understanding function of FRG1. These findings can form key molecular basis of its evolutionary conservation among various species. Further research and functional validation in animal (tumor) models is required to make a conclusive point that FRG1 is a negative regulator of tumor growth.



Homi Bhabha National Institute

SYNOPSIS OF Ph.D. THESIS

1. **Name of the Student: Ankit Tiwari**
2. **Name of the Constituent Institution: National Institute of Science Education and Research**
3. **Enrolment No.:LIFE11201004013**
4. **Title of the Thesis: Controlling an Angiogenic Switch: Dissecting out the Role and Molecular Mechanism of *FRG1* in Tumorigenesis”**
5. **Board of Studies: LIFE SCIENCES**

SYNOPSIS

(Limited to 10 pages in double spacing)

Introduction:

Angiogenesis is critical for development, wound healing and disease physiology. Abnormal angiogenesis has been associated with various diseases *viz.* Ischemia, Atherosclerosis, Diabetic retinopathy, Stroke, Alzheimer’s disease, Cancer and many more [1]. Angiogenesis is regulated by pro-angiogenic and anti-angiogenic factors, which in turn balance the process and lead to formation of new blood vessels. During tumor progression, the balance is tipped off and the process is known as “Angiogenic switch”. Angiogenesis is essential for tumor progression [2]. During tumor progression, the angiogenic regulators are released from other stromal components *viz.* cancer cells, immune cells and, tumor associated fibroblasts. Since tumors are angiogenesis dependent, anti-angiogenic therapies were developed for the treatment of cancer [3]. Endothelial cells were considered to be stable target, as the genomic integrity was well maintained compared to cancer cells [4]. The regulation of pro-angiogenic and anti-angiogenic

factors is not well coordinated in cancer as it is, during normal physiology [5]. Hence, the blood vessels formed during tumor angiogenesis, are leaky and succulent with poor cell-cell adhesion [5, 6]. This change in properties of tumor blood vessels lead to lower efficacy of anti-angiogenic therapy [6]. Thus, inefficacy of anti-angiogenic therapy poses a question regarding proper understanding of tumor angiogenesis. Various molecules and associated molecular mechanism regarding tumor angiogenesis is known but it has not led to improvement in tumor therapy. Further improvement of anti-angiogenic therapy requires identification of novel molecules and molecular mechanism which may be critical for tumor angiogenesis. One such molecule is FSHD region gene 1 (FRG1) which is a putative angiogenic regulator.

FRG1, which is primarily known to be a candidate gene for Facioscapulohumeral Muscular Dystrophy (FSHD), was discovered in 1996 [7]. *FRG1* is highly conserved and has been associated with muscle development in various organisms, including *Drosophila*, *C.elegans*, *Xenopus*, Mice and Humans [8-11]. The other dysfunction associated with FSHD, is retinal vasculature abnormalities in 50-75 % of FSHD patients [12]. A study on *Xenopus* demonstrated that FRG1 levels dictate blood vessel formation during *Xenopus* development, specifically via angiogenesis [13]. Here interesting point to be noted was, FRG1 over expression promoted vessel formation but with disturbed vascular phenotype, like enhanced vessel branching, vessel dilation and development of edemas in blood vessels [13]. This vascular phenotype resembled that of tumor angiogenesis. This was the first indication of FRG1's role in angiogenesis or tumorigenesis. Additionally, developmental studies in *Xenopus* revealed that FRG1 is crucial for muscle development, altered levels of *FRG1* led to abnormal musculature. FRG1 alteration affected the migration of muscle cells [10]. Reduction of FRG1 led to reduced levels of Vimentin, an Epithelial-Mesenchymal Transition (EMT) marker, generally over expressed in solid tumors and associated with accelerated tumor growth, invasion and metastasis [14], suggesting the possible role of FRG1 in tumor angiogenesis and tumorigenesis. Apart from development of muscle and blood vessel, FRG1 also plays crucial role in odontogenesis, as FRG1 is differentially expressed during tooth development [15]. Bone Morphogenetic Protein 4 (BMP4), a known tumor suppressor, is also a regulator of odontogenesis [15, 16] and the study showed the BMP4 treatment of murine Dental Epithelial Cells (mDEC6) led to change in localization of FRG1. Indirectly, indicating association of FRG1 with tumorigenesis. Moreover, domain analysis of FRG1 revealed that it consists of a Lipocalin domain, Fascin Like domain and nuclear localization signals. Fascins are family of proteins that promote tumor progression

and affect tumor cell migration and invasiveness [17]. Hence, indicating involvement of FRG1 in tumorigenesis.

Overall, involvement of FRG1 in various developmental processes and association with various molecules regulating tumor led us to hypothesize that **FRG1 may be involved in tumor progression and tumor angiogenesis**. Therefore, we formulated following objectives to validate the proposed hypothesis. Each objective will eventually make one chapter of the thesis.

Objectives/Chapters:

Chapter 1: To investigate effect of FRG1 expression in angiogenesis

Chapter 2: To establish tumorigenic properties of FRG1 *in vivo* and *in vitro*

Chapter 3: Identifying role and molecular mechanism of FRG1 in Prostate cancer

Chapter 4: To determine role and molecular mechanism of FRG1 in Breast cancer

Results:

Chapter 1: To investigate effect of FRG1 in angiogenesis

1.1 FRG1 over expression reduces tubule formation and migration of HUVECs

Human Umbilical Vein Endothelial Cells (HUVECs) were treated with conditioned media obtained from HEK293T cells transfected with FRG1 over expression vector. Matrigel tubule formation assay was performed and it was observed that HUVECs, treated with conditioned media obtained from FRG1 expressing HEK293T, showed significant reduction in tubule formation, compared to empty vector control. Further, migratory ability of endothelial cells was determined by transwell migration assay, with HEK293T conditioned media. The migration was significantly reduced in FRG1 expression set compared to empty vector set. Further, we also explored effect of FRG1 expression on cell proliferation of HUVECs. No significant difference in cell proliferation was observed between HUVECs treated with conditioned media from over expression set, compared to empty vector control. Overall, our result clearly indicated that ectopic expression of FRG1 (in HEK293T) led to reduction in endothelial cell differentiation and migration but had no effect on cell proliferation.

1.2 No correlation of tumor FRG1 levels with tumor Micro Vessel Density (MVD)

To further ascertain involvement of FRG1 in tumor angiogenesis, immunohistochemistry based correlation analysis was performed. FFPE tumor tissue blocks were obtained from tissue archive of SRL diagnostics from year 2014 - 2016. Immunohistochemistry was performed for FRG1 and CD31 (vascular marker) expression. Scoring for Immunohistochemistry of FRG1 was done. Measurement of Micro Vessel Density (MVD) was done as per Wiedner et al. [18]. Pearson correlation coefficient was derived between Allred score of tumor vs. tumor MVD, but no

significant correlation was observed between FRG1 levels and tumor MVD. p value of ≤ 0.05 was considered to be significant.

Chapter 2: To establish tumorigenic properties of FRG1 *in vivo* and *in vitro*

2.1 *In silico* analysis shows reduced FRG1 expression in tumors and poor prognosis

Oncomine analysis was performed for FRG1 expression in various types of cancers, with threshold of ≥ 1.5 – fold change and p value of ≤ 0.05 . Oncomine analysis revealed that, out of total 462 analyses, FRG1 expression was significantly affected in 43 analyses. Specifically, 26 out of 43 analyses showed significant reduction in FRG1 expression. On the contrary, only 17 analyses showed significant up regulation of FRG1. Overall, *in silico* analysis of FRG1 expression showed that FRG1 expression was reduced in higher number of Oncomine datasets.

To further assert the importance of FRG1 expression, Kaplan Meier plotter analysis was done for available cancer types, viz. breast, lung, gastric and ovarian. Survival analysis revealed that low FRG1 expression was associated with poor prognosis in overall survival of patients, in lung cancer (HR= 0.84, p value = 0.0058) and in gastric cancer (HR= 0.56, p value = 1.8×10^{-08}).

2.2 *In vivo* analysis shows reduced FRG1 protein levels in tumors

To determine the expression levels and localization of FRG1 in tumor tissue and in uninvolved counterpart, immunohistochemistry based approach was used. Blocks of 124 surgically resected tumor tissues with uninvolved region were obtained from the tissue archives.

To probe the role of FRG1 in tumor progression a pan-cancer approach was followed. HeLa cell block was used as positive control during the staining procedure.

In oral cancer, we observed that FRG1 levels were reduced in 61.11 % of tumor cases i.e. in 11/18 cases, compared to uninvolved region. FRG1 levels in 90 % cases were moderate in terms of staining, in uninvolved region. On the other hand, staining in tumor area was weak to negative, in 80 % cases. Comparison of Allred score for FRG1 expression in tumor and uninvolved tissue, showed significant reduction of FRG1 levels in tumor.

Similarly, in case of gastric and colon cancer, FRG1 levels in tumor were reduced in 66.66 % (6/9) and 63.63 % (7/11) cases respectively, compared to the uninvolved control. Distribution pattern of FRG1 staining in gastric cancer revealed that more than 40 % cases showed strong staining and 60 % cases showed moderate staining in uninvolved tissue, whereas in tumor only 40 % cases belonged to strong to moderate group, in terms of staining intensity. Comparison of Allred score showed significant reduction in tumors compared to uninvolved tissue, with p value ≤ 0.05 . In colon cancer, distribution pattern revealed ~80 % cases had strong FRG1 staining in

uninvolved tissue, compared to ~40 % cases in tumor tissue. Allred score analysis revealed significant ($p \leq 0.05$) reduction in Allred score for tumor compared to uninvolved tissue.

We observed nuclear localization of FRG1 in gastric cancer and colon cancer. No significant association was derived between tumor progression parameters and nuclear localization of FRG1. In case of squamous epithelium of oral cavity, FRG1 was strictly localized at cytoplasm. A larger and well stratified sample size of these cancer types could provide proper insights into nuclear localization of FRG1 in tumors.

2.3 Altered FRG1 levels has no effect on cell proliferation in non-cancer, HEK293T cells

Unchecked cell proliferation being a hallmark of cancer, it was critical to identify effect of FRG1 on cell proliferation, to ascertain its role in tumorigenesis. In our study, we chose HEK293T (Human Embryonic Kidney) cells to test the oncogenic effects of FRG1 in a non-cancer cell line. Ectopic expression of FRG1 and FRG1 knockdown showed no significant change in cell proliferation, compared to empty vector set and scrambled vector control, respectively. Hence, FRG1 may have discrete effect on cell proliferation depending on cell type as over expression of FRG1 led to reduced cell proliferation in myoblasts cells, as previously reported [19].

2.4 Altered FRG1 expression level affects cellular migration

Cellular migration is essential for progression of tumor as it is associated with tumor metastasis. Thus, we further evaluated effect of FRG1 expression on cellular migration. In a 6 well plate, 0.25×10^6 cells were seeded and were transfected, after 24 hour. Once the cells formed a confluent monolayer, scratch was made using P200 tip and imaging was done for wound healing at different time points. Ectopic expression of FRG1 led to significant reduction in wound healing in HEK293T. Knockdown of FRG1 significantly enhanced cellular migration, compared to scrambled control vector in HEK293T.

To further validate effect of FRG1 expression on cell migration transwell migration assay was also performed. Ectopic expression of FRG1 led to reduction in transwell migration of HEK293T. This result further strengthened our claim that FRG1 affects the migration of cells. FRG1 knockdown sets showed reverse trends of migration than ectopic expression set. FRG1 knockdown led to significant increase in transwell migration of HEK293T. Thus, above results from scratch wound healing assay and transwell migration are matching and clearly shows the effect of FRG1 expression levels on cell migration which also justifies reduction of FRG1 levels in tumor tissues.

2.5 Altered FRG1 level affects invasiveness of cells

Metastasis is a hallmark of tumor and could be correlated to invasiveness. During tumor progression, malignant cells invade through the extracellular matrix and metastasize into various organs. Thus, we performed Matrigel Invasion Assay to determine whether FRG1 expression affects invasiveness of the cell. Invasion data followed the trend of cellular migration data. Ectopic expression of FRG1 led to significant reduction in cell invasion in HEK293T. FRG1 knockdown led to enhanced cell invasion compared to scrambled shRNA in HEK293T. Accordingly, we can infer that FRG1 expression levels have a significant effect on invasiveness of non-cancer cell lines.

2.6 FRG1 modulates cell migration and invasion by regulating expression of various cytokines and MMPs in HEK293T

RNA extraction was done from HEK293T cells, transfected with FRG1 expression vector and FRG1 knockdown vector with their respective controls. cDNA was made from the extracted RNA. Q-RT PCR was done using the above-mentioned cDNA sample for 11 tumor and angiogenesis associated cytokines and 7 MMPs. In HEK293T knockdown, MMP10 was significantly up regulated (p value ≤ 0.05 , Fold change ≥ 1.5). In case of ectopic expression of FRG1 G-CSF was significantly reduced in HEK293T cells (p value ≤ 0.05 , fold change ≥ 1.5).

Chapter 3: Identifying role and molecular mechanism of FRG1 in Prostate cancer

3.1 In vivo analysis shows reduced FRG1 protein levels in Prostate cancer

In Prostate cancer 20 Needle core biopsy cases were identified of which, only 10 cases had uninvolved tissue. Out of which five tumor cases showed reduced FRG1 levels, compared to the uninvolved tumor tissue. But no significant difference was observed in Allred scores. We found that 80 % cases were moderately stained in case of tumor tissues. On the contrary, 60 % of uninvolved tissue samples had strong staining. Prostate cancer was the only tumor type in our study, where reduction in FRG1 levels was not significantly associated with tumor progression.

3.2 Altered FRG1 levels have discrete effect on cell proliferation of Prostate cancer cell lines

PC3 and DU145 cells were used to test the oncogenic effects of FRG1 in prostate cancer. Ectopic expression of FRG1 showed no significant change in cell proliferation compared to empty vector set, in case of DU145 cells but PC3 cells showed significant reduction in cell proliferation. To decipher effect of FRG1 knockdown on cell proliferation stable FRG1 knockdown line was prepared for DU145 but for PC3 transient knockdown was done. DU145 showed significant increase in cell proliferation, on FRG1 knockdown, but PC3 did not show

any significant change in cell proliferation. Hence, FRG1 may have discrete effect on cell proliferation depending on cell type.

3.3 Altered FRG1 expression level affects cellular migration

Cellular migration is a key property in tumorigenesis as it promotes tumor metastasis. Further we wanted to evaluate the effect of FRG1 expression on cell migration, which was assessed by scratch wound healing assay and transwell migration assay.

Ectopic expression of FRG1 led to significant reduction in wound healing in DU145 and PC3 cell lines. Knockdown of FRG1 significantly enhanced cellular migration, compared to scrambled control vector. Our observation clearly demonstrated that FRG1 affects cell migration. To further validate effect of FRG1 expression on cell migration, transwell migration assay was also performed. Ectopic expression of FRG1 led to reduction in transwell migration of DU145 and PC3. This result further strengthened our claim that FRG1 affects the migration of cells. FRG1 knockdown in both DU145 and PC3 cell lines led to significant increase in transwell migration of cells. Therefore, above results from scratch wound healing assay and transwell migration are matching and clearly show the effect of FRG1 expression levels on cell migration which also justifies reduction of FRG1 levels in tumor tissues.

3.4 Altered FRG1 level affects invasiveness of cells

Invasion data followed the trend of cellular migration data. Ectopic expression of FRG1 led to significant reduction in cell invasion in DU145 and PC3 cell lines. FRG1 knockdown led to enhanced cell invasion compared to scrambled shRNA in both the prostate cancer cell lines. Accordingly, we can infer that FRG1 expression levels have a significant effect on invasiveness of these two cancer cell lines.

3.5 FRG1 modulates cell migration and invasion by regulating expression various cytokines and MMPs

RNA extraction was done from DU145 and PC3, transfected with FRG1 expression vector and FRG1 knockdown vector with their respective controls. Q-RT PCR was done using the above mentioned cDNA sample for 11 tumor and angiogenesis associated cytokines and 7 MMPs. In DU145 knockdown GM-CSF, PLGF and MMP1 were significantly up regulated (p value ≤ 0.05 , fold change ≥ 1.5). In case of PC3 cells, knockdown of FRG1 showed significant up regulation of MMP1, GM-CSF, PDGFA and CXCL1 (p value ≤ 0.05 , fold change ≥ 1.5).

Chapter 4: To determine role and molecular mechanism of FRG1 in Breast cancer

4.1 In vivo analysis shows reduced FRG1 protein levels in Breast cancer

46 surgically resected Breast tumor tissues were identified along with uninvolved region. A total of 38, out of 46 tumor cases showed significant ($p \text{ value} \leq 0.05$) reduction in FRG1 levels compared to their paired uninvolved sample. 50 % cases of tumor tissues were stained negatively; on the other hand 60 % of uninvolved ductal epithelial cells were stained strongly. Allred score of FRG1 levels for tumor tissue showed a significant reduction, compared to uninvolved control.

4.2 Altered FRG1 levels affected cell proliferation of MCF7 cells

MCF7 cells were used to validate *in vivo* findings of breast cancer. Cell proliferation assay was performed to determine effect of FRG1 on oncogenic growth potential of MCF7. Ectopic expression of FRG1 showed reduction in cell proliferation. To decipher effect of FRG1 knockdown on MCF7 cell proliferation, stable FRG1 knockdown lines were prepared. MCF7 showed significant increase in cell proliferation, on FRG1 knockdown.

4.3 Altered FRG1 expression level affects cellular migration in MCF7 cells

Cellular migration was assessed by scratch wound healing assay and transwell migration assay. Ectopic expression of FRG1 led to significant reduction in wound healing in MCF7, with inverse trends being observed in FRG1 knockdown i.e. reduced FRG1 expression led to enhanced cellular migration.

To further validate effect on cellular migration, transwell migration assay was done. Ectopic expression of FRG1 led to reduction in transwell migration of MCF7, on the contrary FRG1 knockdown showed enhanced migration. Consequently, above result from scratch wound healing assay and transwell migration are complementary and clearly show the effect of FRG1 expression levels on cell migration. Thus, we can conclude that reduced FRG1 in breast cancer may promote tumor cell migration.

4.4 Altered FRG1 level affects invasiveness of MCF7 cells

Matrigel invasion assay was performed to determine whether FRG1 expression affects invasiveness of the cells. Invasion data followed the trend of cellular migration data. Ectopic expression of FRG1 led to significant reduction in cell invasion of MCF7 and FRG1 knockdown led to enhanced cell invasion compared to scrambled shRNA. Thus, asserting that FRG1 might be a crucial molecule for cancer cell metastasis.

4.5 FRG1 regulates cell proliferation, migration and invasion of MCF7 by regulating expression various cytokines and MMPs

Q-RT PCR was done in MCF7 cells with ectopic FRG1 expression and knockdown sets, using the above-mentioned cDNA sample for 11 tumor and angiogenesis associated cytokines and 7 MMPs. In MCF7 knockdown set MMP2, MMP13, PDGFA, PDGFB, CXCL1, CXCL8, FGF2 and PLGF were significantly up regulated (p value ≤ 0.05 , Fold change ≥ 1.5). No significant change was observed in any molecule in case of ectopic FRG1 expression set.

Discussion and Conclusion:

Prior to our study FRG1 was considered to be a FSHD candidate gene with possibility of involvement in angiogenesis regulation. FRG1 levels dictate angiogenesis in *Xenopus* development, but we have reported for the first time that it also regulates mammalian endothelial cell differentiation *in vitro*. Involvement of FRG1 in angiogenesis needs thorough understanding, as our *in vitro* data suggest otherwise of *Xenopus* study. Further we could not correlate FRG1 tumor levels with MVD, which measures neoangiogenesis in tumors. These finding sheds light into study of FSHD patients with retinal vasculature abnormalities where FRG1 levels were unchanged. To decipher involvement of FRG1 in tumor angiogenesis we need to look into large cohorts of sample with higher sample size.

The study reports for the first-time involvement of FRG1 in tumorigenesis. In our study, we have demonstrated for the first-time tissue based localization and distribution of FRG1 protein in tumor. Prior to our study there was only single study, which reported about distribution of FRG1 in human tissue i.e. in muscle biopsy of FSHD patients. In our study, we could observe that FRG1 is indeed, both cytoplasmic and nuclear protein and localization might vary based on the tissue type; in oral cavity squamous epithelial lining it was strictly cytoplasmic. This suggests that FRG1 may perform different fundamental cellular functions depending on the tissue type. One of the major findings of our study was, FRG1 levels are reduced in tumors, this trend was conserved all through various tumor types. To further understand effect of FRG1 on tumorigenesis we used various cell lines to understand effect on cell proliferation, migration and invasion. We could consistently observe that loss of FRG1 levels increased cellular migration and invasion which contradicted the earlier finding where FRG1 over expression lead to enhanced delamination and migration of muscle cells during *Xenopus* development. It may be possible that FRG1 functions differently in various cell types and presence of different stromal components determines the function. Variation in our cell line proliferation data also advocates it. Enhanced expression of FRG1 is known to reduce proliferation of myoblasts, causing

muscular atrophy, which is evident in FRG1 over expressing transgenic mice. In our study, altered FRG1 expression affected cell proliferation in MCF7 with FRG1 ectopic expression and knockdown sets, DU145 with FRG1 knockdown set, PC3 with ectopic expression set, but had no effect in HEK293T cells. This suggests that the regulation of proliferative property of cells by FRG1 depends on the cell type and various other stromal components.

FRG1 expression levels affect the expression of various cytokines and MMPs including CXCL1, CXCL8, PLGF, GCSF, GMCSF, MMP10, MMP2, IL10 and MMP13. These cytokines and MMPs are very well associated with tumor progression. These molecules play significant role in tumor progression. Overall, in our study we provide an overview that loss of FRG1 may be essential for tumor progression, which is mediated through change in expression levels of these cytokines. A step further has to be taken to understand the molecular mechanism, which is essential to pin point the importance of the FRG1 in tumor progression and angiogenesis.

References

1. Carmeliet, P., *Angiogenesis in life, disease and medicine*. Nature, 2005. **438**: p. 932-936.
2. Hanahan, D. and R.A. Weinberg, *The hallmarks of cancer*. Cell, 2000. **100**: p. 57-70.
3. Chung, A.S., J. Lee, and N. Ferrara, *Targeting the tumour vasculature: insights from physiological angiogenesis*. Nature Rev. Cancer, 2010. **10**: p. 505-514.
4. Carmeliet, P. and R.K. Jain, *Principles and mechanisms of vessel normalization for cancer and other angiogenic diseases*. Nature reviews. Drug discovery, 2011. **10**(6): p. 417-27.
5. Bergers, G. and D. Hanahan, *Modes of resistance to anti-angiogenic therapy*. Nature Rev. Cancer, 2008. **8**: p. 592-603.
6. Potente, M., H. Gerhardt, and P. Carmeliet, *Basic and Therapeutic Aspects of Angiogenesis*. Cell, 2011. **146**(6): p. 873-887.
7. Grewal, P.K., et al., *FRG1, a gene in the FSH muscular dystrophy region on human chromosome 4q35, is highly conserved in vertebrates and invertebrates*. Gene, 1998. **216**(1): p. 13-19.
8. Ferri, G., et al., *Direct interplay between two candidate genes in FSHD muscular dystrophy*. Human Molecular Genetics, 2016. **24**(5): p. 1256-1266.
9. Gabellini, D., et al., *Facioscapulohumeral muscular dystrophy in mice overexpressing FRG1*. Nature, 2006. **439**(7079): p. 973-977.
10. Hanel, M.L., R.D. Wuebbles, and P.L. Jones, *Muscular dystrophy candidate gene FRG1 is critical for muscle development*. Developmental Dynamics, 2009. **238**(6): p. 1502-1512.
11. Liu, Q., et al., *Facioscapulohumeral muscular dystrophy region gene-1 (FRG-1) is an actin-bundling protein associated with muscle-attachment sites*. Journal of cell science, 2011. **123**(Pt 7): p. 1116-23.
12. Padberg, G.W., et al., *On the significance of retinal vascular disease and hearing loss in facioscapulohumeral muscular dystrophy*. Muscle & nerve. Supplement, 1995. **2**: p. S73-80.

13. Wuebbles, R.D., M.L. Hanel, and P.L. Jones, *FSHD region gene 1 (FRG1) is crucial for angiogenesis linking FRG1 to facioscapulohumeral muscular dystrophy-associated vasculopathy*. Disease models & mechanisms, 2009. **2**(5-6): p. 267-74.
14. Liu, C.-Y., et al., *Vimentin contributes to epithelial-mesenchymal transition cancer cell mechanics by mediating cytoskeletal organization and focal adhesion maturation*, in *Oncotarget*. 2014. p. 15966-15983.
15. Hasegawa, K., et al., *Facioscapulohumeral muscular dystrophy (FSHD) region gene 1 (FRG1) expression and possible function in mouse tooth germ development*. Journal of Molecular Histology, 2016. **1**.
16. Fang, W.-T., et al., *Downregulation of a putative tumor suppressor BMP4 by SOX2 promotes growth of lung squamous cell carcinoma*. International journal of cancer, 2014. **135**(4): p. 809-819.
17. Adams, J.C., *Roles of fascin in cell adhesion and motility*. Current opinion in cell biology, 2004. **16**(5): p. 590-596.
18. Weidner, N., et al., *Tumor angiogenesis and metastasis correlation in invasive breast carcinoma*. New England Journal of Medicine, 1991. **324**(1): p. 1.
19. Chen, S.C., et al., *Decreased proliferation kinetics of mouse myoblasts overexpressing FRG1*. PLoS One, 2011. **6**(5): p. 1932.

Publications in Refereed Journal:

a. Published:

Arman K Hansda*, **Ankit Tiwari***, Manjusha Dixit; Current Status and Future Prospect on FSHD Region Gene 1. Journal of Biosciences, 42(2), 345-353.

* Equal contribution by authors

b. Accepted:

Ankit Tiwari, Bratati Mukherjee, Manjusha Dixit; MicroRNA Key to Angiogenesis Regulation: miRNA Biology and Therapy; Current Cancer Drug Targets

c. Communicated:

Ankit Tiwari, NiharikaPattanaik, ArchitaMohanty Jaiswal, Manjusha Dixit. FRG1 is a Putative tumor suppressor (Communicated)

Ankit Tiwari, MdKhurshidul Hassan, NiharikaPattanaik, ArchitaMohanty Jaiswal, Manjusha Dixit. Reduced FRG1 expression promotes prostate cancer progression and affects prostate cancer cell migration and invasion (Communicated)

Other Publications:

a. Book/Book Chapter

b. Conference/Symposium

Ankit Tiwari, S.P. Singh, Manjusha Dixit; Finding out role of FRG1 expression in angiogenesis and cancer, Indian Cancer Genetics Conference, 2013, Navi Mumbai, India.

Ankit Tiwari, Manjusha Dixit; Association of FRG1 with DAB2, a tumor suppressor gene in cancer cells, IACR, 2014, Kollam, Kerala, India

Signature of Student: *Ankit Tiwari*

Date: *29th May 2017*

Doctoral Committee:

S. No.	Name	Designation	Signature	Date
1.	Dr. Sanjib Kar	Chairman	<i>Sanjib Kar</i>	<i>29/05/2017</i>
2.	Dr. Manjusha Dixit	Guide/ Convener	<i>Manjusha</i>	<i>29/05/2017</i>
3.		Co-guide (if any)		
4.	Dr. Asima Bhattacharyya	Member	<i>Asima Bhattacharyya</i>	<i>29.5.17</i>
5.	Dr. Subhasis Chattopadhyay	Member	<i>Subhasis Chattopadhyay</i>	<i>30/05/17</i>
6.	Dr. Rajeeb Swain	Member	<i>Rajeeb Swain</i>	<i>30/05/17</i>

Chapter 1

To Investigate the Effect of FRG1 Expression in Angiogenesis

This section has been published in following research article

Ankit Tiwari, Niharika Pattanaik, Archita Mohanty Jaiswal, Manjusha Dixit; Increased FRG1 expression reduces in vitro cell migration, invasion and angiogenesis, ex vivo supported by reduced expression in tumors. *Bioscience Reports*, 2017, 37 (5).

5.1.1. Introduction:

FRG1 was the first gene to be associated with FSHD and therefore primary focus on FRG1 research is centered towards muscle function and development [74, 76]. The relation between FRG1 and angiogenesis were derived from the observation made in FSHD patients; 75 % of FSHD patients harbor retinal vasculature abnormalities [82, 83]. Thus to verify the association between FRG1 and angiogenesis gene expression analysis were performed between FSHD patients and healthy individuals. Expression analysis data did not associate FRG1 with retinal vasculature abnormalities [17]. The first report to associate FRG1 with angiogenesis was in *Xenopus laevis*. Frg1 knockdown in *Xenopus* embryos led to reduced expression of vascular marker dab2 suggesting of inhibition of angiogenesis [16]. The same study also reported poor vessel organization in developing *Xenopus* embryos with transgenic expression of FRG1 [16]. These findings provided us with primary concept of association of FRG1 and angiogenesis. Hence, we decided to look into the effect of FRG1 expression on tumor endothelial cells.

5.1.2. Results:

5.1.2.1. FRG1 Levels Affect Endothelial Cell Functions:

To assess role of FRG1 in angiogenesis we used co-culture set up of endothelial cells (HUVECs) with epithelial cells (HEK293T). Firstly, to identify effect on endothelial cell differentiation, tubule formation assay was done. Treatment of HUVECs with conditioned medium, obtained from HEK293T cells transfected with FRG1 expression vector, led to reduced tubule formation compared to its control (Figure 5.1.1.A). The analysis revealed, 13 out of 20 angiogenesis related criteria, were significantly affected ($p \text{ value} \leq 0.05$) (Table 5.1.1). Further, to identify effect of

FRG1 expression on endothelial cell proliferation, we performed cell proliferation assay on HUVECs. No effect was observed, on HUVEC cell proliferation, when treated with conditioned media obtained from HEK293T cells transfected with FRG1 expression vector (Figure 5.1.1.B).

Migratory properties of endothelial cells are essential for blood vessel development. Therefore, we checked the effect of FRG1 expression on HUVEC migration in the same co-culture set up in which other assays were done. We observed a reduction in migration of HUVECs; there was statistically significant (p value = 0.009) difference between FRG1 over expression set and empty vector control set (Figure 5.1.1.C, 5.1.1.D).

Table (5.1.1): Data from tubule formation assay showing change in various parameters of angiogenesis

S. No.	Angiogenesis Parameter	Analyzer	FRG1 over expression vector	Control vector	P value
1	Number of Extremities		132 ± 25	107 ± 14	0.026
2	Number of Nodes		263 ± 98	371 ± 96	0.039
3	Number of Junctions		79 ± 28	110 ± 28	0.041
4	Number of Master Junctions		32 ± 16	46 ± 15	0.073
5	Number of Master Segments		51 ± 29	80 ± 28	0.057
6	Total Master Segment Length		6288 ± 2837	9571 ± 2576	0.028
7	Number of Meshes		16 ± 12	27 ± 12	0.057
8	Total Meshes Area		127029 ± 120136	306016 ± 163722	0.022
9	Number of Pieces		183 ± 33	218 ± 36	0.052
10	Number of Segments		83 ± 41	130 ± 43	0.039
11	Number of Branches		69 ± 7	70 ± 8	0.41
12	Number of Isolated Segments		30 ± 11	17 ± 8	0.025
13	Total Length		13624 ± 1677	15602 ± 1613	0.029
14	Total Branching Length		11200 ± 2393	14257 ± 2200	0.029
15	Total Segment Length		5964 ± 2756	9165 ± 2562	0.029
16	Total Branches Length		5236 ± 683	5091 ± 777	0.36
17	Total Isolated Branches Length		2424 ± 867	1345 ± 620	0.014
18	Branching Interval		87 ± 43	132 ± 41	0.046
19	Mesh Index		200 ± 26	212 ± 28	0.22
20	Mean Mesh Size		6830 ± 1740	10358 ± 3523	0.024

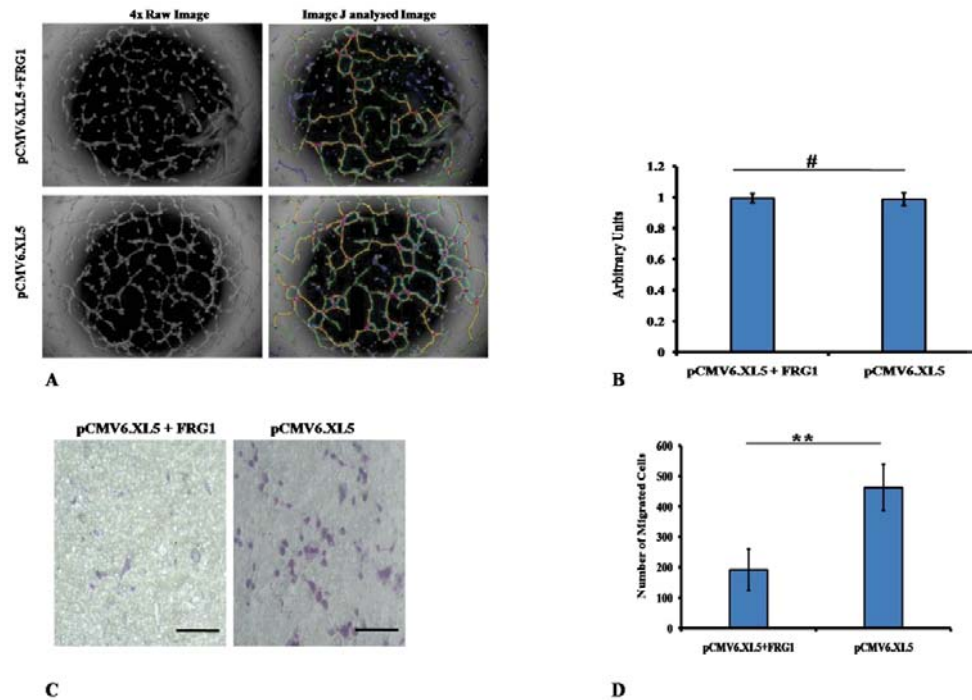


Figure (5.1.1): Effect of FRG1 Expression on endothelial cell function. **A.** Representative images showing matrigel tubule formation assay in HUVECs treated with conditioned medium, obtained from FRG1 expressing HEK293T cells and respective vector control; image shows reduced tubule formation in FRG1 over expression set. **B.** Graphical representation of cell proliferation assay data showing no significant change in proliferation of HUVECs when treated with conditioned medium obtained from HEK293T transfected with respective sets. **C.** Representative images of HUVEC transwell migration assay in co-culture with HEK293T cells, transfected with FRG1 expression vector and empty vector control. **D.** Graphical representation of HUVEC transwell migration assay showing significant reduction in HUVEC migration co-cultured with HEK293T expressing FRG1 (pCMV6.XL5.FR1), compared to empty vector (pCMV6.XL5). ** represents $p < 0.01$, # represents $p > 0.05$.

5.1.2.2. FRG1 Levels in Tumor Samples do not Correlate with MVD Count:

Since earlier studies suggest association of FRG1 with vascular abnormalities and our *in vitro* data shows that higher levels of FRG1 lead to reduction of tubule formation, therefore we checked whether FRG1 level is associated with tumor angiogenesis. To identify we performed a correlation analysis between Allred score of tumors with Micro Vessel Density (MVD) count of the respective tumor type. The correlation coefficient for MVD vs. Allred score of oral, gastric and colon cancers were $r^2 = 0.115$ (p value = 0.16), $r^2 = 0.026$ (p value = 0.63) and $r^2 = 0.006$ (p value = 0.83),

respectively (Figure 5.1.2). Generally, correlation analysis suggests that FRG1 expression levels may not have a role in tumor angiogenesis.

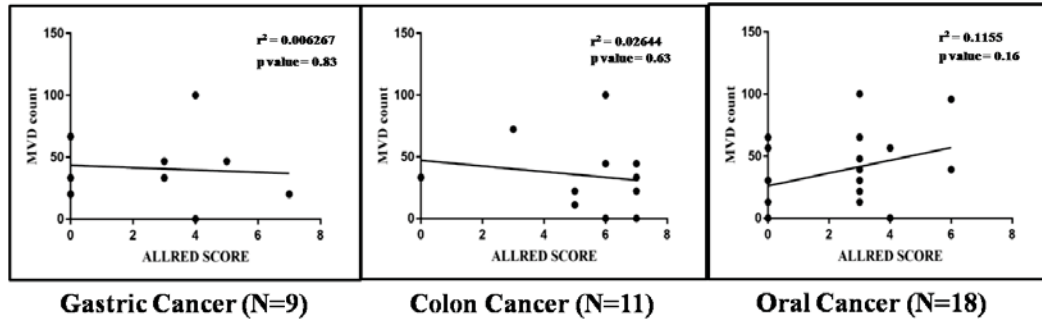


Figure (5.1.2): Correlation between FRG1 expression and MVD count. Row represents correlation analysis between FRG1 staining Allred score and MVD count for each tumor type. N shows the sample number in each tumor type. No significant correlation was observed between FRG1 Allred score and MVD count in all three cancer types.

5.1.3. Discussion:

FRG1 has been very well implicated in FSHD but in recent times, studies have reported functional insights into various cellular and physiological processes [16, 71, 93]. Based on the indirect indications, we decided to investigate the role of FRG1 in angiogenesis and tumorigenesis. The reason to use HEK293T cells for co culture set up with endothelial cell was, that we wanted to observe whether FRG1 can change the angiogenic switch in non-cancerous cells, inducing pro/ anti-angiogenic environment. The first-time study reports the effect of FRG1 expression on cellular properties of primary endothelial cell and epithelial origin cell line. The role of FRG1 in angiogenesis remains questionable. The first idea of involvement of FRG1 in angiogenesis regulation was formed by a simple observation, that is, 75 % of FSHD patients were diagnosed with retinal vasculature abnormalities [17, 82, 83]. To elucidate the involvement of FRG1 in angiogenesis, FRG1 transcription signatures of FSHD patients (N = 19) were compared to healthy individuals (N = 30). The findings

of the study showed unaltered FRG1 levels in the patients with vasculature abnormalities [17]. On the contrary, developmental studies on *Xenopus* showed that *frg1* is crucial for angiogenesis but not for vasculogenesis [16]. Our *in vitro* data suggests the involvement of FRG1 in angiogenesis, as we observed that FRG1 overexpression led to reduction in tubule formation and migration of endothelial cell. This finding was further supported by CAM assay and matrigel plug assay (work done in M.Sc. thesis of Mr. Pratush Brahma) performed using conditioned media from MCF7 cells transfected with FRG1 expression vector and knockdown vector. In this study also, he found reduced angiogenic activity with FRG1 ectopic expression. Further, we could not observe an association between FRG1 levels in tumor and tumor MVD. The underlying reason could be the small sample size used for the association. Moreover, we did not have enough number of tumors from different stages and grades. It is possible that FRG1 expression correlates with angiogenesis only in the initial stage of tumorigenesis. We screened the cytokines associated with angiogenesis in HEK293T cells but we did not observe any change in VEGF levels. A direct manipulation of FRG1 levels in HUVECs can provide better understanding regarding its involvement in VEGF/VEGFR signaling axis. Henceforth, a study with better sample size, where stratification is possible, and with direct manipulation of FRG1 expression in HUVECs, can help us ascertain the role of FRG1 in angiogenesis.

Overall *in vitro* data provide us with first-hand information regarding the involvement of FRG1 in angiogenesis in humans. The question remains to be answered in case of tumor samples; currently it provides insights parallel to the findings in FSHD patients with vasculature abnormalities [17].

Chapter 2

To Establish Tumorigenic Properties of FRG1 *In vivo* and *In vitro*

This section has been published as research article, reference

Ankit Tiwari, Niharika Pattanaik, Archita Mohanty Jaiswal, Manjusha Dixit; Increased FRG1 expression reduces *in vitro* cell migration, invasion and angiogenesis, ex vivo supported by reduced expression in tumors. *Bioscience Reports*, 2017, 37 (5).

5.2.1. Introduction:

FSHD region gene 1 (FRG1) is highly conserved from invertebrates to vertebrates [14]. Its exact function is unknown. FRG1 has been a candidate gene for Facioscapulohumeral muscular dystrophy (FSHD) [14]. Ectopic expression of FRG1 causes abnormal splicing of specific genes in mice, which leads to development of FSHD like phenotype [74]. The majority of studies have proposed a role of FRG1 in muscle development [14, 18, 66, 74-76]. FRG1 over expression leads to reduction in myoblast cell proliferation, suggesting of muscular atrophy [84]. Reduction of *frg1* levels in *Xenopus laevis* leads to disrupted muscle organization. Further, over expression of *frg1* also leads to abnormal epaxial and hypaxial muscle development [18]. Altered expression of FRG1 not only affects muscle, but also the vasculature of the organism [16]. Vascular abnormalities have been observed in 75 % of FSHD patients [17, 82, 83]. Reduction in *frg1* levels in *Xenopus laevis* reduced the levels of vascular marker *dab2*, and vice versa [16]. Apart from above-mentioned studies, isolated studies are available about its role at a cellular level. Sub-cellular localization studies revealed that FRG1 is an actin bundling protein and localized in nucleolus or spliceosome complex, suggesting its role in RNA biogenesis [70, 93]. Ectopically expressed FRG1 is localized in nuclear region, predominantly into nucleolus, cajal bodies, and transcriptionally active chromatin regions [71, 93]. Nonetheless, FRG1's accurate function remains uncertain.

Various studies have indirectly associated FSHD with cancer. Treatment of dental epithelial cell line, mDEC6 with Bone Morphogenetic Protein 4 (BMP4), a known tumor inhibitor, led to translocation of FRG1 from the nucleus to the cytoplasm [19]. Moreover, FRG1's functional domain analysis revealed that it consists of a fascin like

domain, a lipocalin domain and two nuclear localization signals [70]. Fascins are actin bundling proteins which are crucial for tumor progression [94-97]. Transcriptional signature of FSHD myotubes and myocytes resemble highly with Ewing's sarcoma [86]. Patients of muscular dystrophy such as DMD, are known to develop cancer [85, 98-100]. In terms of FSHD, there has been a single case report where FSHD patient was diagnosed with breast cancer [87].

Until now, there is no direct evidence showing the role of FRG1 in tumor angiogenesis and tumor progression. Similarly, effect of FRG1 expression on other cell types, apart from myocytes and other muscle cells is unknown. Above mentioned studies suggest the role of FRG1 in development of various organs and angiogenesis. Therefore, FRG1 expression levels might be crucial for tumor progression through tumor angiogenesis or independently. Present study was taken up to explore the association of FRG1 expression with tumor progression.

5.2.2. Results:

5.2.2.1. Altered FRG1 Levels do not Affect Cell Proliferation but it Affects Cell Migration:

We chose HEK293T cells to test the oncogenic effects of FRG1, as these cells are not derived from cancer. Ectopic expression of FRG1 (Figure 5.2.1.A) showed no change in cell proliferation compared to empty vector set (p value = 0.33) (Figure 5.2.1.C). Similar results were observed when RNAi based silencing reduced FRG1 levels (Figure 5.2.1.B), no alteration in cell proliferation was observed compared to scrambled shRNA set (p value = 0.55) (Figure 5.2.1.D).

Further we evaluated the effect of FRG1 expression on cell migration. Effect on cell migration was assessed by scratch wound assay and transwell migration assay. In FRG1 over expression set, healed wound area was found to be smaller than the empty

vector control (Figure 5.2.1.E). There was statistically significant (p value < 0.0001) difference in healed area between empty vector set (94.88 ± 0.66 %) and FRG1 over expression set (80.78 ± 0.35 %) (Figure 5.2.1.G). Similar trends were observed in transwell migration assay (Figure 5.2.2.A). Significantly (p value = 0.029) less number of cells migrated through the membrane in FRG1 over expression set (3055 ± 110), compared to the control set (3425 ± 86) (Figure 5.2.2.C).

To see whether reduction of FRG1 expression has opposite effect on migration, scratch wound healing assay was performed with HEK293T silenced for FRG1. As expected, the trends were observed to be just opposite to the over expression set. Knockdown of FRG1 led to increased migration of cells, compared to scrambled control (Figure 5.2.1.F). Statistically significant (p value = 0.036) more area (64 ± 6.28 %) was healed in case of FRG1 knockdown compared to scrambled shRNA (53 ± 2.91 %) (Figure 5.2.1.H). Results of transwell migration assay supported the scratch wound healing assay data (Figure 5.2.2.B). Number of cells (1069 ± 320) migrated in FRG1 knockdown set, was significantly (p value = 0.021) higher compared to cells (371 ± 71) migrated in scrambled shRNA set (Figure 5.2.2.D). To sum up, all above assays advocate the role of FRG1 in cellular migration.

5.2.2.2. FRG1 Regulates Cell Invasion:

During tumor progression, malignant cells invade through the extracellular matrix and metastasize into various organs. Thus, we performed Matrigel invasion assay to determine whether FRG1 expression affects invasiveness of the cell. Invasion data followed the trend of cellular migration (Figure 5.2.2.E). Ectopic expression of FRG1 led to significant (p value = 0.026) reduction in cell invasion, with 520 ± 55 invasive cell count compared to 948 ± 208 , of empty vector (Figure 5.2.2.G). FRG1

knockdown led to significantly (p value = 0.029) enhanced cell invasion compared to scrambled shRNA (cell count 445 ± 70 vs. 263 ± 65) (Figure 5.2.2.H). From this data, we can infer that FRG1 expression levels have a significant effect on invasiveness of HEK293T cells.

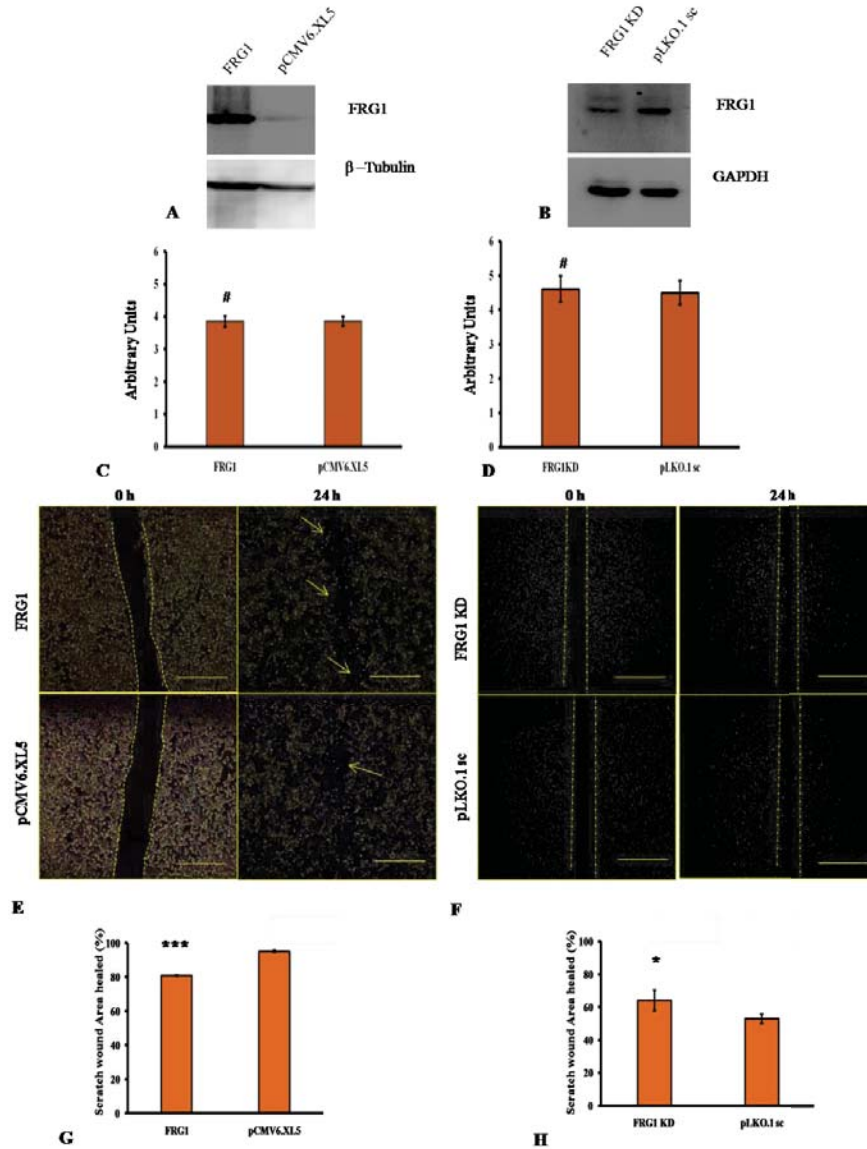


Figure (5.2.1): Effect of FRG1 expression on HEK293T cell proliferation and scratch wound healing. A. shows western blot to confirm ectopic expression FRG1 in HEK293T. B. shows verification of reduced FRG1 levels after RNAi silencing in HEK293T, by western blot. C. represents measurement of cell proliferation in HEK293T with ectopic expression of FRG1 compared to empty vector control (pCMV6.XL5), by MTS reagent. D. represents measurement of cell proliferation in HEK293T with knockdown of FRG1 compared to scrambled vector control (pLKO1.sc), by MTS reagent. E. shows representative images of scratch wound healing assay of HEK293T cells with ectopic expression of FRG1 and respective vector control (pCMV6.XL5). F. shows representative images of scratch wound healing assay of HEK293T with FRG1 knockdown and respective scrambled vector control (pLKO1.sc). G. shows representative graph for scratch wound healing assay of HEK293T cells with ectopic expression of FRG1, compared to empty vector control (pCMV6.XL5). H. shows representative graph for scratch wound healing assay of HEK293T cells with FRG1 knockdown, compared to empty vector control (pLKO1.sc). * represents $p < 0.05$, *** represents $p < 0.001$, # represents $p > 0.05$

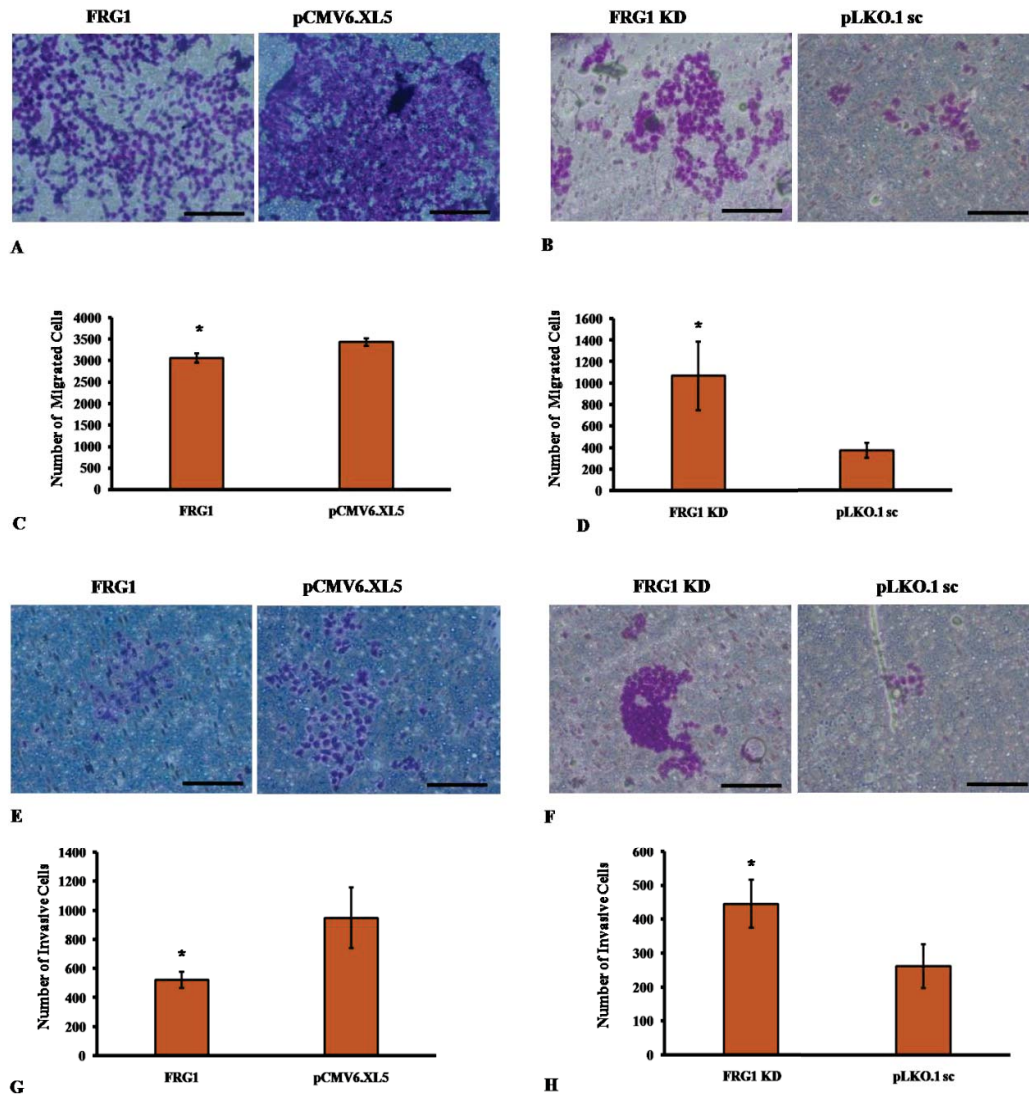


Figure (5.2.2): Effect of FRG1 expression on transwell migration and invasion. **A.** shows representative images of transwell migration assay of HEK293T cells with ectopic expression of FRG1 and respective vector control (pCMV6.XL5). **B.** shows representative images of transwell migration assay of HEK293T with FRG1 knockdown and respective scrambled vector control (pLKO1.sc). **C.** represents representative graph for transwell migration assay of HEK293T cells with ectopic expression of FRG1, compared to empty vector control (pCMV6.XL5). **D.** shows representative graph for transwell migration assay of HEK293T cells with FRG1 knockdown, compared to empty vector control (pLKO1.sc). **E.** shows representative images of matrigel invasion assay of HEK293T cells with ectopic expression of FRG1 and respective vector control (pCMV6.XL5). **F.** shows representative images of matrigel invasion assay of HEK293T with FRG1 knockdown and respective scrambled vector control (pLKO1.sc). **G.** represents representative graph for matrigel invasion assay of HEK293T cells with ectopic expression of FRG1, compared to empty vector control (pCMV6.XL5). **D.** shows representative graph for matrigel invasion assay of HEK293T cells with FRG1 knockdown, compared to empty vector control (pLKO1.sc). * represents $p < 0.05$

5.2.2.3. FRG1 expression levels alter expression of GCSF and MMP10:

Further, we identified the signaling molecules affecting these cell properties through FRG1. Quantitative real time PCR was performed for 7 matrix metalloproteinase's (MMPs) and 11 tumor associated cytokines. Only granulocyte colony stimulating Factor (G-CSF) and matrix metalloproteinase 10 (MMP10) showed significant effect on their gene expression, in response to change in FRG1 expression. Expression analysis revealed that ectopic expression of FRG1 led to reduction (3.3-fold, p value = 0.021) of G-CSF expression, which is key molecule associated with cell migration and tumor progression (Figure 5.2.3.A). Knockdown of FRG1 showed no specific effect on G-CSF expression, but led to increased expression of MMP10 by 2.48-fold (p value = 0.013) (Figure 5.2.3.B). MMPs are known to play important role in tumor metastasis. These findings support the possible role of FRG1 in cell migration and invasion and identified the downstream molecules, which might mediate the effect on cellular migration and invasion.

5.2.2.4. *In silico* Analysis Shows Reduced FRG1 Expression in Tumors and Poor Prognosis:

To look into FRG1 levels in tumor progression *in silico* analysis was done. Oncomine analysis revealed that, out of total 462 analyses, *FRG1* expression was significantly affected in 43 analyses. 26 out of 43 analyses showed significant reduction in *FRG1* expression. On the contrary, 17 analyses showed significant up regulation of *FRG1* (Figure 5.2.4.A). Overall, *in silico* analysis of FRG1 expression showed that FRG1 expression is reduced in more Oncomine datasets.

To further assert the importance of FRG1 expression, Kaplan Meier plotter analysis was done for available cancer types, viz. breast, lung, gastric, and ovarian. Survival

analysis revealed that low *FRG1* expression was associated with poor prognosis in overall survival of patients, in lung cancer (HR = 0.84, p value = 0.0058) (Figure 5.2.4.C) and in gastric cancer (HR = 0.56, p value = 1.8×10^{-08}) (Figure 5.2.4.B). Out of these four cancer types Oncomine data suggests that *FRG1* expression was reduced in breast, lung, and ovarian cancer but in gastric cancer, not a single analysis was found to be significant.

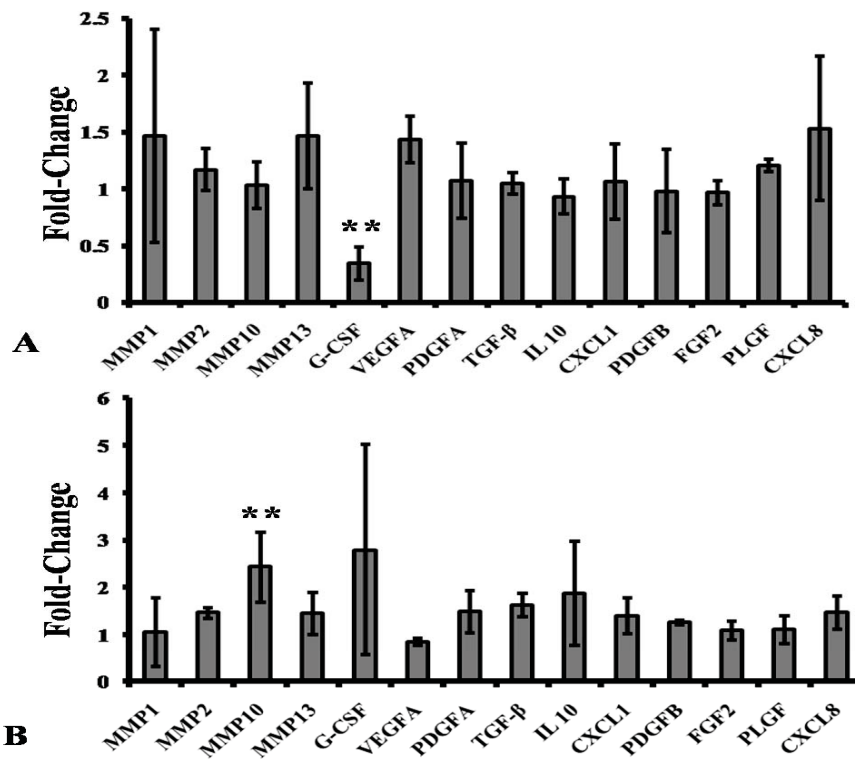


Figure (5.2.3): Effect of FRG1 expression on cell signaling molecules. A. q-RT PCR expression analysis shows effect of FRG1 expression on levels of various cytokines and MMPs, in HEK293T cells, transfected with FRG1 expression vector, compared to empty vector control. **B.** Expression analysis of various cytokines and MMPs, in HEK293T cells with FRG1 knockdown, compared to scrambled vector control). X-axis shows the name of various signaling molecules and Y-axis shows the fold change in expression of these molecules compared to their controls** represents p < 0.01,

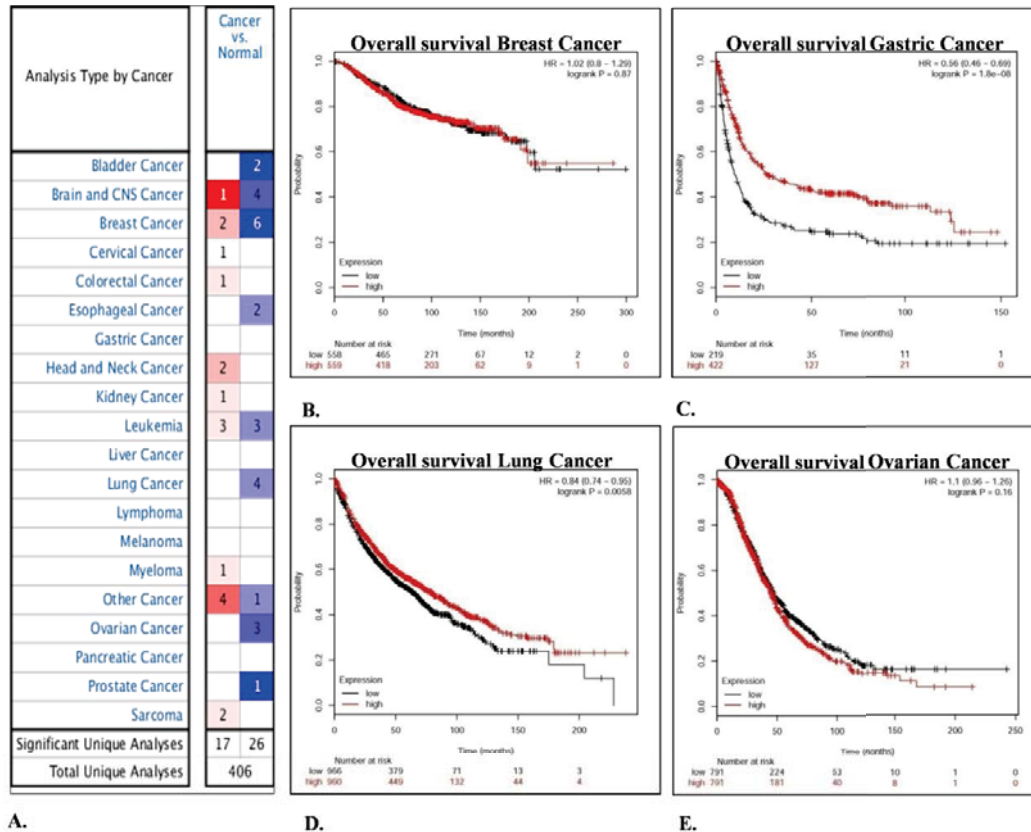


Figure (5.2.4): Determination of FRG1 expression levels and prognostic value by *in silico* analysis. A. shows FRG1 gene summary overview by OncoPrint analysis. The view represents FRG1 expression in various, tumor vs. normal datasets. The blue color represents down regulation of FRG1 levels and red color represents up regulation of FRG1 expression in a particular number of datasets. Intensity of color represents the level of up-regulation or down-regulation. B-E. Represents Kaplan Meier Plotter analysis of, B -Breast Cancer, C - Gastric cancer, D - Lung Cancer and E - Ovarian Cancer. Red line shows patients with expression above the median and black line shows patients with expression below the median. X-axis denotes the number of patient at risk with time in months and Y-axis denotes the probability of survival.

5.2.2.5. *In vivo* Analysis Shows Reduced FRG1 Protein Expression in Tumors:

To further validate *in silico* data and to derive correlation from cell-based studies, we checked FRG1 expression levels in tumor tissues. Additionally, we wanted to determine the general trend of FRG1 expression in tumors so we took various cancer types and compared expression with its uninvolved counterpart. Surgically resected tumor tissue with uninvolved region of oral cancer, gastric cancer and colon cancer were stained with FRG1 antibody. Significant reduction of FRG1 expression levels was observed in tumor, when compared to levels in uninvolved tissue.

In oral cancer, we observed that FRG1 levels were reduced in 61.11 % of tumor cases i.e. in 11/18 cases, compared to uninvolved region. FRG1 levels were mostly (90 % cases) moderate in terms of staining in uninvolved region. On the other hand, staining in tumor area was weak to negative, in 80 % cases (Figure 5.2.5). Comparison of Allred score for FRG1 in tumor and uninvolved tissue, showed significant (p value = 0.0001) reduction of FRG1 levels in tumor (median value = 3) to uninvolved (median value = 6) (Figure 5.2.5).

Similarly, in gastric and colon cancer, FRG1 levels in tumor were reduced in 66.66 % (6/9) and 63.63 % (7/11) compared to the uninvolved control, respectively. Distribution pattern of FRG1 staining in gastric cancer revealed that more than 40 % cases had strong staining and 60 % cases had moderate staining in uninvolved tissue, whereas in tumor total 40 % cases belonged to strong to moderate group (Figure 5.2.5). Comparison of Allred score showed significant (p value = 0.0078) reduction in tumor (median = 3), compared to uninvolved (median = 6) (Figure 5.2.5). In colon cancer, distribution pattern showed that ~80 % cases had strong FRG1 staining in uninvolved tissue, compared to ~40 % cases with strong FRG1 staining in tumor tissue (Figure 5.2.5). Allred score analysis indicated significant (p value = 0.0195) reduction in Allred score for tumor (median = 5), compared to uninvolved tissue (median = 7) (Figure 5.2.5). Overall, this data indicates possible role of FRG1 in tumor progression.

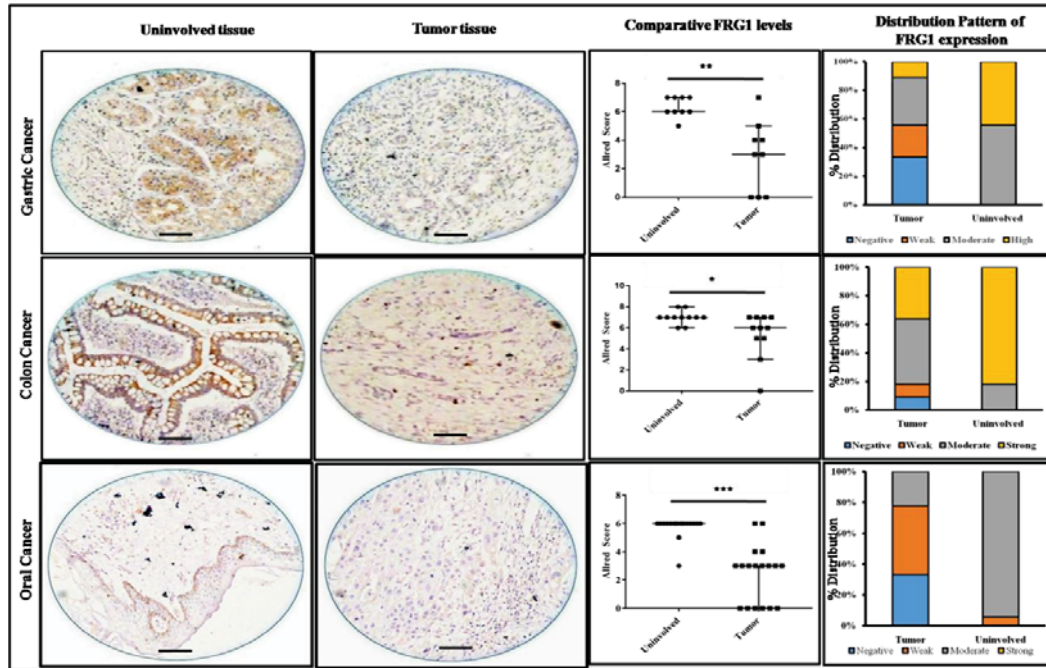


Figure (5.2.5): FRG1 levels and distribution pattern in tumor tissues. Top row represents-Gastric cancer, the middle row represents- Colon cancer and bottom row represents- Oral cavity cancer. First two columns show representative images of FRG1 staining in uninvolved tissue and tumor tissue staining respectively. The third column illustrates comparison of Allred score for FRG1 staining, between uninvolved tissue and tumor tissue. Distribution of staining pattern for the above-mentioned tumor types is represented at the fourth column.* represents $p < 0.05$, ** represents $p < 0.01$, *** represents $p < 0.0001$.

5.2.3. Discussion:

Developmental studies in *Xenopus* reported that FRG1 over expression led to increased delamination and migration of muscle cells from myotome. This study concluded that FRG1 may be essential for Epithelial to Mesenchymal Transition (EMT) or Mesenchymal to Epithelial Transition (MET) [18]. Our findings suggest other way, as we observed reduction in cellular migration and invasion, on FRG1 over expression and vice versa. Another study supports our data indirectly, where FRG1 expression is reduced in migratory breast cancer cells [20]. FRG1 over expression led to atrophy in muscle cells and reduced cell proliferation of C2C12 myoblasts, which was restored over time with reduction in FRG1 expression [84]. Nevertheless, an

important question still remains to be answered, i.e. whether FRG1 expression affects cell proliferation during tumor progression. In present study FRG1 levels did not affect cell proliferation of HEK293T cell line. FRG1 may possess tumor suppressor activity as it inhibits cellular migration and invasion; these properties are enhanced in tumor cells which lead to metastatic growth of tumor. Further, evidence can be drawn from regulation of angiogenesis by FRG1. Reduced angiogenesis during FRG1 over expression clearly points towards tumor suppressive role of FRG1. To further characterize involvement of FRG1 in tumorigenesis, animal model based studies are required. The statement is noteworthy as mouse model with FRG1 over expression is available but no animal models is known for FRG1 knock out/ knock down, which would be appropriate model to provide insights into tumorigenesis.

To find the insights of molecular mechanism of FRG1 mediated tumorigenesis, we checked expression of various signaling molecules. We found that ectopic expression of FRG1 leads to reduction in expression of G-CSF, a hematopoietic growth factor that induces proliferation and differentiation of hematopoietic stem cells of neutrophils [101-104]. Studies have established role of G-CSF in tumor progression. Administration of G-CSF leads to increase in pro-tumorigenic factors, VEGF and TGF beta [105-107]. Also, G-CSF enhances migration and proliferation of gastric and colon carcinoma cells which is further supported by findings in head and neck cancer [108-110]. Reduction of G-CSF levels could be primary reason for reduction of cellular migration and invasion of HEK293T cells, on ectopic expression of FRG1. G-CSF levels might be critical for our *in vitro* finding regarding endothelial cell function. G-CSF levels are known to promote angiogenesis and tumorigenesis [111]. Direct mediation of G-CSF facilitates angiogenesis and reduces ischemia, as observed in

ischemic model system [112]. Therefore, the effects observed in our *in vitro* study could be attributed to reduced G-CSF expression, with FRG1 over expression in HEK293T.

Knockdown of FRG1 in HEK293T showed increased expression of MMP10. MMPs are family of zinc related endoproteases involved in tumor invasion, metastasis, and angiogenesis [113]. MMP10 belongs to stromelysin sub family of MMPs. Higher MMP10 expression has been reported in lung cancer [114, 115], head and neck cancer [116, 117], oral cavity cancer esophagus cancer [118], and cervical tumors [119]. Higher expression of MMP10 directly modulates cell migration and enhances invasiveness of the cell [120]. Above mentioned studies support that up regulation of MMP10 on FRG1 silencing, might be responsible for enhanced cell migration and invasiveness.

Since G-CSF and MMP10, which are known to promote tumor growth, levels were affected by FRG1; we looked for FRG1 expression in tumor tissues. Ours is the first study is to identify reduced expression of FRG1 in tumor tissues. Expression of FRG1 was higher in uninvolved epithelial tissues, compared to the tumor. Previous study has shown positive staining of FRG1 in skin epithelial lining and sweat glands [76]. The staining patterns were consistent in our study, as basal layer of stratified epithelium, sweat glands and sebaceous glands were positively stained for FRG1. We observed that FRG1 is predominantly localized in cytoplasm but nuclear positivity was also observed in some cases, as reported previously [70, 71, 76]. Further, change in cellular migration and invasion properties with altered FRG1 levels, supported its role in tumorigenesis. One aspect, which suggests that FRG1 can be multi functional, is localization. FRG1 is known to be associated with spliceosome complex and, have

role in mRNA transport and RNA splicing [71, 93]. On the other hand, it is an actin bundling protein, providing structural integrity to the cell [71]. The localization of FRG1 is predominantly nuclear in cell lines such as mDEC6 and C2C12 [19, 76]. Whereas it is predominantly cytoplasmic in, human skeletal muscle myoblasts (HSMMs) and muscle derived stem cells (MDSCs) [76]. BMP4 treatment in mDEC6 cells, leads to change in FRG1 localization from nucleus to cytoplasm [19]. Since localization of FRG1 is critical to its function, with above mentioned studies, we can get a clear idea that FRG1 functionality may vary among different systems and it depends on the activity of stromal components, as observed in animal models.

In summary, this study provides first insights into role of FRG1 in tumorigenesis. *In silico*, *in vivo* and *in vitro* analysis of FRG1 levels revealed that loss of FRG1 expression promotes tumorigenesis [16]. Effect of FRG1 expression on cellular migration and invasion might be through G-CSF and MMP10, which might have also dictated the *in vitro* endothelial cell function. However, the specific molecular mechanism of FRG1 is yet to be understood.

Chapter 3

Identifying Role and Molecular Mechanism of FRG1 in Prostate Cancer

This section has been communicated as the following research article

Ankit Tiwari, Md Khurshidul Hassan Niharika Pattanaik, Archita Mohanty Jaiswal, Manjusha Dixit; Reduced FRG1 expression promotes prostate cancer progression and affects prostate cancer cell migration and invasion.*BMC Cancer, second revision*

5.3.1. Introduction:

Prostate cancer is the most common male cancer, and is the second and third most common cause of cancer-related death of men, in the US and Europe, respectively [21, 121, 122]. It is a heterogeneous disease in early stages, which requires rigorous stratification, so that the progression to the advanced stage could be predicted more accurately [123]. Advances are being made in the treatment and etiological understanding of prostate cancer. Still the abundant presence of resistant tumor types and the burden of prostate cancer related death, poses a question regarding better etiological understanding of the disease [124]. Consequently, the search for novel regulators and molecular mechanism, associated with prostate cancer, is of the utmost significance.

To enhance the understanding about additional players in prostate cancer, FRG1 can be a good candidate. FRG1 is a candidate gene for Facioscapulohumeral muscular dystrophy (FSHD) [14] but it has also been shown to affect vasculature [16]. 75 % of FSHD patients have retinal vasculature abnormalities [17, 83]. Reduction in *frg1* levels in *Xenopus laevis*, reduced the levels of vascular marker *dab2* and increase in *frg1* levels led to vascular abnormalities [16]. Our research work focused on establishing the role of FRG1 as an angiogenic regulator, indicated towards possible role of FRG1 in tumorigenesis, in prostate cancer. Human homolog of *dab2* has been reported to be associated with prostate cancer progression [125]. Functional domain analysis of FRG1 revealed that it consists of a fascin like domain. Fascin is an actin bundling protein which is known to be involved in tumor progression [72]. FRG1 is also essential for differentiation of amleoblasts, odontoblasts and matrix formation, associating it with BMP4, which is well known tumorigenesis regulator [19]. Above

mentioned studies provide indications of possible involvement of FRG1 in tumorigenesis. Therefore, we intend to understand the etiological function of FRG1 in prostate cancer and its association with tumor angiogenesis.

5.3.2. Results:

5.3.2.1. FRG1 Levels in Prostate Adenocarcinoma:

FRG1 expression was analyzed in prostate cancer by immunohistochemistry in 20 needle core biopsies. Out of them, uninvolved prostate tissue was present in 10 biopsies. Figure 5.3.1.A shows strong FRG1 staining in control tissue compared to tumor tissue. The staining pattern revealed significant reduction of FRG1 expression levels in tumor cells, compared to uninvolved secretory ductal epithelial cells of prostate. Immunoreactive score (IRS), quantified for the staining pattern, revealed 7/10 cases (p value = 0.0078) had reduced FRG1 expression in tumor tissue (Figure 5.3.2.B). FRG1 staining was moderate to strong in 40 % of tumor samples and weak to negative in remaining 60 % of tumor ductal epithelial cells compared to 80 % of uninvolved tissue with moderate to strong staining (Figure 3.2.1.C).

Further, to understand the effect of FRG1 expression on tumor angiogenesis, correlation analysis was done for FRG1 IRS and MVD. No significant correlation could be derived between FRG1 protein expression levels and MVD (p value = 0.17, $r^2 = 0.102$) (Figure 5.3.1.D). Overall, patient IHC data revealed that FRG1 expression is reduced in tumor tissue but does not correlate with MVD count.

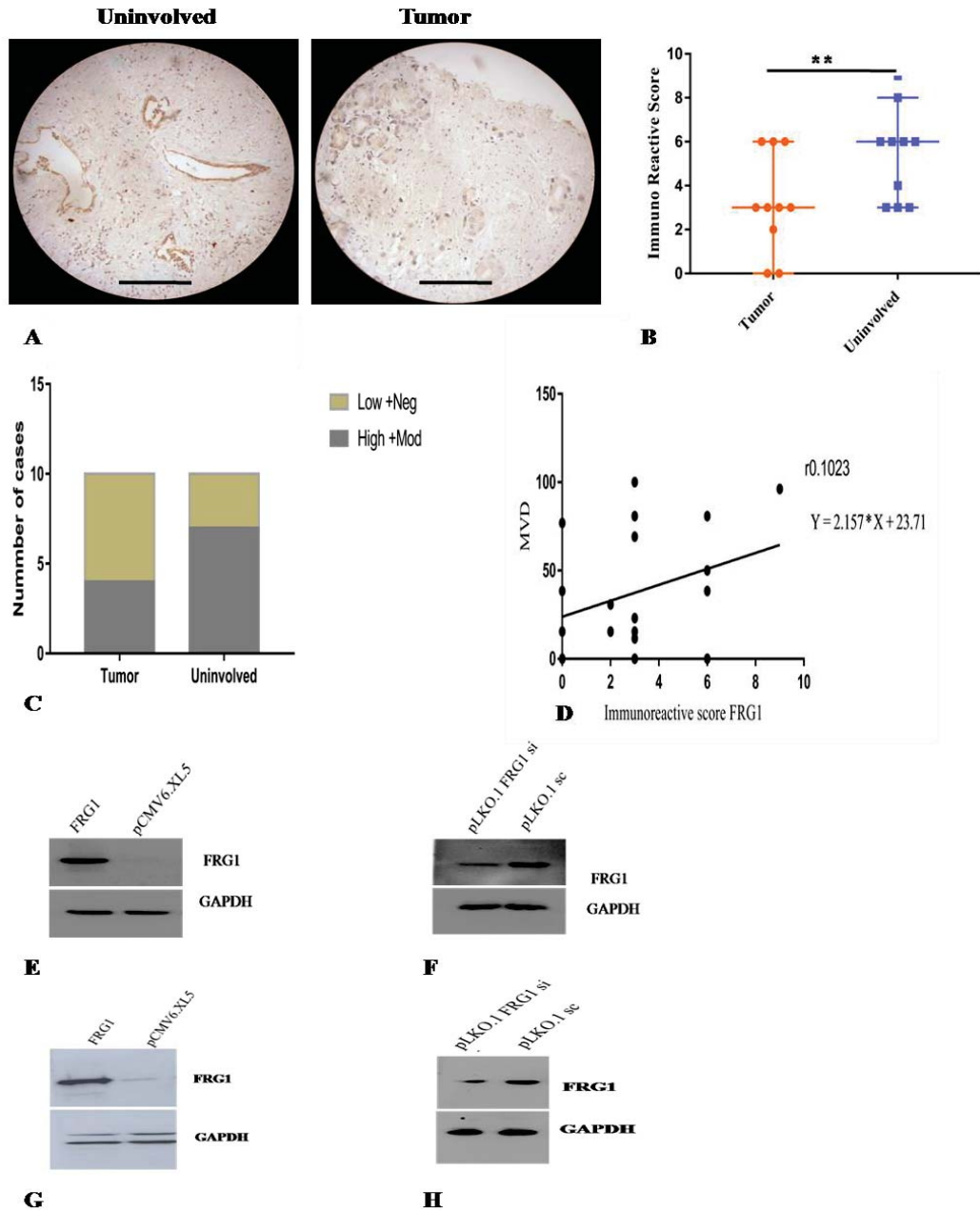


Figure (5.3.1): FRG1 expression levels in prostate tumor and cell lines. **A.** Representative Images of tumor and uninvolved tissues of prostate, column from left, first (uninvolved) and second (tumor) **B.** Comparison of IRS between tumor and uninvolved tissue. Graph shows that the reduction of IRS in tumor tissue was significant ($p = 0.0078$). **C.** Distribution of staining pattern for FRG1 in the prostate tumor and uninvolved tissue. **D.** Graphical representation of correlation analysis between tumor IRS and MVD count. **E.** Western blot to confirm ectopic expression of FRG1 in DU145 cells **F.** Western blot showing reduced FRG1 levels after RNAi silencing in DU145. **G.** Western blot image validating ectopic expression of FRG1 levels in PC3 cells. **H.** Reduction in FRG1 levels in FRG1 silenced PC3 cells confirmed by western blot. ** represents p value < 0.01

5.3.2.2. Varying Effect of FRG1 on Proliferation of Prostate Cancer Cells:

Cell proliferation assay revealed that FRG1 over expression had no significant effect on proliferation of DU145 cells (Figure 5.3.2.A) but FRG1 knockdown led to significant increase in cell proliferation (Figure 5.3.2.B). PC3 cells had significantly reduced proliferation in response to ectopic expression of FRG1 (Figure 5.3.2.C) but no significant effect was observed on cell proliferation of PC3 cells with FRG1 knockdown (Figure 5.3.2.D).

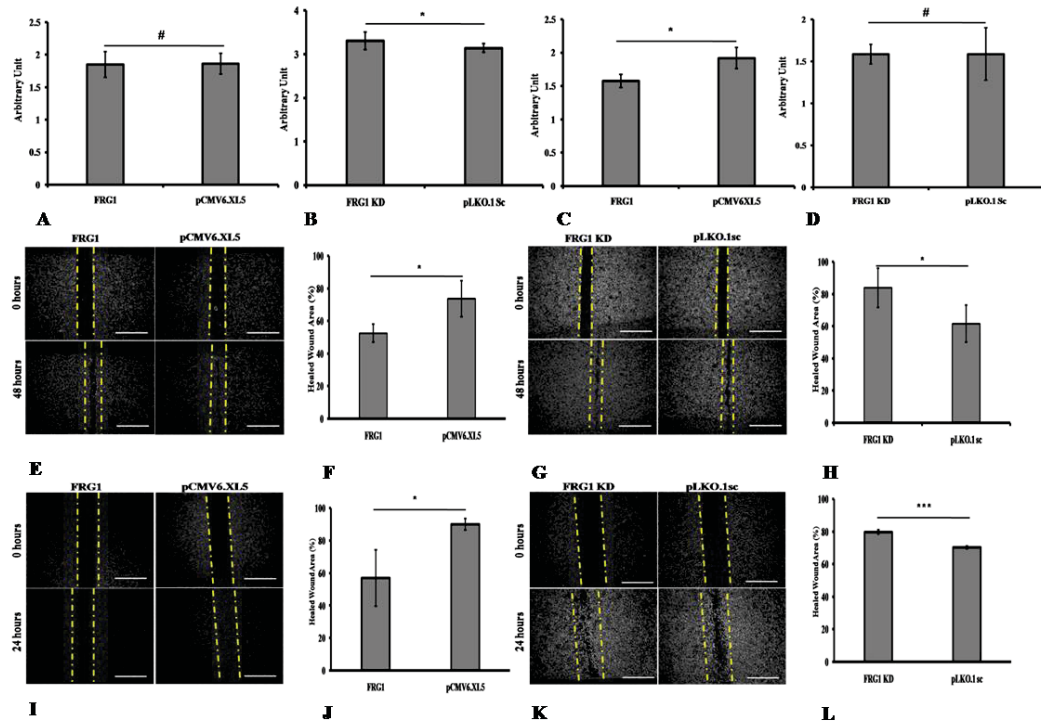


Figure (5.3.2): Effect of FRG1 expression on cell proliferation and scratch wound healing. A. Ectopic expression of FRG1 has no significant (p value = 0.91) effect on cell proliferation in DU145, compared to empty vector control. **B.** Measurement of cell proliferation in DU145, knockdown of FRG1 showing significant increase in cell proliferation (p value = 0.029), compared to scrambled vector control. **C.** Measurement of cell proliferation in PC3 with ectopic expression of FRG1, compared to empty vector control, showing significant reduction (p -value = 0.013). **D.** Quantitation of cell proliferation in PC3 with knockdown of FRG1, compared to scrambled vector control, showing no significant (p value = 0.97) effect. **E.** Representative images of scratch wound healing assay of DU145 cells, with ectopic expression of FRG1 and respective vector control. **F.** Graph of scratch wound healing assay of DU145 cells with ectopic expression of FRG1, showing 52 % reduced wound area, compared to empty vector control with 72 % reduced wound area (p value = 0.04). **G.** Representative Images of scratch wound healing assay of DU145 with FRG1 knockdown and respective scrambled vector control. **H.** Graph of scratch wound healing assay of DU145 cells with FRG1 knockdown showing 83 % reduced wound area, compared to scrambled vector control with 61 % reduced wound area (p value = 0.01). **I.** Representative images of scratch wound healing assay of PC3 cells with ectopic expression of FRG1 and respective vector control. **J.** Graph of scratch wound healing assay of PC3 cells with ectopic expression of FRG1, showing 57 % reduced wound area, compared to empty vector control with 90 % reduced wound are (p value = 0.03). **K.** Representative Images of scratch wound healing assay of PC3 with FRG1 knockdown and respective scrambled vector control. **L.** Graph of scratch wound healing assay of PC3 cells with FRG1 knockdown, showing 79 % reduced wound area, compared to scrambled vector control with 70 % reduced wound area (p value = 0.004). * \leq 0.05, *** $<$ 0.005, # $>$ 0.05

5.3.2.3. FRG1 Affects Prostate Cancer Cell Motility and Invasiveness:

Enhanced cell motility and invasiveness are important features of tumor progression. Therefore, to investigate the role of FRG1 in cell migration and invasion we performed scratch wound healing, transwell cell migration and matrigel invasion assays.

Wound healing was significantly (p value = 0.04) reduced in cells ectopically expressing FRG1, with 52 % area healed in FRG1 expression set compared to 72 % of empty vector, in DU145. In PC3 cell line, FRG1 expression led to 57 % area being healed, compared to 90 % of empty vector set (p value = 0.03) (Figure 5.3.2.E-F; Figure 5.3.2.I-J respectively). To confirm the findings, scratch wound healing assay was done in FRG1 knockdown set. Increased wound healing in FRG1 knockdown set was observed, compared to scrambled control vector set (83 % vs. 61 % respectively, p value = 0.01) in DU145. In PC3 cells, FRG1 knockdown led to 79 % reduced wound area compared to 70 % of scrambled vector set (p value = 0.004) (Figure 5.3.2.G-H; Figure 5.3.2.K-L respectively).

Further support was provided by transwell cell migration data, which was decreased in cells ectopically expressing FRG1, compared to empty vector control, in both DU145 (p value = 0.0106) and PC3 (p value = 0.036) cell lines (Figure 5.3.3.A-B; Figure 5.3.3.E-F respectively). This observation was reversed when FRG1 expression was silenced, in both DU145 (p value = 0.023) and PC3 (p value = 0.01) (Figure 5.3.3.C-D; Figure 5.3.3.G-H respectively). Ectopic expression of FRG1 led to significant reduction in cell invasion in both DU145 (p value = 0.005) and PC3 (p value = 0.028) cells (Figure 5.3.3.I-J; Figure 5.3.3.M-N respectively). FRG1 knockdown had opposite effect on cell migration, as FRG1 knockdown led to increase in cell invasion

in both DU145 (p value = 0.017) and PC3 (p value = 0.043) cells (Figure 5.3.3.K-L; Figure 5.3.3.O-P respectively). These results clearly indicate that FRG1 reduces cell migration and invasion in prostate cancer cells *in vitro*.

5.3.2.4. FRG1 Expression Level Dictates Expression of Various Cytokines and MMP1:

To identify the associated cytokines affected by FRG1 expression q-RT PCR analysis for 13 cytokines and 7 Matrix metalloproteinases was done (Table 4.6). Ectopic expression of FRG1 led to no significant change in expression of cytokine and matrix metalloproteinases in PC3 cells (Figure 5.3.5.A-B) but in DU145 ectopic expression of FRG1 led to reduction of PLGF (fold change ≤ 5 and p value ≤ 0.05) (. On the other hand, FRG1 knockdown showed significant change in expression of certain targets in cell line specific manner. FRG1 knockdown in DU145 led to significant increase in expression of GM-CSF, PLGF and MMP1 (fold change ≥ 1.5 and p value ≤ 0.05) (Figure 5.3.4.A). By FRG1 silencing in PC3 cells, expression of GM-CSF, MMP1, PDGFA and CXCL1 showed significant increase in expression by ≥ 1.5 fold (p value ≤ 0.05) (Figure 5.3.4.B). Here we can infer that FRG1 may affect proliferative, migratory and invasiveness properties of cells by modulating expression of above mentioned cytokines and MMPs.

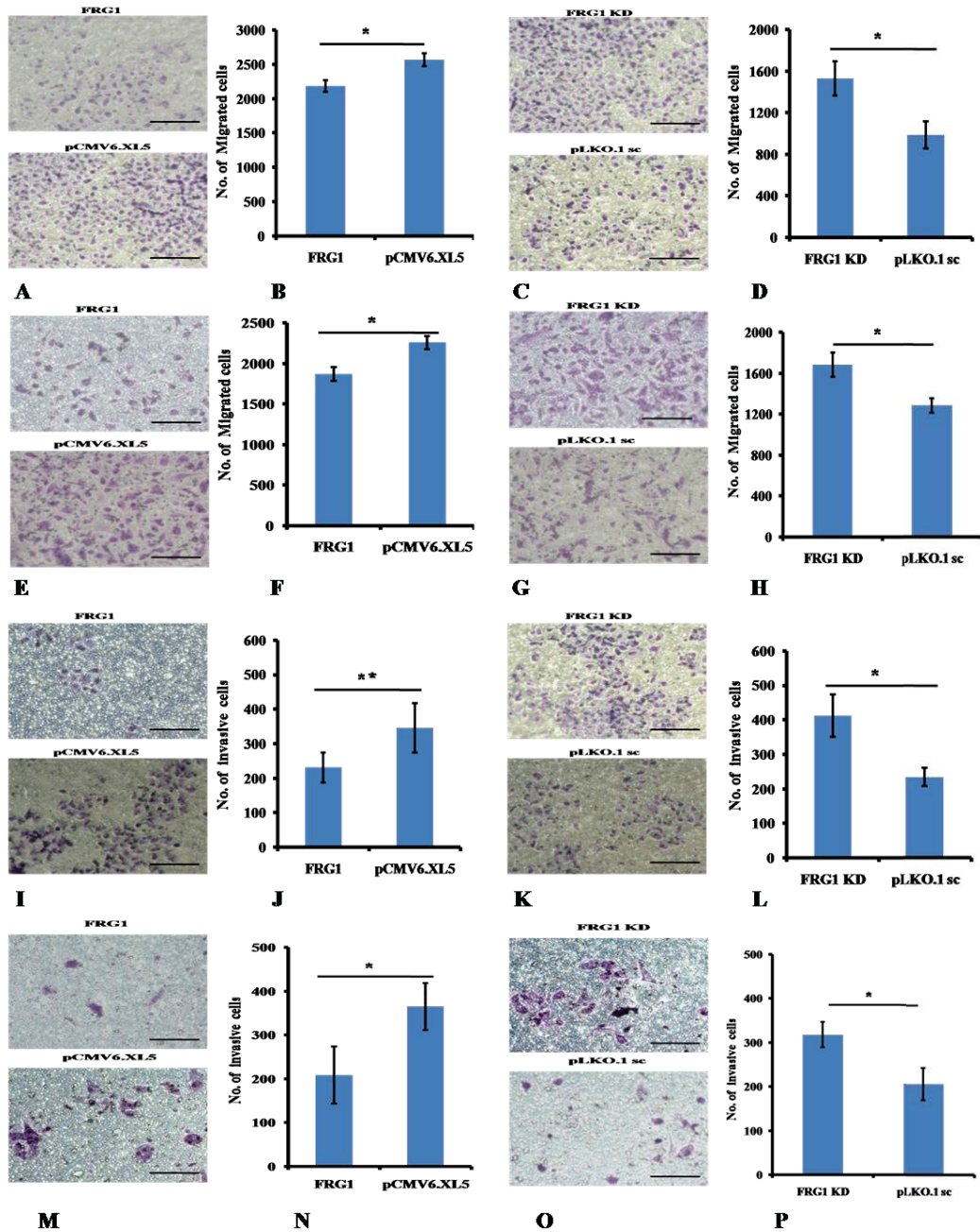


Figure (5.3.3): Effect of FRG1 expression on transwell migration and invasion. A. Representative images of transwell migration assay of DU145 cells with ectopic expression of FRG1 and respective vector control. B. Representative images of transwell migration assay of DU145 cells with FRG1 knockdown and respective scrambled vector control. C. Graphical representation of transwell migration assay of DU145 cells with ectopic expression of FRG1 (2183 ± 84), showing reduction in transwell migration, compared to empty vector control (2565 ± 93.7) (p value = 0.0106). D. Graph of transwell migration assay of DU145 cells with FRG1 knockdown (1532 ± 165), showing enhanced transwell migration, compared to scrambled vector control (987 ± 131) (p value = 0.023). E. Representative images of transwell migration assay of PC3 cells with ectopic expression of FRG1 and respective vector control. F. Representative images of transwell migration assay of PC3 cells with FRG1 knockdown and respective scrambled vector control. G. Graphical representation of transwell migration

assay of PC3 with ectopic expression of FRG1 (1532 ± 165), showing reduction (p value = 0.036) in transwell migration, compared to empty vector control (1869 ± 86.37). **H.** Graphical representation of transwell migration assay of PC3 cells with FRG1 knockdown (1685 ± 120.3), showing enhanced (p value = 0.01) transwell migration, compared to scrambled vector (1281 ± 71). **I.** Representative images of matrigel invasion assay of DU145 cells with ectopic expression of FRG1 and respective vector control. **J.** Representative images of matrigel invasion assay of DU145 with FRG1 knockdown and respective scrambled vector control. **K.** Graphical representation of matrigel invasion assay of DU145 cells with ectopic expression of FRG1 (231 ± 43.5) compared to empty vector control (346 ± 71.3) (p value = 0.005). **L.** Representative Graph of matrigel invasion assay of DU145 cells with FRG1 knockdown (412 ± 61.7) compared to scrambled vector control (234 ± 26.8) (p value = 0.017). **M.** Representative images of matrigel invasion assay of PC3 cells with ectopic expression of FRG1 and respective vector control. **N.** Representative images of matrigel invasion assay of PC3 with FRG1 knockdown and respective scrambled vector control. **O.** Representative graph of matrigel invasion assay of PC3 cells with ectopic expression of FRG1 (208.7 ± 65) compared to empty vector control (365 ± 53.2) (p value = 0.028). **P.** Representative graph of matrigel invasion assay of PC3 cells with FRG1 knockdown (318 ± 29) compared to scrambled vector control (206 ± 37) (p value = 0.043). * ≤ 0.05 , ** < 0.01 ,

5.3.2.5. FRG1 Silencing Enhances p38 MAPK Activation:

To identify effect of FRG1 expression on critical signaling pathways we checked the activation levels of ERK and p38 MAPK. FRG1 knockdown showed enhanced phosphorylation of p38 MAPK, in both DU145 (Figure 5.3.6.A) and PC3 (Figure 5.3.6.B). Total ERK level was increased during FRG1 knockdown in DU145 cells with mild increase in ERK phosphorylation in case of FRG1 knockdown in PC3 cells (Figure 5.3.6.B).

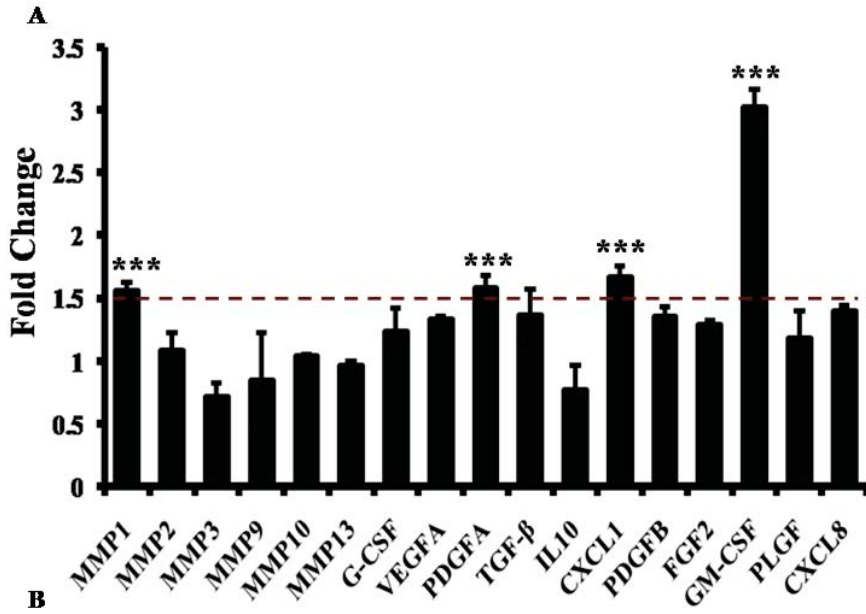
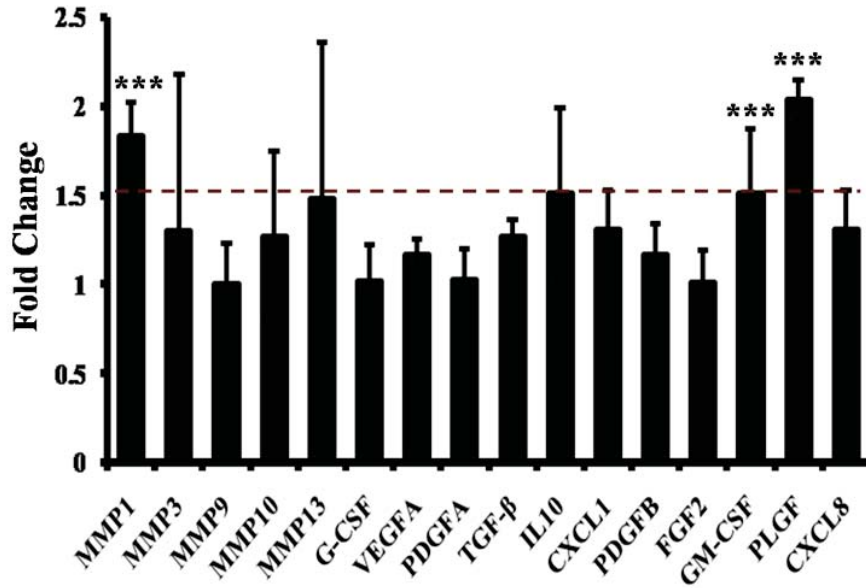
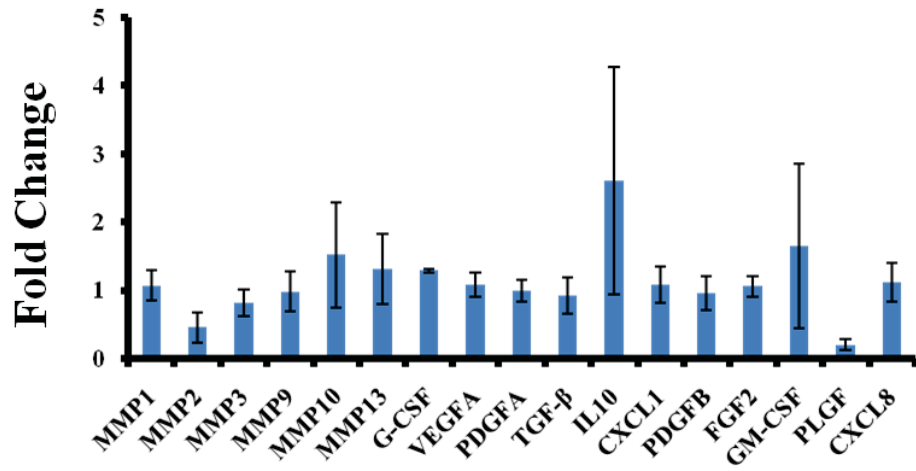
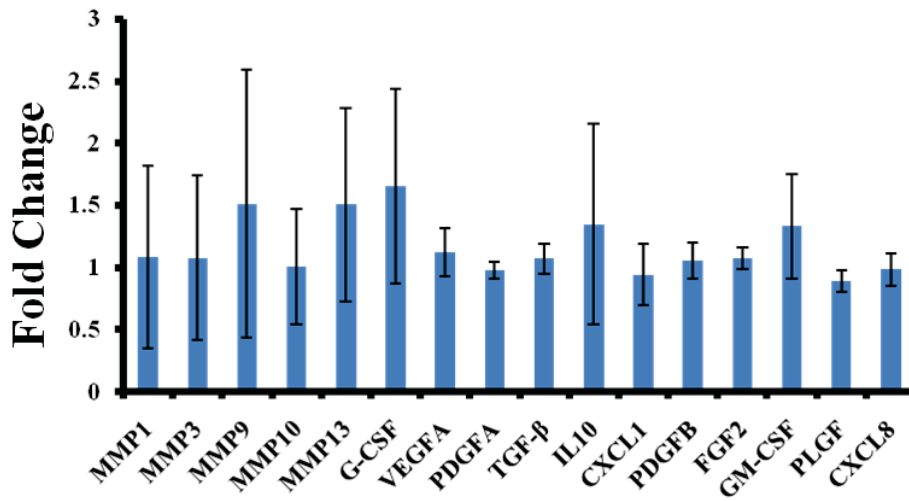


Figure (5.3.4): Expression analysis of listed cytokines and MMPs in prostate cancer cells during FRG1 knockdown. **A.** q-RT PCR expression analysis of listed genes in (Table 4.6) in DU145 cells transfected with FRG1 silencing vector compared to scrambled vector control, **B.** q-RT PCR Expression data of listed gene in (Table 4.6) in PC3 cells knockdown for FRG1 versus scrambled vector control. Dotted line represents 1.5-fold cut off and p value = *** < 0.005.



A



B

Figure (5.3.5): Expression analysis of listed cytokines and MMPs in prostate cancer cells during ectopic expression of FRG1.A.q-RT PCR expression analysis of genes listed in (Table 4.6) in DU145 cells with ectopic expression of FRG1 compared empty vector control **B.** q-RT PCR expression analysis of genes listed in (Table 4.6) in PC3 cells with ectopic expression of FRG1 compared empty vector control.

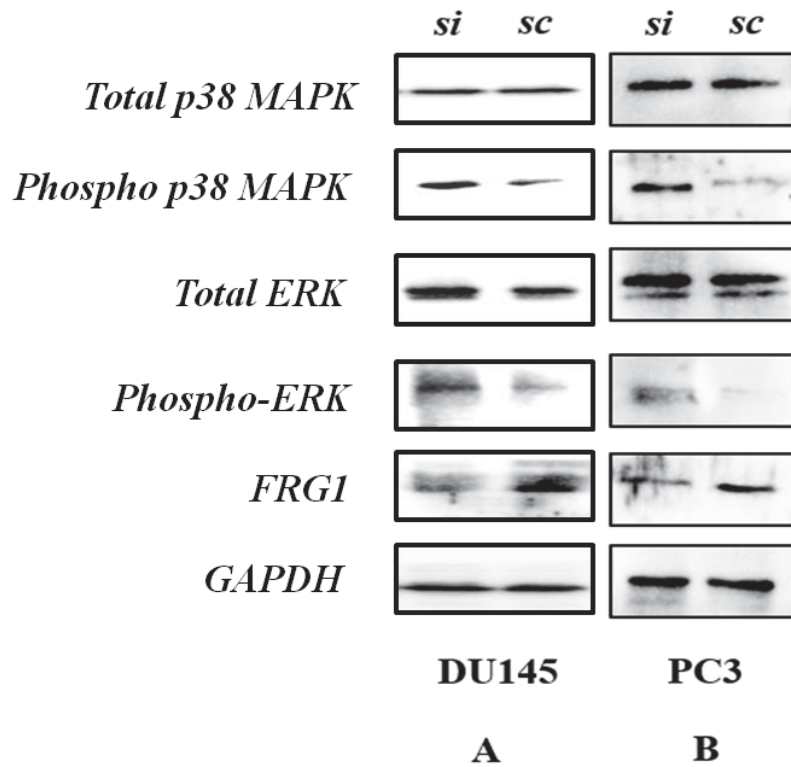


Figure (5.3.6): Reduced FRG1 expression enhances p38 MAPK phosphorylation. **A.** Panel of blots showing enhanced p38 MAPK phosphorylation with FRG1 knockdown in DU145 cells followed by increase in total ERK levels. **B.** Panel of blots showing enhanced p38 MAPK phosphorylation with FRG1 knockdown in PC3 cells with mild increase in phospho ERK levels. si represents protein lysate from FRG1 knockdown cells and sc represents cells expressing scrambled vector control.

5.3.3. Discussion:

Studies about FRG1 are primarily focused on FSHD pathophysiology and muscle development [18, 74]. Functional studies have shown FRG1 to be actin bundling and RNA binding protein [71, 76], accordingly claiming that FRG1 localizes in both, cytoplasm and nucleus. Our study first time revealed FRG1 expression level and localization in prostate cancer tissue; showed the significant loss of FRG1 expression in tumor tissues. FRG1 expression was predominantly cytoplasmic but sporadic cases with nuclear localization were also observed. FRG1 levels regulate angiogenesis during *Xenopus* development by affecting *dab2* levels [16]. In our study, no

significant association between FRG1 levels and neo-angiogenesis was observed. Involvement of FRG1 in angiogenesis remains unclear as FSHD patients with retinal vasculature abnormalities, showed no change in FRG1 expression [17]. Thus, a well stratified and higher sample size could provide a more conclusive picture regarding localization and role of FRG1 in tumor angiogenesis. Since our study is first to elucidate effect of FRG1 on tumor cell lines, we had no idea regarding behavior of tumor cells with altered FRG1 expression. FRG1 expression increases during FSHD phenotype and our observation in cancer patient showed reduction of FRG1 levels compared to uninvolved tissue. Therefore, to check effect of FRG1 expression in prostate cancer cell lines we decided to proceed with ectopic expression and knockdown of FRG1 in both PC3 and DU145 cells. Our study for the first time demonstrates the effect of FRG1 expression on cell properties *viz.* proliferation, migration and invasion, which are important for tumorigenesis. Prior reports of FRG1 affecting cellular migration, was of myoblast cells in *Xenopus* development, where FRG1 over expression enhanced migration and invasion [18]. On the contrary, in our data FRG1 knockdown enhanced cell migration in prostate cancer cells *in vitro*. Which is supported by prior study, where reduced expression of FRG1 was observed in breast cancer cells with higher migratory levels, compared to average non-migratory breast cancer cells [20]. This observation suggests role of FRG1 in migration but in opposite way, indicating that FRG1 function may vary in tumor and developmental set up. Earlier reports have also shown that FRG1 over-expression reduces cell proliferation of mice myoblasts [84]. With varying effect of FRG1 levels in these cell types an argument can be placed that FRG1 may have discrete effect on various cell types and may dictate cellular properties based on the stromal components.

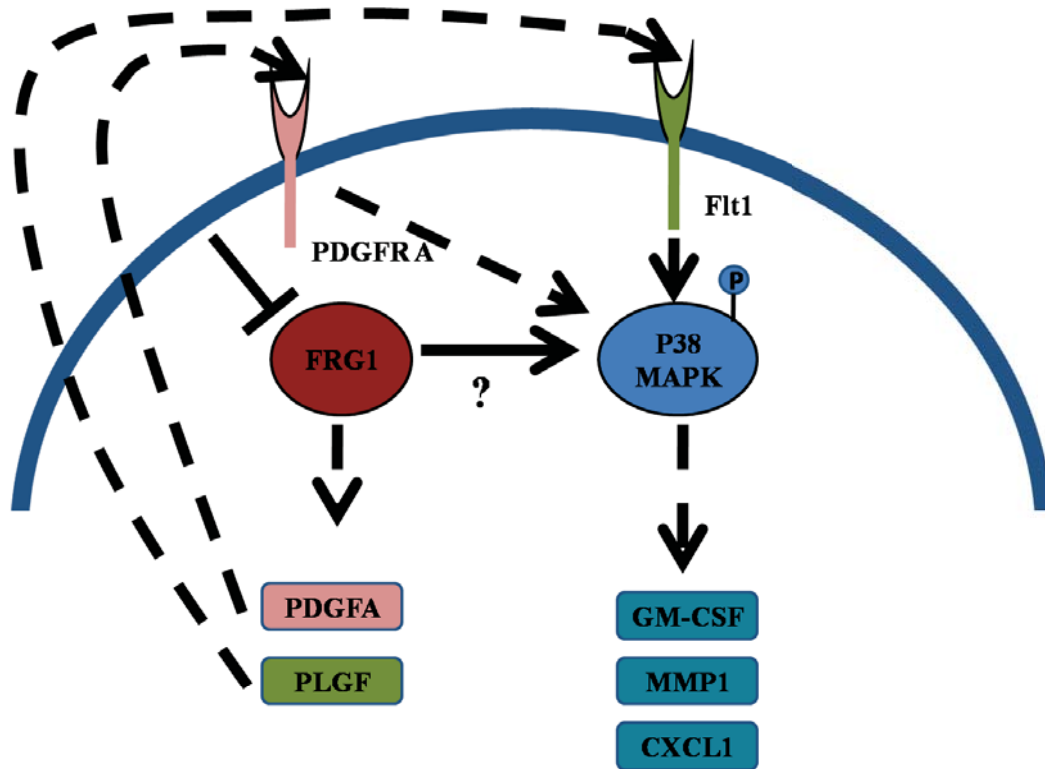


Figure (5.3.7): Model for possible molecular interaction during FRG1 knockdown in prostate cancer cells. The model suggests FRG1 knockdown in prostate cancer cells leads to activation of p38 MAPK pathway via enhanced expression of mitogens (PDGFA, PLGF). Activation of p38 MAPK might lead to increased expression of GM-CSF, MMP1, and CXCL1, which in turn promotes cell migration, invasion and proliferation. Model also speculates that FRG1 may directly regulate p38 MAPK activation but the mechanism is unknown.

FRG1 over expression had no effect on expression levels of cytokines and MMPs except for PLGF in DU145 cells, but FRG1 knockdown, in both the prostate cancer cell lines, led to enhanced expression of MMP1, GM-CSF, PLGF, PDGFA and CXCL1 in DU145. MMP1 and GM-CSF were up regulated in both DU145 and PC3 cell lines. MMP1 belongs to collagenase family and promotes tumor progression and metastasis [126]. FRG1 knockdown led to enhanced MMP1 expression, which can be very well related with reduced expression of FRG1 in tumor tissue. It is possible that reduction in FRG1 expression leads to increased expression of MMP1, giving it tumorigenic property. GM-CSF production has been reported in both DU145 and PC3

cell lines [127] . In various tumors, it shows antagonistic effects on immune system [128]. There is no report on tumor promoting activity of GM-CSF till date, in prostate cancer. Thus, a proper understanding of FRG1 and GM-CSF loop is required to delineate role of FRG1 in prostate cancer cell migration and invasion.

PLGF is a member of VEGF family, its inhibition in the stromal components reduces growth of prostate tumor, in mice xenograft model [129]. CXCL1 is tumor-promoting cytokine with enhanced expression in high-grade prostate cancer, promoting tumor invasion and migration [130, 131]. PDGFA levels along with PDGFR- α , is increased in carcinoma, compared to normal prostate epithelium and stroma, promoting tumor progression [132].

FRG1 knockdown led to activation of p38 MAPK. p38 MAPK activation has been associated with tumor progression in various tumor types [133]. In prostate cancer p38 MAPK activation has been shown through TNF α and IL6 [133, 134]. We are first time reporting the involvement of FRG1 in p38 MAPK mediated signaling, which can be very well connected with our expression data on various cytokines and the cell based assays. We found that GMCSF was up regulated in both DU145 and PC3 cell lines, with reduced FRG1 expression; earlier study has shown that both these cell lines are positive for GM-CSF receptor [135]. Treatment of DU145 and PC3 cells with GM-CSF has been shown to enhance colonogenicity and chemo taxis [135]. Accordingly, up regulation of GM-CSF during FRG1 knockdown in prostate cancer cells might be one of the factors affecting cell migration and invasiveness. Prior studies in human monocytes and bronchial epithelial cells have shown that p38 MAPK activation regulates GM-CSF production [136]. However, we could not find any reports suggesting p38 MAPK activation by GMCSF. TNF α based activation of

p38MAPK regulates expression of CXCL1 in vascular endothelial cells [137]. TNF α regulates GM-CSF levels in bronchial epithelial cells via p38 MAPK activation [136]. Additionally, activation of p38 MAPK also induces expression of MMP1, promoting invasiveness in cell lines, as observed in both DU145 and PC3 cells [138, 139]. PDGFA signaling is known to activate p38 MAPK in porcine aortic endothelial cells, leading to enhanced cellular migration [140]. Prior reports suggest that PC3 cells but not DU145, is positive for PDGFA receptor [141], which can be associated with activated p38 MAPK via enhanced PDGFA expression. Similar to PDGF signaling, PLGF also activates p38 MAPK and is known to enhance cellular migration in colon cancer cells and leukemia [142]. PLGF binds to Flt 1 receptor and exert activation of p38 MAPK in DU145 cells [143]. Thus, p38 MAPK activation in DU145 and PC3 might be induced via independent mechanisms.

However, there is an impending question, regarding the mechanism of p38 activation during FRG1 knockdown. With no prior reports of association of FRG1 with above-mentioned molecules, which regulate tumor progression, further mechanistic study needs to be done to obtain a clear picture of FRG1's role in prostate tumor progression.

4. MATERIALS AND METHODS

4. MATERIALS AND METHODS:

4.1. Oncomine Analysis:

Oncomine cancer microarray database ([http:// www.oncomine.org](http://www.oncomine.org)) [88] was used to determine gene expression of FRG1 in various tumor types. For analysis, we set thresholds of p value ≤ 0.05 and fold change ≥ 1.5 and, comparisons were drawn between tumor and normal group.

4.2. Kaplan Meier Plotter Analysis:

Kaplan Meier plotter (<http://kmplot.com/analysis>) [89] analysis was done to determine the prognostic value of FRG1 gene expression. Overall survival (OS) was analyzed in Breast (N = 4142), Ovarian (N = 1648), Lung (N = 2437) and, Gastric (N = 1065) cancer. Patients were divided into two groups, FRG1 high and FRG1 low, based on gene expression. Comparative survival analysis was done between both the groups. To ascertain the effect of FRG1 expression on survival, Hazard Ratio (HR) with 95% CI, was calculated, along with the log rank p value. p value of ≤ 0.05 , was considered to be significant.

4.3. Immunohistochemistry:

4.3.1. Reagents for Immunohistochemistry: Buffered Formalin (10 % Formalin; 0.025 M sodium dihydrogen phosphate; 0.046 M disodium hydrogen phosphate in distilled water), Poly-L-Lysine (Sigma), Acetone (Merck), Xylene (Merck), Ethanol (Merck), Fibrinogen (Instrumentation laboratory), Paraffin (Fischer scientific), Haematoxylin (HiMedia), Eosin (HiMedia), Tris Buffered Saline pH 7.2 (0.05 M Tris, 0.8 % NaCl), Tris-EDTA buffer pH 9 (10 mM Tris, 1 mM EDTA), EnVision Flex HRP (Dako), EnVision Flex DAB + Chromogen (Dako), EnVision Flex Peroxidase

Blocking Reagent (Dako), EnVision Flex Substrate Buffer (Dako), DPX mountant (Fisher scientific).

4.3.2. Poly-L-Lysine Coating of Slides: Glass slides were washed with detergent followed by 1 % acetic acid ethanol solution. Slides are dried completely prior to Poly-L Lysine coating using hot air oven until all traces of liquid disappears. Washed slides are immersed into 0.01 % Poly-L-Lysine solution for 20 minutes followed by two dips of distilled water. Slides were dried at 37⁰ Celsius overnight prior to use, for immunohistochemistry.

4.3.3. Preparation of Control Cell Block: HeLa cells were harvested from a T25 flask. Harvested cells were mixed with fibrinogen at 1:2 ratios and incubated at 37⁰ Celsius for 1 minute. Cell coagulant was fixed in 10 % buffered formalin followed by dehydration using alcohol gradient from 50 % - 100 %. Dehydrated cell coagulant was washed with acetone for 30 minutes followed by two rounds of incubation in xylene for 1 hour each. Cell coagulant was incubated in paraffin at 36⁰ Celsius for 1 hour and paraffin embedding was done.

4.3.4. Immunohistochemistry Protocol: FFPE blocks of various tumor types were identified from tissue archives of SRL Diagnostics Bhubaneswar. Ethical clearance for the study was taken from Institutional Ethics Committee (BioEthics # MD-1), NISER, Bhubaneswar. Information regarding list of antibodies used for immunohistochemistry along with protocols and clones is given in the (Table 4.1). 4 µm thick sections of FFPE blocks were cut and placed on Poly-L-Lysine coated slides. Sections were deparaffinized and rehydrated using alcohol gradient from 100 % to 50 %. Endogenous Peroxidase activity of the rehydrated sections was blocked using EnVision Flex Peroxidase Blocking Reagent by incubating at room temperature for 10

minutes. Primary antibody incubation was done as per the conditions given in table 4.1, followed by incubation with EnVision Flex HRP secondary antibody for 30 minutes. EnVision Flex DAB + Chromogen and EnVision Flex Substrate Buffer was applied for 5 minutes for development of color, proceeded by counter stain with haematoxylin HeLa cell block was used as positive control for anti-FRG1 antibody and mouse IgG isotype was used as negative control.

4.3.5. Immunohistochemistry Scoring: Immunohistochemistry (IHC) scoring was performed by two independent pathologists. FRG1 expression levels were scored in paired tumor tissue and uninvolved (normal) tissue, for intensity of staining and percent positive cells. Intensity of staining was scored in a scale of 0-3; where 0 = negative, 1 = weak, 2 = moderate and, 3 = strong. Percent positivity of cells was scored in a scale of 0-5; where 0 = negative, 1 < 1 %, 2 = 1 – 10 %, 3 = 11 – 33 %, 4 = 34 – 66 % and, 5 ≥ 67 %. To calculate FRG1 expression levels, Allred scores were derived, using the following formula; **Allred score = Staining intensity + Percent positive cells**. Allred scores were categorized in Low = 1 – 2, Moderate = 3 – 6, High = 7 – 8 [90]. Accordingly FRG1 expression levels were categorized into these three groups, in both tumor and uninvolved tissues.

4.3.6. Micro-Vessel Density Analysis: CD31 a known vascular marker was used to stain blood vessel. Micro vessel density (MVD) analysis was performed as per Weidner et al. [6]. Three highly vascularized areas were identified at low magnification (40 X) and micro vessels at these hotspots were counted at higher magnification (200 X). The hotspot with highest number of micro vessel was considered as MVD count.

Table (4.1): List of Immunohistochemical Markers and Protocols

IHC Markers	Antibody Clone	Vendor	Dilution	Antigen Retrieval Buffer	Incubation Time for the Antibody	Antigen Retrieval Instrument	Detection Kit
CD31	JC70A	Dako, USA	Prediluted	High pH	60 minutes	Microwave	Envision+ System-HRP Labeled Polymer-Anti-mouse
FRG1	N/A	Biorbyt, UK	1:100	High pH	60 minutes	Microwave	Envision+ System-HRP Labeled Polymer-Anti-mouse

4.4. Plasmid Preparation:

4.4.1. Reagents for Plasmid Preparation: LB Agar (Miller) (HiMedia), L B Broth (Miller) (HiMedia), Ampicillin (100 mg/ml in autoclaved Mili Q water) (Sigma), Kanamycin (50 mg/ml in autoclaved Mili Q water) (Sigma), Ethanol (Merck), Isopropanol (Sigma), Plasmid mini kit (Qiagen), Plasmid midi kit (Qiagen), PIPES (0.5 M in distilled water, pH 6.7) (Sigma), KOH (Sigma), MnCl₂.4H₂O (HiMedia), CaCl₂.2H₂O (HiMedia), KCl (Sigma), DMSO (MP Biomedicals), Glycerol (50 % in autoclaved Mili Q water) (HiMedia), Inoue Buffer (55 mM MnCl₂.4H₂O, 15 mM CaCl₂.2H₂O, 250 mM KCl, 10 mM PIPES in autoclaved Mili Q water).

4.4.2. Plasmids: FRG1 coding sequence, cloned into pCMV6.XL5 mammalian expression vector, was procured from Origene, along with pCMV6.XL5 empty vector. We procured FRG1 shRNA- pLKO.1 vector from Sigma, along with scrambled shRNA in pLKO.1 vector.

4.4.3. Preparation of *E. coli* (DH5 α) Competent Cells: DH5 α ultra competent cells were prepared as per Inoue method [91]. Single colony of DH5 α grown in LB agar

plate for 16 hours at 37⁰ Celsius, was picked and transferred to 5 ml of Lysogeny Broth (LB) and incubated for 16 hours at 37⁰ Celsius. 0.5 ml of starter culture was transferred to 250 ml of LB Broth and incubated at 18⁰ Celsius and 125 rpm. Culture was grown until the OD reached 0.55, once the desired OD was obtained; culture flask was transferred to ice and incubated for 10 minutes. Cells were harvested by centrifugation at 2,500 g for 10 minutes at 4⁰ Celsius in a 50 ml falcon tube. Media was completely removed and cells were re-suspended gently in 80 ml Inoue buffer. Cells were further centrifuged at 2,500 g for 10 minutes at 4⁰ Celsius, supernatant was discarded and pellet was re-suspended gently in 20 ml Inoue buffer. 1.5 ml of DMSO was added to the bacterial cell suspension followed by 10 minutes incubation in ice. To make aliquots for future use, 50 µl of suspension was added to chilled 1.5 ml micro centrifuge tubes. The micro centrifuge tubes were snap chilled in liquid nitrogen and moved to -80⁰ Celsius freezer.

4.4.4. Transformation Protocol: Transformation was performed as per heat shock method [92]. DH5 α competent cells were taken out from -80⁰ Celsius freezer, kept in ice and incubated for 10 minutes after adding 50 ng of plasmid DNA. Heat shock treatment was given to the bacterial cells by incubating in a circulating water bath at 42⁰ Celsius for 45 seconds and immediately transferred on ice for 2 minutes. 1 ml of warm LB broth was added to the transformed cells and incubated for 20 minutes, at 37⁰ Celsius and 225 rpm. 100 µl of transformed cell suspension was plated to LB agar plate with respective antibiotic for positive clone selection.

4.4.5. Plasmid Purification Protocol: Plasmid purification was done at miniprep and midiprep scales. 5 ml culture was set up for miniprep plasmid preparation and plasmid purification was done using QIAprepSpin Miniprep Kit (Qiagen) as per

manufacturer's instructions (refer to appendix 8.1). 100 ml of culture was prepared for midiprep plasmid preparation; plasmid purification was done using Qiagen Plasmid Midi Kit (Qiagen) as per the maker's protocol (refer to appendix 8.2).

4.4.6. Preparation of Glycerol Stock: Confirmed positive clones were grown in 2 ml LB broth using appropriate antibiotic, for 12 hours. 2 ml of 50 % glycerol was added to the culture and an aliquot of 1 ml mix was transferred to each cryovial. The cryovials were stored at -80⁰ Celsius freezer until use.

4.5. Cell Culture:

4.5.1. Reagents for Cell Culture: DMEM (Pan Biotech), HiGlutaXL RPMI1640 (HiMedia), HiEndoXl Endothelial Cell Growth Medium (HiMedia), PBS pH 7.4 (HiMedia) DPBS pH 7.4 (Pan Biotech), Trypsin-EDTA (Pan Biotech), Fetal Bovine Serum (Pan Biotech), Penicillin Streptomycin (Pan Biotech), Amphotericin B (HiMedia), Trypan-Blue (0.4 % in PBS) (HiMedia), Puromycin (1 mg/ml in autoclaved Mili Q water) (MP Biomedicals), DMSO (MP Biomedicals), Lipofectamine 3000 (Invitrogen).

4.5.2. Preparation of Media: DMEM and RPMI1640 were supplemented with 100 units/ml of Penicillin, 50 µg/ml Streptomycin, 0.25µg/ml Amphotericin B and 10 % FBS. Complete media was filtered through 0.2 µm vacuum driven filter unit (Biofil); thereafter it was stored at 4⁰ Celsius. HiEndoXL endothelial cell growth medium was constituted by mixing part A and part B components. Complete endothelial cell growth medium was filtered through 0.2 µm vacuum driven filter unit (Biofil) and stored at 4⁰ Celsius. Freezing medium was prepared for cryopreservation of cells, by adding 10 % DMSO to FBS.

4.5.3. Cell Culture Protocol: HEK293T cell line is a derivative of Human Embryonic Kidney 293 cells with SV40 T antigen. HEK293T cell line was procured from National Centre for Cell Science (NCCS) and maintained in complete DMEM. Human Umbilical Vein Endothelial Cells, which are isolated from endothelium of veins of umbilical cord, were procured from HiMedia, Mumbai. HUVECs were maintained in complete HiEndoXL endothelial cell growth medium. DU145 cell line is derived from metastatic lesion of primary adenocarcinoma prostate, at central nervous system of 69 year old Caucasian male. DU145 was obtained from Dr. Rajeeb Swain's Lab from Institute of Life Sciences, Bhubaneswar and was maintained in complete DMEM. PC3 cell line was established from grade IV adenocarcinoma bone metastatic lesion from a 62 year old Caucasian male and was procured from NCCS, Pune. PC3 cell line was maintained in complete RPMI1640. MCF7 cell line is derived from pleural effusion of malignant adenocarcinoma of breast, from 69 year old Caucasian female. MCF7 cell line was obtained from NCCS, Pune and was maintained in complete DMEM. All cell lines were grown at 37⁰ Celsius and 5 % CO₂, for various experiments.

4.5.4. Revival of Cells: Frozen vial of cell line was retrieved from liquid nitrogen dewar and placed in water bath maintained at 37⁰ Celsius. Thawed cell suspension was transferred to pre warmed complete media in a 15 ml centrifuge tube. Cell suspension was centrifuged at 200 g for 5 minutes. Thereafter supernatant was discarded and pellet was resuspended into 6 ml pre-warmed complete media and transferred to a T-25 cm² cell culture flask and incubated, at 37⁰ Celsius and 5 % CO₂.

4.5.5. Subculture, Splitting and Trypsinization of Cells: Splitting or sub culture of cell lines/ primary cells was done once cells reached at confluency of 80 %. Cells were washed twice with DPBS, subsequently trypsin-EDTA was added to cell culture

flasks and incubated at 37⁰ Celsius until cells detach from surface. Complete medium was added to neutralize trypsin activity; acquired cell suspension was centrifuged at 200 g for 5 minutes. Supernatant was discarded and pellet was re-suspended in complete medium. Total viable cell count was determined using trypan-blue stain in haemocytometer and required numbers of viable cells were seeded into culture plates. Culture plates were incubated into humidified incubator, at 37⁰ Celsius and 5 % CO₂.

4.5.6. Cell Freezing and Cryopreservation: Cells with around 70 – 80 % confluency were washed twice with PBS and trypsinized. Total cell count was determined and cells were centrifuged at 200 g for 5 minutes. Supernatant was discarded and pellet was re-suspended in freezing medium at cell concentration of 1 x 10⁶ cells per ml. One ml of suspension was dispensed into each cryovial and transferred into – 1⁰ Celsius per minute cooler and kept - 80⁰ Celsius freezer. 24 hours later vials were transferred into liquid nitrogen dewar for long term storage.

4.5.7. Transient Transfection: To identify effect of FRG1 expression on various cell lines transient transfection was performed in HEK293T, DU145, PC3 and MCF7 cell lines for FRG1-pCMV6.XL5 or its empty vector pCMV6.XL5. 0.5 x 10⁶ cells were seeded in a 6 well plate; transfection was carried out after 24 hours of seeding as per the instructions provided in the product manual of Lipofectamine 3000 (refer to appendix 8.3). Transient transfections were also performed for PC3 cell line for FRG1 knockdown using FRG1sh-pLKO.1 vector along with pLKO.1-scrambled vector control (refer to appendix 8.3).

4.5.8. Stable Transfection: Stable line was prepared to determine effect of FRG1 knockdown (FRG1sh-pLKO.1) along with scrambled vector control (pLKO.1-scrambled) in HEK293T, DU145 and MCF7 cell lines. Cells were transfected as per

the manufacturer's 3000 (refer to appendix 8.3) for all three cell lines cells were subjected to antibiotic selection by adding 0.5 µg/ml puromycin in the growth medium after 48 hours. Stable clones were selected at 2 µg/ml of puromycin and expression levels were verified by western blot.

4.6. Cell Proliferation Assay:

4.6.1. Reagents for Cell Proliferation Assay: CellTiter 96 AQueous One solution Reagent (Promega).

4.6.2. Protocol for Cell Proliferation Assay in Transiently Transfected Cells: 2×10^3 cells were seeded into individual wells of 96 well plates. Transfections were performed (refer to section 4.5.7) and transfection mix was replaced after six hours with 5 % serum containing medium. Cells were grown for 96 hours and replaced with 100 µl of fresh medium prior to addition of 20 µl CellTiter 96 AQueous One solution reagent. Cells were incubated for two hours after addition of CellTiter 96 AQueous One solution reagent and absorbance was measured at 490 nm wavelength in Bio-rad iMark Microplate absorbance reader (Bio-rad). Experiments were performed three times with nine replicates in each group.

4.6.3. Protocol for Cell Proliferation Assay in Stable Cells: 3×10^3 cells were seeded in a 96 well plate. 24 hours after seeding, the growth medium was replaced with 5 % serum containing growth medium, subsequently cells were grown for 96 hours in 5 % serum containing growth medium. 96 hours later cells were replenished with 90 µl fresh medium followed by addition of 20 µl CellTiter 96 AQueous One solution reagent. After two hours of incubation absorbance was measured at 490 nm wavelengths in Bio-rad iMark Microplate absorbance reader (Bio-rad). Experiments were performed three times with nine replicates in each group.

4.6.4. Protocol for Cell Proliferation Assay in HUVECs: 5×10^3 HUVECs were seeded in 96 well plates. 24 hours after seeding cells media was replaced with conditioned medium obtained from transfected HEK293T. HUVECs were grown for 96 hours in conditioned media and henceforth replaced with 100 μ l fresh medium along with 20 μ l CellTiter 96 AQueous One solution reagent. Plates were incubated for two hours followed by measurement of absorbance at 490 nm wavelength using Bio-Rad iMark Microplate absorbance reader (Bio-Rad). Experiments were performed three times with nine replicates in each group.

4.7. Scratch Wound Healing Assay:

4.7.1. Reagents for Scratch Wound Healing Assay: Phosphate Buffered Saline (pH 7.4) (HiMedia).

4.7.2. Protocol for Scratch Wound Healing Assay for Transiently Transfected Cells: 0.25×10^6 cells were seeded in a 6 well plate. 24 hours after seeding, cells were transfected and grown for 48 hours. Thereafter, scratch was made using a P200 tip and cells were washed with PBS. Cells were grown in reduced serum medium (2 % FBS) and images of scratch wound were taken at 0, 24 and 48 hours for each cell line, depending on the wound closure speed. Imaging was done under Primovert inverted microscope (Ziess). Cell migration was analyzed using NIH ImageJ software. The experiments were conducted in triplicates.

4.7.3. Protocol for Scratch Wound Healing Assay of Stable Cells: 0.5×10^6 cells were seeded in a 6 well plate, a scratch was made with P200 tip after cells formed a fully confluent monolayer, which was subsequently washed with PBS. Images of scratch were taken at 0, 24 and 48 hours for each cell line, grown in reduced serum

medium (2 % FBS), under Primovert inverted microscope (Zeiss). Cell migration was analyzed using NIH ImageJ software. The experiments were conducted in triplicates.

4.8. Transwell Migration Assay:

4.8.1. Reagents for Transwell Migration Assay: 8 μm pore size 12 well plate transwell growth chambers (Milipore), Methanol (Merck), Giemsa (Fisher scientific), PBS (pH-7.4) (HiMedia).

4.8.2. Transwell Migration Assay Protocol for Cell lines: 2×10^4 cells (transfected transiently or stable lines) suspended in 500 μl serum free medium, were seeded in the 8 μm pore size transwell growth chamber. Prior to addition of cells, one ml complete medium was added in the lower chambers of the well plates. The plates were incubated at 37⁰ Celsius and 5 % CO₂. After 24 hours of incubation, media was removed from transwell inserts and washed with PBS twice, afterwards cells were fixed and permeabilized by adding 200 μl of methanol and incubated at 4⁰ Celsius for 20 minutes. Following the incubation, inserts were retrieved and cells were washed with PBS twice. 300 μl of Giemsa stain was added to the washed inserts and incubated in dark for 15 minutes at room temperature. Further, cells were washed with PBS and the upper layer of cells was removed using a cotton swab. Imaging was performed using CKX41 inverted microscope and the cells were counted in five different view fields, using NIH ImageJ software. The experiment was conducted in triplicate.

4.8.3. Transwell Migration Assay Protocol for HUVECs: 0.2×10^6 HEK293T cells transfected with FRG1 over expression vector along with empty vector control was grown in a 12 well plate. 36 hours after transfection of HEK293T, 2×10^4 HUVECs were seeded in the upper chamber of the transwell growth inserts. The plates were

incubated for 24 hours at 37⁰ Celsius and 5 % CO₂. Further, media was removed from the inserts and washed with PBS, which was followed by addition of 300 µl methanol for permeabilization and fixation of the cells. Inserts were washed with PBS and incubated in 200 µl of Giemsa stain for 15 minutes. Inserts were washed with PBS and cells at the upper layer were removed by cotton swab. Imaging was performed using CKX41 inverted microscope (Olympus) and the cells were counted in five different view fields at 10 X magnification, using NIH ImageJ software. The experiment was conducted in triplicate.

4.9. Matrigel Invasion Assay:

4.9.1. Reagents for Matrigel Invasion Assay: Growth Factor Reduced Matrigel (Corning), 8 µm pore size 12 well plate transwell growth chambers (Milipore), Methanol (Merck), Giemsa (Fisher scientific), PBS (pH 7.4) (HiMedia), DMEM (Pan Biotech).

4.9.2. Matrigel Invasion Assay Protocol: Growth factor reduced matrigel was thawed and diluted in DMEM with final protein concentration of 0.5 mg/ml. 100 µl diluted matrigel was added to transwell inserts and incubated at 37⁰ Celsius for two hours. Transiently transfected and stable cells were harvested and cell count was done. 2 x 10⁴ cells suspended in 500 µl of serum free medium were seeded into the chamber of transwell growth inserts; prior to that, 1 ml of complete media was dispensed into the lower chamber. The plates were incubated for 24 hours at 37⁰ Celsius and 5 % CO₂. Media from the insert was removed and washed with PBS; cells were fixed and permeabilized by addition of 300 µl of methanol with incubation at 4⁰ Celsius for 20 minutes. Inserts were washed with PBS and stained with Giemsa for 15 minutes, in dark. Inserts were washed with PBS and cells at the upper layer were removed by

cotton swab. Imaging was performed using CKX41 inverted microscope (Olympus) and the cells were counted in five different view fields, using NIH ImageJ software. The experiments were conducted in triplicates.

4.10. Matrigel Tubule Formation Assay:

4.10.1. Reagents for Matrigel Tubule Formation Assay: Matrigel (Corning), PBS (HiMedia).

4.10.2. Matrigel Tubule Formation Assay Protocol: Matrigel was thawed overnight at 4⁰ Celsius, following which, 50 µl of matrigel was plated into individual wells of a 96 well plate. Plate was incubated for 1 hour at 37⁰ Celsius to allow the matrigel to solidify. HUVECs were harvested from T75 flask and re-suspended in conditioned media; subsequently 5 x 10³ cells in 100 µl of conditioned medium were seeded into the matrigel coated wells and incubated at 37⁰ Celsius and 5 % CO₂. Images were acquired after six hours of incubation using a CKX41 inverted microscope (Olympus) at 4X magnification. Image analysis was performed using angiogenesis analyzer plugin in NIH ImageJ software.

4.11. Preparation of Cell Lysate:

4.11.1. Reagents for Preparation of Cell Lysate: RIPA lysis buffer (25 mM Tris-HCl pH 7.6, 150 mM NaCl, 1 % NP-40, 1 % Sodium deoxycholate, 0.1 % Sodium dodecyl sulphate) (Thermo), SIGMAFAST Protease Inhibitor (AEBSF 2 mM, Aprotinin 0.3 µM, Bestatin 130 µM, EDTA 1 mM, E-64 14 µM, Leupeptin 1 µM) (Sigma), PhosSTOP phosphatase inhibitor cocktail (Roche).

4.11.2. Protocol for Preparation of Cell Lysate: Cells were grown up to 80 – 90 % confluency in cell culture dishes and well plates. Cells were washed with PBS and lysed by adding ice-cold RIPA lysis buffer followed by incubation of 20 minutes in

ice. Lysate was centrifuged at 14,000 g for 15 minutes; supernatant was collected in a fresh micro centrifuge tube and stored at -80⁰ Celsius freezer for further use.

4.12. Estimation of Protein by BCA Method:

4.12.1. Reagents for Protein Estimation by BCA Method: Pierce BCA protein assay kit (Thermo), Bovine serum albumin (MP Biomedicals).

4.12.2. Protocol for Protein Estimation by BCA Method: Bovine serum albumin standards were prepared by making serial dilutions at 1.5 fold from 2 mg/ml BSA stock to 20 µg/ml, total of 8 dilutions of standard were prepared simultaneously working reagent (WR) was prepared by mixing BCA reagent A and BCA reagent B at 50:1 ratio. 10 µl of sample and BSA standard were dispensed to individual wells of 96 well plates. BSA standard were added in triplicates and samples were added in duplicates. Following addition of samples and BSA standard, 200 µl of working reagent (WR) was added to the wells, 10 µl RIPA buffer was used as blank. Plate was covered and incubated at 37⁰ Celsius for 30 minutes. Plate was retrieved and incubated at room temperature for 10 minutes and absorbance was measured at 562 nm using in iMark Microplate absorbance reader (Bio-Rad).

4.13. SDS-PAGE Electrophoresis:

4.13.1. Reagents for SDS-PAGE Electrophoresis: 30 % Acrylamide Bisacrylamide [29 g acrylamide, (Invitrogen) and 1 g Bis acrylamide, (Sigma) dissolved in 100 ml autoclaved Mili Q water], Laemmli buffer (0.1 % 2-Mercaptoethanol, 0.0005 % Bromophenol blue, 10 % Glycerol, 2 % SDS, 63 mM Tris-HCl pH 6.8), SDS-PAGE running buffer (25 mM Tris-HCl, 250 mM Glycine, 0.1 % SDS), Tris 1.5 M (pH 8.8), Tris 1 M (pH 6.8), 10 % SDS, 10 % APS (MP Biomedicals), TEMED (Sigma).

4.13.2. Protocol for SDS-PAGE Electrophoresis: 30 µg of Protein lysates were mixed with equal volume of 2X Laemmli buffer and boiled at 95⁰ Celsius for 5 minutes. 10 % or 12 % SDS PAGE resolving gel was prepared depending on the respective protein to be analyzed. 4 % stacking gel was prepared and protein samples were loaded into the wells and ran at constant voltage of 100V for the separation of protein samples. The composition of SDS-PAGE gel is mentioned in (Table 4.2).

Table (4.2): Composition of SDS-PAGE gel

Resolving Gel Constituents	Resolving Gel		Stacking Gel Constituents	Stacking Gel 4 % (2 ml)
	10 % (5 ml)	12 % (5 ml)		
30 % Acrylamide	1.66 ml	2.08 ml	30 % Acrylamide	340 µl
Mili Q H ₂ O	1.98 ml	1.57 ml	Mili Q H ₂ O	1.36 ml
1.5 M Tris (pH 8.8)	1.25 ml	1.25 ml	1 M Tris (pH 6.8)	250 µl
10 % SDS	50 µl	50 µl	10 % SDS	20 µl
10 % APS	50 µl	50 µl	10 % APS	20 µl
TEMED	5 µl	5 µl	TEMED	2 µl

4.14. Coomassie staining:

4.14.1. Reagents for Coomassie Staining: Coomassie staining solution (0.25 % Coomassie Brilliant Blue R 250, 45 % Methanol, 10 % acetic acid in distilled water), Destaining Solution (45 % Methanol, 10 % Acetic acid in distilled water).

4.14.2. Protocol for Coomassie Staining: SDS-PAGE gel was retrieved and immersed in Coomassie staining solution for 2 - 4 hours at room temperature under constant shaking. After completion of incubation, staining solution was replaced with destainer, consequently after removal of background stain, gels were kept in distilled water and scanned for future records.

4.15. Western Blot:

4.15.1. Reagents for Western Blot: Semi-dry transfer buffer, Tris-buffered saline (150 mM NaCl, 10 mM TrisHCl pH 8.0), Methanol (Merck), Tris-buffered saline TWEEN 20 (TBS-T) (0.1 % TWEEN 20 (v/v)), 150 mM NaCl, 10 mM TrisHCl (pH 8.0), Ponceau Staining solution (0.2 % Ponceau stain in 5 % acetic acid), Blocking buffer (3 % BSA in TBS or 5 % Milk powder in TBS), Antibody dilutions were prepared in 2.5 % BSA in TBS, Super Signal West Femto Maximum Sensitivity Substrate (Thermo scientific), Restore Western Blot Stripping Buffer (Thermo scientific), Immobilon-P Membrane, PVDF, 0.45 µm (Milipore), Ponceau (HiMedia), TWEEN 20 (Sigma), BSA (MP Biomedicals), Skimmed Milk (HiMedia).

4.15.2. Protocol for Western Blot: Protein samples were resolved in SDS-PAGE gel; followed by transfer of proteins from gel to methanol activated Immobilon PVDF membrane, using semidry transfer buffer in Bio-Rad Transblot SD Semidry Transfer Cell (Bio-Rad) at 17 V for 1 hour. Visualization of transferred protein, was done by staining membrane with Ponceau Staining solution, which was later washed with MiliQ water to remove stain. Complete removal of Ponceau staining solution, was done by washing TBS-T for two minutes. The blot was incubated in blocking buffer for one hour, followed by three times TBS-T wash for five minutes each. Blot was incubated in diluted primary antibody overnight at 4⁰ Celsius. After completion of incubation, blot was washed with TBS-T, three times for five minutes each. Thereafter blot was incubated in HRP conjugated secondary antibody with respective dilutions as mentioned in (Table 4.3) at room temperature for one hour on the rocker. Secondary antibody was removed and blot was washed with TBS-T. Blot was developed by using SuperSignal West Femto Maximum Sensitivity Substrate as per manufacturer's

instructions in Chemidoc XRS+ (Bio-Rad). Exposure time intervals were determined as per the signal strength. To characterize another protein in same blot, stripping was performed using Restore Western Blot Stripping Buffer according to manufacturer's protocols. The lists of antibodies used are mentioned in table 4.3.

Table (4.3): List of Antibodies Used in Western Blotting

Antibody	Dilution	Vendor	Catalog	Origin
FRG1	1:1000	Novus Biologicals	H00002483-2146	Mouse
GAPDH	1:20000	Sigma	G9545	Rabbit
Beta Tubulin	1:2000	Cell Signaling Technologies	2146	Rabbit
Total - p38	1:1000	Cell Signaling Technologies	9212	Rabbit
Phospho - p38	1:1000	Cell Signaling Technologies	9211	Rabbit
Total – ERK	1:1000	Cell Signaling Technologies	9120	Rabbit
Phospho - ERK	1: 1000	Sigma	9102	Rabbit
HRP tagged mouse IgG	1:10000	Thermo Scientific	31452	Rabbit
HRP tagged Rabbit IgG	1: 10000	Cell Signaling Technologies	7074	Goat

4.16. RNA Extraction and cDNA Synthesis:

4.16.1. Reagents for RNA Extraction and cDNA Synthesis: RNeasy mini kit (Qiagen), Superscript IV Reverse Transcriptase (Invitrogen), Agarose (Lonza), Tris-Acetate-EDTA buffer (40 mM Tris-acetate and 1 mM EDTA).

4.16.2. Protocol for RNA Extraction and cDNA Synthesis: Cells were grown in six well plates until a confluency of 80 – 90 % is achieved. RNA extraction was done using RNeasy mini kit as per the manufacturer's instructions (refer to appendix 8.4), once the cells reach desired confluency. RNA quality was verified by resolving samples in 1 % agarose gel using 120 V for 15 minutes, simultaneously RNA concentration was determined by using Nanodrop 2000 (Thermo). After verification of RNA quality and quantity, 5 µg of each sample was subsequently used for cDNA synthesis using one unit of Superscript IV Reverse Transcriptase. cDNA synthesis thus was followed as per manufacturer's instructions (refer to appendix 8.5). cDNA was stored at -80⁰ Celsius, until further use for expression analysis.

4.17. Quantitative –Real Time PCR:

4.17.1. Reagents for Quantitative –Real Time PCR: Nuclease Free Water (Genei), Fast SYBR GREEN (Roche), Primers (Integrated DNA Technologies) (Primer set for individual genes are provided with respective sequence in table 4.6).

4.17.2. Protocol for Quantitative – Real Time PCR: cDNA from various samples were diluted to 5 ng/µl concentration and a total of 10 ng of cDNA was used for expression analysis. Reaction was setup in an optically clear 96 well plate as mentioned in table 4.4. Each reaction was set up in triplicates, added by a no template control (NTC). Optically clear sealing film was applied to the plates; the plates were centrifuged (Eppendorf, 5810R) at 1500 rpm in a swinging rotor for two minutes.

Reaction was set in ABI7500 real time PCR machine, using parameters as mentioned in table 4.5. GAPDH was used as reference gene, to quantify the expression levels by $\Delta\Delta C_t$ methods. List of primers are provided in table 4.6.

Table (4.4): Reaction mix for q-RT-PCR

Composition	cDNA	No Template Control
Template	2 μ l	0
2X SYBR GREEN	10 μ l	10 μ l
Primer Forward (2.5 μ M)	1 μ l	1 μ l
Primer Reverse (2.5 μ M)	1 μ l	1 μ l
H ₂ O	6 μ l	8 μ l
Total	20 μ l	20 μ l

Table (4.5): ABI 7500 Run protocol

Stage	Temperature	Time
Holding	50 ⁰ C	2 minutes
Holding	95 ⁰ C	10 minutes
Melting x 40 cycles	95 ⁰ C	15 seconds
(Annealing + extension) x 40 cycles	60 ⁰ C	1 minute

Table (4.6): List of Primers

Gene	Primer 5' ---- 3'
MMP1 F	AGAGCAGATGTGGACCATGC
MMP1 R	TTGTCCCGATGATCTCCCCT
MMP2 F	CGTCGCCCATCATCAAGTTC
MMP2 R	CAGGTATTGCACTGCCAACTC
MMP3 F	CACTCACAGACCTGACTCGG
MMP3 R	AGTCAGGGGGAGGTCCATAG
MMP8 F	AAGCCAGGAGGGGTAGAGTT
MMP8 R	TTTTCCAGGTAGTCCTGAACAGT
MMP9 F	TTCAGGGAGACGCCCATTTT
MMP9 R	AACCGAGTTGGAACCACGAC
MMP10 F	AGTTTGGCTCATGCCTACCC
MMP10 R	TTGGTGCCTGATGCATCTTCT
MMP13 F	GTTTGCAGAGCGCTACCTGA
MMP13 R	GACTGCATTTCTCGGAGCCT
FGF2F	GCTGTACTGCAAAAACGGGG
FGF 2 R	TAGCTTGATGTGAGGGTCGC
PLGF F	CCATGCAGCTCCTAAAGATCC
PLGF R	TCCTCCTTTCCGGCTTCA
CXCL1 F	AACCGAAGTCATAGCCACAC
CXCL1 R	GTTGGATTTGTCAGTTCAGC
CXCL8 F	ACCGGAAGGAACCATCTCAC
CXCL8 R	GGCAAAACTGCACCTTCACAC
IL 10 F	AAGACCCAGACATCAAGGCG
IL 10 R	AATCGATGACAGCGCCGTAG
PDGFA F	GCCAACCAGATGTGAGGTGA
PDGFA R	GGAGGAGAACAAGACCGCA

PDGFB F	ACCTGCGTCTGGTCAGC
PDGFB R	ATCTTCCTCTCCGGGGTCTC
GM-CSF F	CTGGAGCTGTACAAGCAGGG
GM-CSF R	ACAGGAAGTTTCCGGGGTTG
G-CSF F	AGCAAGTGAGGAAGATCCAGG
G-CSF R	TTGTAGGTGGCACACTCACTC
VEGFA-F	ATCTGCATGGTGATGTTGGA
VEGFA-R	GGGCAGAATCATCACGAAGT
TGF-beta-F	GCAACAATTCTGGCGATACC
TGF-beta-R	AAAGCCTCAATTTCCCCTCC

4.18. Statistical Analysis:

Continuous data of two groups was compared by student's t-test. For correlation analysis, statistical significance was determined by Pearson Correlation coefficient. p value ≤ 0.05 was considered statistically significant. Graphpad Prism (Version 7) was used to perform statistical analysis.

6. REFERENCES

7. REFERENCES:

1. Schmidt, T. and P. Carmeliet, *Blood-vessel formation: Bridges that guide and unite*, in *Nature*. 2010. p. 697-699.
2. Carmeliet, P., *Angiogenesis in health and disease*. *Nature Med.*, 2003. **9**: p. 653-660.
3. Flamme, I. and W. Risau, *Induction of vasculogenesis and hematopoiesis in vitro*. *Development*, 1992. **439**: p. 435-439.
4. Gilbert, S.F., *Developmental Biology* 6th ed. 2000.
5. Folkman, J., *Tumor angiogenesis: therapeutic implications*. *The New England journal of medicine*, 1971. **285**(21): p. 1182-1186.
6. Weidner, N., et al., *Tumor angiogenesis: a new significant and independent prognostic indicator in early-stage breast carcinoma*. *Journal of the National Cancer Institute*, 1992. **84**(24): p. 1875-1887.
7. Bergers, G., L.E. Benjamin, and S. Francisco, *TUMORIGENESIS AND THE ANGIOGENIC SWITCH*. *Nature Rev. Cancer*, 2003. **3**(June): p. 1-10.
8. Folkman, J. and P.A.D. Amore, *Blood Vessel Formation : What Is Its Molecular Basis ?* *CELL*, 1996. **87**(7): p. 1153-1155.
9. Potente, M., H. Gerhardt, and P. Carmeliet, *Review Basic and Therapeutic Aspects of Angiogenesis*. *Cell*, 2011. **146**(6): p. 873-887.
10. Streubel, B., et al., *Lymphoma-specific genetic aberrations in microvascular endothelial cells in B-cell lymphomas*. *The New England journal of medicine*, 2004. **351**(3): p. 250-259.
11. Chung, A.S., J. Lee, and N. Ferrara, *Targeting the tumour vasculature: insights from physiological angiogenesis*. *Nature Rev. Cancer*, 2010. **10**: p. 505-514.
12. Bergers, G. and S. Song, *The role of pericytes in blood-vessel formation and maintenance I*. *Neuro Oncol.*, 2005. **7**: p. 452-464.
13. Goel, S., et al., *Normalization of the vasculature for treatment of cancer and other diseases*. *Physiological reviews*, 2011. **91**(3): p. 1071-1121.
14. Grewal, P.K., et al., *FRG1, a gene in the FSH muscular dystrophy region on human chromosome 4q35, is highly conserved in vertebrates and invertebrates*. *Gene*, 1998. **216**(1): p. 13-19.
15. Gabellini, D., M.R. Green, and R. Tupler, *Inappropriate gene activation in FSHD: a repressor complex binds a chromosomal repeat deleted in dystrophic muscle*. *Cell*, 2002. **110**(3): p. 339-348.
16. Wuebbles, R.D., M.L. Hanel, and P.L. Jones, *FSHD region gene 1 (FRG1) is crucial for angiogenesis linking FRG1 to facioscapulohumeral muscular dystrophy-associated vasculopathy*. *Disease models & mechanisms*, 2009. **2**(5-6): p. 267-274.
17. Osborne, R.J., et al., *Expression profile of FSHD supports a link between retinal vasculopathy and muscular dystrophy*. *Neurology*, 2007. **68**(8): p. 569-577.
18. Hanel, M.L., R.D. Wuebbles, and P.L. Jones, *Muscular dystrophy candidate gene FRG1 is critical for muscle development*. *Developmental dynamics*, 2010. **238**(6): p. 1502-1512.

19. Hasegawa, K., et al., *Facioscapulohumeral muscular dystrophy (FSHD) region gene 1 (FRG1) expression and possible function in mouse tooth germ development*. Journal of Molecular Histology, 2016. **1**(2).
20. Patsialou, A., et al., *Selective gene-expression profiling of migratory tumor cells in vivo predicts clinical outcome in breast cancer patients*. Breast Cancer Research, 2012. **14**(5): p. R139-R139.
21. Ferlay, J., et al., *Cancer incidence and mortality worldwide : Sources , methods and major patterns in GLOBOCAN 2012*. International journal of cancer, 2015. **136**: p. E359-E386.
22. Fong, G.H., et al., *Role of the Flt-1 receptor tyrosine kinase in regulating the assembly of vascular endothelium*. Nature, 1995. **376**(6535): p. 66-70.
23. Shalaby, F., et al., *Failure of blood-island formation and vasculogenesis in Flk-1-deficient mice*. Nature, 1995. **376**(6535): p. 62-66.
24. Carmeliet, P., et al., *Role of tissue factor in embryonic blood vessel development*. Nature, 1996. **383**(6595): p. 73-75.
25. Ferrara, N., et al., *Heterozygous embryonic lethality induced by targeted inactivation of the VEGF gene*. Nature, 1996. **380**(6573): p. 439-442.
26. Ribatti, D., *Endogenous inhibitors of angiogenesis: a historical review*. Leukemia research, 2009. **33**(5): p. 638-644.
27. Ribatti, D., A. Vacca, and M. Presta, *The discovery of angiogenic factors: a historical review*. General pharmacology, 2000. **35**(5): p. 227-231.
28. Hanahan, D. and R.A. Weinberg, *The Hallmarks of Cancer Cell*, 2000. **100**: p. 57-70.
29. Hanahan, D. and R.A. Weinberg, *Review Hallmarks of Cancer : The Next Generation*. Cell, 2011. **144**(5): p. 646-674.
30. Hanahan, D. and J. Folkman, *Patterns and emerging mechanisms of the angiogenic switch during tumorigenesis*. Cell, 1996. **86**(3): p. 353-364.
31. Baeriswyl, V. and G. Christofori, *Seminars in Cancer Biology The angiogenic switch in carcinogenesis*. Seminars in Cancer Biology, 2009. **19**: p. 329-337.
32. Armstrong, L.C. and P. Bornstein, *Thrombospondins 1 and 2 function as inhibitors of angiogenesis*. Matrix Biology, 2003. **22**(1): p. 63-71.
33. Carmeliet, P., *VEGF as a Key Mediator of Angiogenesis in Cancer*. Oncology, 2005. **69**(suppl 3): p. 4-10.
34. Ferrara, N., *Vascular Endothelial Growth Factor*. Arterioscler. Thromb. Vasc. Biol., 2009. **29**: p. 789-792.
35. Mac Gabhann, F. and A.S. Popel, *Systems biology of vascular endothelial growth factors*. Microcirculation (New York, N.Y. : 1994), 2008. **15**(8): p. 715-738.
36. Kessenbrock, K., V. Plaks, and Z. Werb, *Matrix metalloproteinases: regulators of the tumor microenvironment*. Cell, 2010. **141**(1): p. 52-67.
37. Kazerounian, S., K.O. Yee, and J. Lawler, *Thrombospondins in cancer*. Cell Mol Life Sci, 2008. **65**(5): p. 700-12.
38. Baluk, P., H. Hashizume, and D.M. McDonald, *Cellular abnormalities of blood vessels as targets in cancer*. Curr. Opin. Genet. Dev., 2005. **15**: p. 102-111.
39. Nagy, J.A., et al., *Heterogeneity of the tumor vasculature*. Semin. Thromb. Hemost., 2007. **36**: p. 321-331.

40. Raica, M., A.M. Cimpean, and D. Ribatti, *Angiogenesis in pre-malignant conditions*. European journal of cancer (Oxford, England : 1990), 2009. **45**(11): p. 1924-1934.
41. Folkman, J., *Role of Angiogenesis in Tumor Growth and Metastasis GROWTH*. Seminars in Oncology, 2002. **29**(6): p. 15-18.
42. Nyberg, P., L. Xie, and R. Kalluri, *Endogenous inhibitors of angiogenesis*. Cancer research, 2005. **65**(10): p. 3967-3979.
43. Raza, A., M.J. Franklin, and A.Z. Dudek, *Pericytes and vessel maturation during tumor angiogenesis and metastasis*. Am. J. Hematol., 2010. **85**: p. 593-598.
44. De Palma, M., et al., *Tie2-expressing monocytes: regulation of tumor angiogenesis and therapeutic implications*. Trends in immunology, 2007. **28**(12): p. 519-524.
45. Murdoch, C., et al., *The role of myeloid cells in the promotion of tumour angiogenesis*. Nature reviews. Cancer, 2008. **8**(8): p. 618-631.
46. Qian, B.Z. and J.W. Pollard, *Macrophage diversity enhances tumor progression and metastasis*. Cell, 2010. **141**: p. 39-51.
47. Zumsteg, A. and G. Christofori, *Corrupt policemen: inflammatory cells promote tumor angiogenesis*. Current opinion in oncology, 2009. **21**(1): p. 60-70.
48. Ferrara, N., *Pathways mediating VEGF-independent tumor angiogenesis*. Cytokine & growth factor reviews, 2010. **21**(1): p. 21-26.
49. Crawford, Y. and N. Ferrara, *VEGF inhibition: insights from preclinical and clinical studies*. Cell Tissue Res., 2009. **335**: p. 261-269.
50. Bergers, G.D.H., *Modes of resistance to anti-angiogenic therapy*. Nature Reviews Cancer, 2009. **8**(8): p. 592-603.
51. Crawford, Y. and N. Ferrara, *Tumor and stromal pathways mediating refractoriness / resistance to anti-angiogenic therapies*. Trends in Pharmacological Sciences, 2009. **30**(12): p. 624-630.
52. Ebos, J.M.L. and R.S. Kerbel, *Antiangiogenic therapy: impact on invasion, disease progression, and metastasis*. Nature reviews. Clinical oncology, 2011. **8**(4): p. 210-221.
53. Van Cutsem, E., et al., *Lessons from the adjuvant bevacizumab trial on colon cancer: what next?*, in *Journal of clinical oncology : official journal of the American Society of Clinical Oncology*. 2011. p. 1-4.
54. Jain, R.K., et al., *Biomarkers of response and resistance to antiangiogenic therapy*. Nature reviews. Clinical oncology, 2009. **6**(6): p. 327-338.
55. Bagri, A., et al., *Effects of Anti-VEGF Treatment Duration on Tumor Growth , Tumor Regrowth , and Treatment Efficacy*. Clinical cancer research, 2010. **16**(15): p. 3887-3901.
56. Francia, G., et al., *Mouse models of advanced spontaneous metastasis for experimental therapeutics*. Nature reviews. Cancer, 2011. **11**(2): p. 135-141.
57. Padera, T.P., *Differential response of primary tumor versus lymphatic metastasis to VEGFR-2 and VEGFR-3 kinase inhibitors cediranib and vandetanib*. Mol. Cancer Ther., 2008. **7**: p. 2272-2279.
58. Miles, D., *Disease course patterns after discontinuation of bevacizumab: pooled analysis of randomized phase III trials*. J. Clin. Oncol., 2010. **29**: p. 83-88.

59. Norden, A.D., J. Drappatz, and P.Y. Wen, *Antiangiogenic therapies for high-grade glioma*. Nature reviews. Neurology, 2009. **5**(11): p. 610-620.
60. Nisancioglu, M.H., C. Betsholtz, and G. Genove, *The absence of pericytes does not increase the sensitivity of tumor vasculature to vascular endothelial growth factor-A blockade*. Cancer research, 2010. **70**(12): p. 5109-5115.
61. Mazzone, M., *Heterozygous deficiency of PHD2 restores tumor oxygenation and inhibits metastasis via endothelial normalization*. Cell, 2009. **136**: p. 839-851.
62. Rolny, C., *HRG inhibits tumor growth and metastasis by inducing macrophage polarization and vessel normalization through downregulation of PlGF*. Cancer Cell, 2011. **19**: p. 31-44.
63. Tiwari, A., B. Mukherjee, and M. Dixit, *MicroRNA Key to Angiogenesis Regulation: miRNA Biology and Therapy*. Current cancer drug targets, 2017.
64. Hansda, A.K., A. Tiwari, and M. Dixit, *Current status and future prospect of FSHD region gene 1*. J Biosci, 2017. **42**(2): p. 345-353.
65. Gabriels, J., et al., *Nucleotide sequence of the partially deleted D4Z4 locus in a patient with FSHD identifies a putative gene within each 3.3 kb element*. Gene, 1999. **236**(1): p. 25-32.
66. Van Deutekom, J.C.T., et al., *Identification of the first gene (FRG1) from the FSHD region on human chromosome 4q35*. Human Molecular Genetics, 1996. **5**(5): p. 581-590.
67. Grewal, P.K., et al., *Recent amplification of the human FRG1 gene during primate evolution*. Gene, 1999. **227**: p. 79-88.
68. Clark, L.N., et al., *Analysis of the organisation and localisation of the FSHD-associated tandem array in primates : implications for the origin and evolution of the 3 . 3 kb repeat family*. Chromosoma, 1996. **105**: p. 180-189.
69. Koningsbruggen, S.V., R.W. Dirks, and A.M. Mommaas, *FRG1P is localised in the nucleolus, Cajal bodies, and speckles*. Journal of Medical Genetics, 2004: p. 1-8.
70. Liu, Q., et al., *Facioscapulohumeral muscular dystrophy region gene-1 (FRG-1) is an actin-bundling protein associated with muscle-attachment sites*. Journal of cell science, 2010. **123**(Pt 7): p. 1116-1123.
71. Sun, C.Y.J., et al., *Facioscapulohumeral muscular dystrophy region gene 1 Is a dynamic RNA-associated and actin-bundling protein*. Journal of Molecular Biology, 2011. **411**(2): p. 397-416.
72. Adams, J.C., *Roles of fascin in cell adhesion and motility*. Current opinion in cell biology, 2004. **16**(5): p. 590-596.
73. Edwards, R.A. and J. Bryan, *Review Fascins , a Family of Actin Bundling Proteins*. Cell motility and Cytoskeleton, 1995. **9**: p. 1-9.
74. Gabellini, D., et al., *Facioscapulohumeral muscular dystrophy in mice overexpressing FRG1*. Nature, 2006. **439**(7079): p. 973-977.
75. Wallace, L.M., et al., *RNA interference improves myopathic phenotypes in mice over-expressing FSHD region gene 1 (FRG1)*. Molecular therapy : the journal of the American Society of Gene Therapy, 2011. **19**(11): p. 2048-2054.
76. Hanel, M.L., et al., *Facioscapulohumeral muscular dystrophy (FSHD) region gene 1 (FRG1) is a dynamic nuclear and sarcomeric protein*. Differentiation, 2011. **81**(2): p. 107-118.

77. Nahabedian, J.F., et al., *Bending amplitude - A new quantitative assay of C. elegans locomotion: Identification of phenotypes for mutants in genes encoding muscle focal adhesion components*. *Methods*, 2012. **56**(1): p. 95-102.
78. Rappsilber, J., et al., *Large-scale proteomic analysis of the human spliceosome*. *Genome research*, 2002. **12**(8): p. 1231-1245.
79. Kim, S.K., et al., *A gene expression map for Caenorhabditis elegans*. *Science (New York, N.Y.)*, 2001. **293**(5537): p. 2087-2092.
80. Sancisi, V., et al., *Altered Tnnt3 characterizes selective weakness of fast fibers in mice overexpressing FSHD region gene 1 (FRG1)*. *American journal of physiology. Regulatory, integrative and comparative physiology*, 2014. **306**(2): p. R124-37.
81. Feeney, S.J., et al., *FHL1 reduces dystrophy in transgenic mice overexpressing FSHD muscular dystrophy region gene 1 (FRG1)*. *PLoS ONE*, 2015. **10**(2): p. 1-29.
82. Fitzsimons, R.B., E.B. Gurwin, and A.C. Bird, *Retinal vascular abnormalities in facioscapulohumeral muscular dystrophy. A general association with genetic and therapeutic implications*. *Brain : a journal of neurology*, 1987. **110** (Pt 3): p. 631-648.
83. Padberg, G.W., et al., *On the significance of retinal vascular disease and hearing loss in facioscapulohumeral muscular dystrophy*. *Muscle & nerve. Supplement*, 1995. **2**: p. S73-80.
84. Chen, S.C., et al., *Decreased proliferation Kinetics of mouse myoblasts overexpressing FRG1*. *PLoS ONE*, 2012. **6**(5): p. e19780-e19780.
85. Chamberlain, J.S., et al., *Dystrophin-deficient mdx mice display a reduced life span and are susceptible to spontaneous rhabdomyosarcoma*. *The FASEB journal*, 2007. **21**(9): p. 2195-2204.
86. Dmitriev, P., et al., *Cancer-related genes in the transcription signature of facioscapulohumeral dystrophy myoblasts and myotubes*. *Journal of Cellular and Molecular Medicine*, 2013. **18**(2): p. 208-217.
87. Yazici, O., et al., *A rare coincidence: Facioscapulohumeral muscular dystrophy and breast cancer*. *Experimental Oncology*, 2015. **35**(4): p. 311-312.
88. Rhodes, D.R., et al., *ONCOMINE: a cancer microarray database and integrated data-mining platform*. *Neoplasia (New York, N.Y.)*, 2004. **6**(1): p. 1-6.
89. Szasz, A.M., et al., *Cross-validation of survival associated biomarkers in gastric cancer using transcriptomic data of 1,065 patients*. *Oncotarget*, 2016. **7**(31): p. 49322-49333.
90. Fedchenko, N. and J. Reifenrath, *Different approaches for interpretation and reporting of immunohistochemistry analysis results in the bone tissue* " a review. *Diagnostic Pathology*, 2014. **9**(221): p. 1-12.
91. Sambrook, J. and D.W. Russell, *The inoue method for preparation and transformation of competent e. Coli: "ultra-competent" cells*. *CSH protocols*, 2006. **2006**(1).
92. Froger, A. and J.E. Hall, *Transformation of Plasmid DNA into E. coli Using the Heat Shock Method*, in *Journal of Visualized Experiments : JoVE*. 2007.
93. van Koningsbruggen, S., et al., *FRGIP-mediated aggregation of proteins involved in pre-mRNA processing*. *Chromosoma*, 2007. **116**(1): p. 53-64.

94. Grothey, A., et al., *C-erbB-2/ HER-2 upregulates fascin, an actin-bundling protein associated with cell motility, in human breast cancer cell lines*. *Oncogene*, 2000. **19**(42): p. 4864-4875.
95. Hashimoto, Y., et al., *Prognostic significance of fascin overexpression in human esophageal squamous cell carcinoma*. *Clinical cancer research : an official journal of the American Association for Cancer Research*, 2005. **11**(7): p. 2597-2605.
96. Jawhari, A.U., et al., *Fascin, an actin-bundling protein, modulates colonic epithelial cell invasiveness and differentiation in vitro*. *The American journal of pathology*, 2003. **162**(1): p. 69-80.
97. Vignjevic, D., et al., *Fascin, a novel target of beta-catenin-TCF signaling, is expressed at the invasive front of human colon cancer*. *Cancer research*, 2007. **67**(14): p. 6844-6853.
98. Fernandez, K., et al., *Mice lacking dystrophin or alpha sarcoglycan spontaneously develop embryonal rhabdomyosarcoma with cancer-associated p53 mutations and alternatively spliced or mutant Mdm2 transcripts*. *Am J Pathol*, 2010. **176**(1): p. 416-34.
99. Hosur, V., et al., *Dystrophin and dysferlin double mutant mice: a novel model for rhabdomyosarcoma*. *Cancer Genet*, 2012. **205**(5): p. 232-41.
100. Schmidt, W.M., et al., *DNA damage, somatic aneuploidy, and malignant sarcoma susceptibility in muscular dystrophies*. *PLoS Genet*, 2011. **7**(4): p. e1002042.
101. Groopman, J.E., J.M. Molina, and D.T. Scadden, *Hematopoietic growth factors. Biology and clinical applications*. *The New England journal of medicine*, 1989. **321**: p. 1449-1459.
102. Nicola, N.A., et al., *Purification of a factor inducing differentiation in murine myelomonocytic leukemia cells. Identification as granulocyte colony-stimulating factor*. *The Journal of biological chemistry*, 1983. **258**: p. 9017-9023.
103. Souza, L.M., et al., *Recombinant human granulocyte colony-stimulating factor: effects on normal and leukemic myeloid cells*. *Science (New York, N.Y.)*, 1986. **232**: p. 61-65.
104. Zsebo, K.M., et al., *Vascular endothelial cells and granulopoiesis: interleukin-1 stimulates release of G-CSF and GM-CSF*. *Blood*, 1988. **71**: p. 99-103.
105. Amariglio, N., et al., *Changes in gene expression pattern following granulocyte colony-stimulating factor administration to normal stem cell sibling donors*. *Acta haematologica*, 2007. **117**: p. 68-73.
106. Fujii, K., et al., *Elevation of serum hepatocyte growth factor during granulocyte colony-stimulating factor-induced peripheral blood stem cell mobilization*. *British journal of haematology*, 2004. **124**: p. 190-194.
107. McGuire, T.R., et al., *Elevated transforming growth factor beta levels in the plasma of cytokine-treated cancer patients and normal allogeneic stem cell donors*. *Cytotherapy*, 2001. **3**: p. 361-364.
108. Amadio, A., et al., *Impact of granulocyte colony-stimulating factors in metastatic colorectal cancer patients*. *Current oncology (Toronto, Ont.)*, 2014. **21**: p. e52-61.
109. Gutschalk, C.M., et al., *Granulocyte colony-stimulating factor and granulocyte-macrophage colony-stimulating factor promote malignant growth*

- of cells from head and neck squamous cell carcinomas in vivo. *Cancer research*, 2006. **66**: p. 8026-8036.
110. Morris, K.T., et al., *G-CSF and G-CSFR are highly expressed in human gastric and colon cancers and promote carcinoma cell proliferation and migration*. *British journal of cancer*, 2014. **110**: p. 1211-1220.
 111. Natori, T., et al., *G-CSF stimulates angiogenesis and promotes tumor growth: potential contribution of bone marrow-derived endothelial progenitor cells*. *Biochemical and biophysical research communications*, 2002. **297**: p. 1058-1061.
 112. Layman, H., et al., *Co-delivery of FGF-2 and G-CSF from gelatin-based hydrogels as angiogenic therapy in a murine critical limb ischemic model*. *Acta biomaterialia*, 2009. **5**: p. 230-239.
 113. Egeblad, M. and Z. Werb, *New functions for the matrix metalloproteinases in cancer progression*. *Nature reviews. Cancer*, 2002. **2**: p. 161-174.
 114. Cho, N.H., et al., *MMP expression profiling in recurred stage IB lung cancer*. *Oncogene*, 2004. **23**: p. 845-851.
 115. Gill, J.H., et al., *MMP-10 is overexpressed, proteolytically active, and a potential target for therapeutic intervention in human lung carcinomas*. *Neoplasia (New York, N.Y.)*, 2004. **6**: p. 777-785.
 116. Muller, D., et al., *Expression of collagenase-related metalloproteinase genes in human lung or head and neck tumours*. *International journal of cancer*, 1991. **48**: p. 550-556.
 117. O-Charoenrat, P., P.H. Rhys-Evans, and S.A. Eccles, *Expression of matrix metalloproteinases and their inhibitors correlates with invasion and metastasis in squamous cell carcinoma of the head and neck*. *Archives of otolaryngology-head & neck surgery*, 2001. **127**: p. 813-820.
 118. Mathew, R., et al., *Stromelysin-2 overexpression in human esophageal squamous cell carcinoma: potential clinical implications*. *Cancer detection and prevention*, 2002. **26**: p. 222-228.
 119. Zhang, G., et al., *Matrix metalloproteinase-10 promotes tumor progression through regulation of angiogenic and apoptotic pathways in cervical tumors*. *BMC cancer*, 2014. **14**: p. 310.
 120. Murray, M.Y., et al., *Macrophage migration and invasion is regulated by MMP10 expression*. *PloS one*, 2013. **8**: p. e63555.
 121. Siegel, R.L., K.D. Miller, and A. Jemal, *Cancer statistics, 2015*. *CA: a cancer journal for clinicians*, 2015. **65**(1): p. 5-29.
 122. Ferlay, J., et al., *Cancer incidence and mortality patterns in Europe: estimates for 40 countries in 2012*. *European journal of cancer (Oxford, England : 1990)*, 2013. **49**(6): p. 1374-1403.
 123. Shtivelman, E., T.M. Beer, and C.P. Evans, *Molecular pathways and targets in prostate cancer*. *Oncotarget*, 2014. **5**(17): p. 7217-7259.
 124. Attard, G., et al., *Prostate cancer*. *Lancet*, 2016. **387**: p. 70-82.
 125. Xie, Y., et al., *Disabled homolog 2 is required for migration and invasion of prostate cancer cells*. *Frontiers of medicine*, 2015. **9**(3): p. 312-321.
 126. Pulukuri, S.M.K. and J.S. Rao, *Matrix metalloproteinase-1 promotes prostate tumor growth and metastasis*. *International journal of oncology*, 2008. **32**(4): p. 757-765.

127. Lang, S.H., et al., *Production and response of human prostate cancer cell lines to granulocyte macrophage-colony stimulating factor*. International Journal of Cancer, 1994. **59**(2): p. 235-241.
128. Parmiani, G., et al., *Opposite immune functions of GM-CSF administered as vaccine adjuvant in cancer patients*. Annals of Oncology, 2007. **18**(2): p. 226-232.
129. Zins, K., et al., *Inhibition of Stromal PlGF Suppresses the Growth of Prostate Cancer Xenografts*. International Journal of Molecular Sciences, 2013. **14**(9): p. 17958-71.
130. Kuo, P.-L., et al., *CXCL1/GRO β increases cell migration and invasion of prostate cancer by decreasing fibulin-1 expression through NF- κ B/HDAC1 epigenetic regulation*. Carcinogenesis, 2012. **33**(12): p. 2477-2487.
131. Miyake, M., et al., *Chemokine (C-X-C motif) ligand 1 (CXCL1) protein expression is increased in high-grade prostate cancer*. Pathology - Research and Practice, 2014. **210**(2): p. 74-78.
132. Fudge, K., D.G. Bostwick, and M.E. Stearns, *Platelet-derived growth factor A and B chains and the α and β receptors in prostatic intraepithelial neoplasia*. The Prostate, 1996. **29**(5): p. 282-286.
133. Koul, H.K., M. Pal, and S. Koul, *Role of p38 MAP Kinase Signal Transduction in Solid Tumors*. Genes & cancer, 2013. **4**(9-10): p. 342-359.
134. Park, J.-I., et al., *Transforming growth factor-beta1 activates interleukin-6 expression in prostate cancer cells through the synergistic collaboration of the Smad2, p38-NF-kappaB, JNK, and Ras signaling pathways*. Oncogene, 2003. **22**(28): p. 4314-4332.
135. Savarese, D.M., et al., *Expression and function of colony-stimulating factors and their receptors in human prostate carcinoma cell lines*. The Prostate, 1998. **34**(2): p. 80-91.
136. Hashimoto, S., et al., *p38 MAP kinase regulates TNF alpha-, IL-1 alpha- and PAF-induced RANTES and GM-CSF production by human bronchial epithelial cells*. Clinical and experimental allergy : journal of the British Society for Allergy and Clinical Immunology, 2000. **30**(1): p. 48-55.
137. Lo, H.M., et al., *TNF-alpha induces CXCL1 chemokine expression and release in human vascular endothelial cells in vitro via two distinct signaling pathways*. Acta Pharmacol Sin, 2014. **35**(3): p. 339-50.
138. Johansson, N., et al., *Expression of collagenase-3 (MMP-13) and collagenase-1 (MMP-1) by transformed keratinocytes is dependent on the activity of p38 mitogen-activated protein kinase*. Journal of cell science, 2000. **113 Pt 2**: p. 227-235.
139. Reunanen, N., et al., *Activation of p38 alpha MAPK enhances collagenase-1 (matrix metalloproteinase (MMP)-1) and stromelysin-1 (MMP-3) expression by mRNA stabilization*. The Journal of biological chemistry, 2002. **277**(35): p. 32360-32368.
140. Matsumoto, T., et al., *Platelet-derived growth factor activates p38 mitogen-activated protein kinase through a Ras-dependent pathway that is important for actin reorganization and cell migration*. J Biol Chem, 1999. **274**(20): p. 13954-60.

141. Liu, Q., et al., *Implication of platelet-derived growth factor receptor alpha in prostate cancer skeletal metastasis*, in *Chinese Journal of Cancer*. 2011. p. 612-619.
142. Casalou, C., et al., *VEGF/PLGF induces leukemia cell migration via P38/ERK1/2 kinase pathway, resulting in Rho GTPases activation and caveolae formation*, in *Leukemia*. 2007. p. 1590-1594.
143. Ferrer, F.A., et al., *Expression of vascular endothelial growth factor receptors in human prostate cancer*. *Urology*, 1999. **54**(3): p. 567-572.
144. Jemal, A., et al., *Cancer Statistics , 2010 BOTH SEXES FEMALE BOTH SEXES ESTIMATED DEATHS*. CA: a cancer journal for clinicians, 2010. **60**(5): p. 277-300.
145. Hutchinson, L., *Breast cancer: Challenges, controversies, breakthroughs*. Nature Publishing Group, 2010. **7**(12): p. 669-670.
146. Chavez, K.J., S.V. Garimella, and S. Lipkowitz, *Triple negative breast cancer cell lines: one tool in the search for better treatment of triple negative breast cancer*. *Breast Dis*, 2010. **32**(1-2): p. 35-48.
147. Polyak, K., *Review series introduction Heterogeneity in breast cancer*. *Journal of Clinical Investigation*, 2011. **121**(10): p. 3786-3788.
148. Brenton, J.D., et al., *Molecular classification and molecular forecasting of breast cancer: ready for clinical application?* *Journal of clinical oncology : official journal of the American Society of Clinical Oncology*, 2005. **23**(29): p. 7350-7360.
149. Devarajan, P., et al., *Structure and expression of neutrophil gelatinase cDNA. Identity with type IV collagenase from HT1080 cells*. *The Journal of biological chemistry*, 1992. **267**(35): p. 25228-25232.
150. Jezierska, A. and T. Motyl, *Matrix metalloproteinase-2 involvement in breast cancer progression: a mini-review*. *Medical science monitor : international medical journal of experimental and clinical research*, 2009. **15**(2): p. RA32-40.
151. Kawamata, H., et al., *Active-MMP2 in cancer cell nests of oral cancer patients: correlation with lymph node metastasis*. *International journal of oncology*, 1998. **13**(4): p. 699-704.
152. Liabakk, N.B., et al., *Matrix metalloprotease 2 (MMP-2) and matrix metalloprotease 9 (MMP-9) type IV collagenases in colorectal cancer*. *Cancer research*, 1996. **56**(1): p. 190-196.
153. Mori, M., et al., *Analysis of MT1-MMP and MMP2 expression in human gastric cancers*. *International journal of cancer*, 1997. **74**(3): p. 316-321.
154. Knauper, V., et al., *Activation of progelatinase B (proMMP-9) by active collagenase-3 (MMP-13)*. *European journal of biochemistry*, 1997. **248**(2): p. 369-373.
155. Yamada, T., et al., *Overexpression of MMP-13 gene in colorectal cancer with liver metastasis*. *Anticancer research*, 2010. **30**(7): p. 2693-2699.
156. Kudo, Y., et al., *Matrix metalloproteinase-13 (MMP-13) directly and indirectly promotes tumor angiogenesis*. *The Journal of biological chemistry*, 2012. **287**(46): p. 38716-38728.
157. Chang, H.-J., et al., *MMP13 is potentially a new tumor marker for breast cancer diagnosis*. *Oncology reports*, 2009. **22**(5): p. 1119-1127.

158. Zhang, B., et al., *Tumor-derived matrix metalloproteinase-13 (MMP-13) correlates with poor prognoses of invasive breast cancer*. BMC cancer, 2008. **8**: p. 83-83.
159. Heldin, C.-H., *Targeting the PDGF signaling pathway in tumor treatment*. Cell communication and signaling : CCS, 2013. **11**: p. 97-97.
160. Bhardwaj, B., et al., *Localization of platelet-derived growth factor beta receptor expression in the periepithelial stroma of human breast carcinoma*. Clinical cancer research : an official journal of the American Association for Cancer Research, 1996. **2**(4): p. 773-782.
161. Coltrera, M.D., et al., *Expression of platelet-derived growth factor B-chain and the platelet-derived growth factor receptor beta subunit in human breast tissue and breast carcinoma*. Cancer research, 1995. **55**(12): p. 2703-2708.
162. Jechlinger, M., et al., *Autocrine PDGFR signaling promotes mammary cancer metastasis*. The Journal of clinical investigation, 2006. **116**(6): p. 1561-1570.
163. Weigel, M.T., et al., *Preclinical and clinical studies of estrogen deprivation support the PDGF/Abl pathway as a novel therapeutic target for overcoming endocrine resistance in breast cancer*. Breast cancer research : BCR, 2012. **14**(3): p. R78-R78.
164. Liu, Q., et al., *The CXCL8-CXCR1/2 pathways in cancer*. Cytokine & Growth Factor Reviews, 2016. **31**(Supplement C): p. 61-71.
165. Singh, J.K., et al., *Recent advances reveal IL-8 signaling as a potential key to targeting breast cancer stem cells*, in *Breast Cancer Research : BCR*. 2013. p. 210-210.
166. Wei, Z.-W., et al., *CXCL1 promotes tumor growth through VEGF pathway activation and is associated with inferior survival in gastric cancer*. Cancer letters, 2015. **359**(2): p. 335-343.
167. Zou, A., et al., *Elevated CXCL1 expression in breast cancer stroma predicts poor prognosis and is inversely associated with expression of TGF- β signaling proteins*. BMC Cancer, 2014. **14**(1): p. 781-781.
168. Zuccari, D.A.P.d.C., et al., *An immunohistochemical study of interleukin-8 (IL-8) in breast cancer*. Acta histochemica, 2012. **114**(6): p. 571-576.
169. Wu, K., et al., *Dachshund inhibits oncogene-induced breast cancer cellular migration and invasion through suppression of interleukin-8*. Proceedings of the National Academy of Sciences of the United States of America, 2008. **105**(19): p. 6924-6929.
170. Gutierrez, M.C., et al., *Molecular changes in tamoxifen-resistant breast cancer: relationship between estrogen receptor, HER-2, and p38 mitogen-activated protein kinase*. Journal of clinical oncology : official journal of the American Society of Clinical Oncology, 2005. **23**(11): p. 2469-2476.
171. Lester, R.D., et al., *Erythropoietin promotes MCF-7 breast cancer cell migration by an ERK/mitogen-activated protein kinase-dependent pathway and is primarily responsible for the increase in migration observed in hypoxia*. The Journal of biological chemistry, 2005. **280**(47): p. 39273-39277.

8. APPENDIX

8. APPENDIX:

8.1. QIAprep spin plasmid extraction kit protocol

1. Pellet 1–5 ml bacterial overnight culture by centrifugation at > 8000 rpm ($6800 \times g$) for 3 min at room temperature (15 – 25°C).
2. Resuspend pelleted bacterial cells in $250 \mu\text{l}$ Buffer P1 and transfer to a micro centrifuge tube.
3. Add $250 \mu\text{l}$ Buffer P2 and mix thoroughly by inverting the tube 4–6 times until the solution becomes clear. Do not allow the lysis reaction to proceed for more than 5 min. If using LyseBlue reagent, the solution will turn blue.
4. Add $350 \mu\text{l}$ Buffer N3 and mix immediately and thoroughly by inverting the tube 4–6 times. If using LyseBlue reagent, the solution will turn colorless.
5. Centrifuge for 10 min at $13,000$ rpm ($\sim 17,900 \times g$) in a table-top micro centrifuge.
6. Apply $800 \mu\text{l}$ supernatant from step 5 to the QIAprep 2.0 spin column by pipetting. Spin at $\geq 10,000 \times g$ for 30–60 s and discard the flow-through.
7. Wash the QIAprep 2.0 spin column by adding 0.75 ml Buffer PE by centrifuging at $\geq 10,000 \times g$ for 30–60 s and discard the flow-through.
8. Centrifuge the QIAprep 2.0 spin column for 1 min at $\geq 10,000 \times g$ to remove residual wash buffer.
9. Place the QIAprep 2.0 column in a clean 1.5 ml micro centrifuge tube. To elute DNA, add $30 \mu\text{l}$ Buffer EB (10 mM TrisCl, pH 8.5) or water to the center of the QIAprep 2.0 spin column, let stand for 1 min, and centrifuge for 1 min at $\geq 10,000 \times g$.

Source: QIAGEN kit handbook or user manual. QIAGEN®, QIAprep®

8.2. QIAprep plasmid midi kit plasmid extraction protocol

1. Pick a single colony from a freshly streaked selective plate and inoculate a starter culture of 2–5 ml LB medium containing the appropriate selective antibiotic. Incubate for approx. 8 h at 37°C with vigorous shaking (approx. 300 rpm). Use a tube or flask with a volume of at least 4 times the volume of the culture.
2. Dilute the starter culture into selective LB medium. For high-copy plasmids, inoculate 25 ml -100 ml medium with starter culture. For low-copy plasmids,

inoculate 100 ml. Grow at 37°C for 12–16 h with vigorous shaking (approx. 300 rpm). Use a flask or vessel with a volume of at least 4 times the volume of the culture.

3. Harvest the bacterial cells by centrifugation at 6000 x g for 15 min at 4°C. Resuspend the bacterial pellet in 4 ml Buffer P1. For efficient lysis, it is important to use a vessel that is large enough to allow complete mixing of the lysis buffers. Ensure that RNase A has been added to Buffer P1.

5. Add 4 ml Buffer P2, mix thoroughly by vigorously inverting the sealed tube 4–6 times, and incubate at room temperature (15–25°C) for 5 min. Do not vortex, as this will result in shearing of genomic DNA. The lysate should appear viscous. Do not allow the lysis reaction to proceed for more than 5 min. If LyseBlue has been added to Buffer P1, the cell suspension will turn blue after addition of Buffer P2. Mixing should result in a homogeneously colored suspension.

6. Add 4 ml of chilled Buffer P3, mix immediately and thoroughly by vigorously inverting 4–6 times, and incubate on ice for 15 min. Precipitation is enhanced by using chilled Buffer P3 and incubating on ice. After addition of Buffer P3, a fluffy white material forms and the lysate becomes less viscous. If LyseBlue reagent has been used, the suspension should be mixed until all trace of blue has gone and the suspension is colorless.

7. Centrifuge at $\geq 20,000$ x g for 30 min at 4°C. Remove supernatant containing plasmid DNA promptly.

8. Centrifuge the supernatant again at $\geq 20,000$ x g for 15 min at 4°C. Remove supernatant containing plasmid DNA promptly.

9. Equilibrate a QIAGEN-tip 100 by applying 4 ml Buffer QBT, and allow the column to empty by gravity flow.

10. Apply the supernatant from step 8 to the QIAGEN-tip and allow it to enter the resin by gravity flow.

11. Wash the QIAGEN-tip with 2 x 10 ml Buffer QC. Allow Buffer QC to move through the QIAGEN-tip by gravity flow.

12. Elute DNA with 5 ml Buffer QF. Collect the eluate in a 15 ml or 50 ml tube.

13. Precipitate DNA by adding 3.5 ml (0.7 volumes) room-temperature isopropanol to the eluted DNA. Mix and centrifuge immediately at $\geq 15,000$ x g for 30 min at 4°C. Carefully decant the supernatant.

14. Wash DNA pellet with 2 ml of room-temperature 70% ethanol, and centrifuge at $\geq 15,000 \times g$ for 10 min. Carefully decant the supernatant without disturbing the pellet.

15. Air-dry the pellet for 5–10 min, and dissolve the DNA in a suitable volume of buffer (e.g., TE buffer, pH 8.0, or 10 mM Tris·Cl, pH 8.5).

Source: QIAGEN® Plasmid Purification Handbook. Trademarks: QIAGEN®,

8.3. Lipofectamine 3000 transfection protocol

1. Initiate transfection protocol when the confluency of cell reaches 70 – 80 %.

2. Prepare the transfection mix I and II as mentioned in (Table 8.1). Mix and incubate both mixes for 5 minutes at room temperature.

3. Add the transfection mix to individual wells and incubate cell culture plates at 37⁰ Celsius and 5 % CO₂ for 36 – 72 hours as per the requirement of downstream process.

Table 8.1: Details of reagents for preparation of transfection mix for single well

Component	96 well	24 well	6 well
Cells	1 - 4 x 10 ⁴	0.5–2 × 10 ⁵	0.25 –1 × 10 ⁶
Serum free medium (Mix I)	5 µl	25 µl	125 µl
Lipofectamine 3000 (Mix I)	0.15 - 0.3 µl	0.75 - 0.5 µl	3.75 - 7.5 µl
DNA (Mix II)	0.2 µg	1 µg	5 µg
Serum free medium (Mix II)	5 µl	25 µl	125 µl
Total volume	10 µl	50 µl	250 µl

Source: Lipofectamine manual (Thermo-scientific)

8.4. RNeasy mini kit RNA extraction protocol:

1. Determine the number of cells. Aspirate the medium, and wash the cells with PBS. Aspirate the PBS, and add 0.1–0.25% trypsin in PBS. After the cells detach from the dish or flask, add medium (containing serum to inactivate the trypsin), transfer the cells to an RNase-free glass or polypropylene centrifuge tube and centrifuge at 300 x g for 5 min. Completely aspirate the supernatant

2. Disrupt the cells by adding Buffer RLT. For pelleted cells, loosen the cell pellet thoroughly by flicking the tube. Add 350 µl Buffer RLT and pipit to mix (if 350 µl is

not enough to cover the dish, use 600 μ l Buffer RLT). Collect the lysate with a rubber policeman. Pipet the lysate into a micro centrifuge tube

3. Homogenize the lysate for 30 s using a rotor–stator homogenizer.
4. Add 1 volume of 70 % ethanol to the homogenized lysate, and mix well by pipetting.
5. Transfer 700 μ l of each sample from step 4, including any precipitate that may have formed, to each RNeasy spin column.
6. Transfer up to 700 μ l of the sample, including any precipitate that may have formed, to an RNeasy spin column placed in a 2 ml collection tube. Close the lid gently, and centrifuge for 15 s at $\geq 8000 \times g$ ($\geq 10,000$ rpm). Discard the flow-through. If necessary, repeat step 6 with the remaining volume.
7. Add 700 μ l Buffer RW1 to the RNeasy spin column. Close the lid gently, and centrifuge for 15 s at $\geq 8000 \times g$ ($\geq 10,000$ rpm) to wash the spin column membrane. Discard the flow-through.
8. Add 500 μ l Buffer RPE to the RNeasy spin column. Close the lid gently, and centrifuge for 15 s at $\geq 8000 \times g$ ($\geq 10,000$ rpm) to wash the spin column membrane. Discard the flow-through.
9. Add 500 μ l Buffer RPE to the RNeasy spin column. Close the lid gently, and centrifuge for 2 min at $\geq 8000 \times g$ ($\geq 10,000$ rpm) to wash the spin column membrane.
10. Place the RNeasy spin column in a new 2 ml collection tube, and discard the old collection tube with the flow-through. Close the lid gently, and centrifuge at full speed for 1 min.
11. Place the RNeasy spin column in a new 1.5 ml collection tube . Add 30–50 μ l RNase-free water directly to the spin column membrane. Close the lid gently, and centrifuge for 1 min at $\geq 8000 \times g$ ($\geq 10,000$ rpm) to elute the RNA.

Source: RNeasy mini handbook. Trademarks: QIAGEN®

8.5. Superscript IV reverse transcriptase protocol for cDNA synthesis:

1. Prepare the RNA primer mix as mentioned in (Table 8.2), vortex and centrifuge the mix.
2. Incubate the RNA primer mix at 65⁰ Celsius for 5 minutes, followed by 1 minute incubation in ice.

Table 8.2: RNA primer mix for cDNA synthesis

Components	Volume
50 μ M Random hexamers	1 μ l
10 mM DNTP	1 μ l
Template RNA (10pg - 5 μ g of total RNA)	Up to 11 μ l
Nuclease Free Water	To 13 μ l

3. Prepare reverse transcriptase enzyme mix as mentioned in (Table 8.3), vortex and briefly centrifuge the mix.

Table 8.3: Reverse transcriptase (RT) mix for cDNA synthesis

Components	Volume
5X SSIV buffer	4 μ l
100 mM DTT	1 μ l
RNASE OUT	1 μ l
Superscript IV Reverse transcriptase	1 μ l

4. RT mix is added to RNA primer mix and incubated at 23⁰ Celsius for 10 minutes, followed by incubation at 55⁰ Celsius for 10 minutes and 80⁰ Celsius for 10 minutes.

5. After completion of the incubation, store the obtained cDNA at -20⁰ Celsius freezer.

Source: Superscript IV manual (Thermo scientific)

8.6. HeLa cell block staining of FRG1

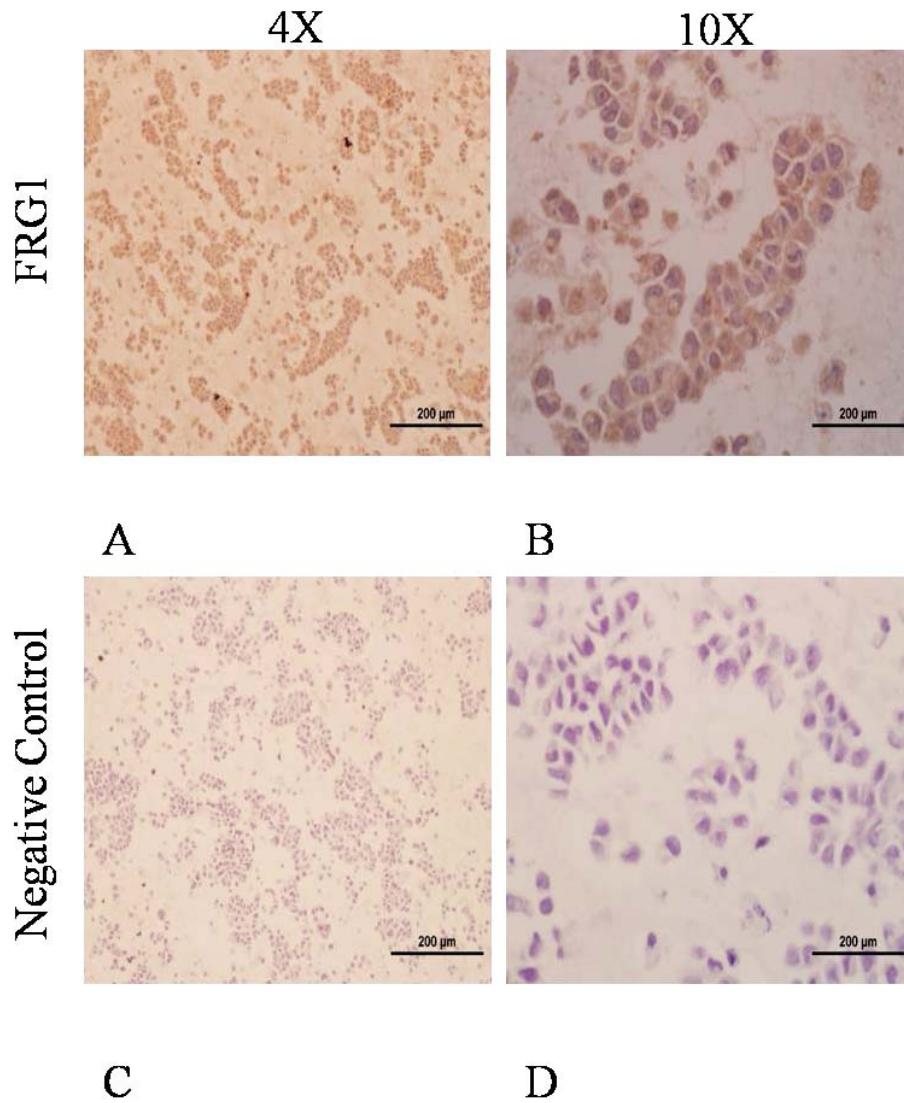


Figure (8.1): Sections of HeLa cell block were stained with anti FRG1 antibody as a positive control. (A – B) as we can observe brown color signals in HeLa cells stained with anti FRG1 antibody. Anti rabbit IgG was used as negative control (C – D), no brown coloration was developed when IHC was performed with anti rabbit IgG.

1. INTRODUCTION

1. INTRODUCTION:

For survival living organisms require a constant supply of nutrients, water, and gaseous exchange. In lower organisms, oxygen simply diffuses to individual cells but in higher organisms, the cardiovascular system is developed which is dedicated for the purpose of transportation of gases and molecules [1]. Blood vessels form a key component of the cardiovascular system [2]. The importance of blood vessels can be further emphasized as they form the largest network in the body, making them essential for the survival of organism [2]. Traversing the body as the largest network, any dysfunction in blood vessel network can be critical for the survival of the organism [2]. While emphasizing the importance of blood vessels, it is important to understand the process of blood vessel formation. Blood vessel formation is dictated via two independent processes *viz.* vasculogenesis and angiogenesis [3]. In higher organisms, blood vessel formation is essential prior to the development of other organs. Angioblasts which are differentiated from hematopoietic stem cells, on activation of FGF signaling further differentiate into endothelial cells, forming primary capillary plexus of the embryo [3]. This process is known as vasculogenesis (Figure 1.1.A), which occurs at the early stage of development. Vasculogenesis is not sufficient for formation of the fully functional vascular network; hence, angiogenesis comes into play. Angiogenesis is the process where blood vessel formation occurs from the pre-existing blood vessels (Figure 1.1.B). Angiogenesis regulates blood vessel formation during development and in maintaining body homeostasis, therefore abnormal angiogenesis can be perceived in the pathological sense.

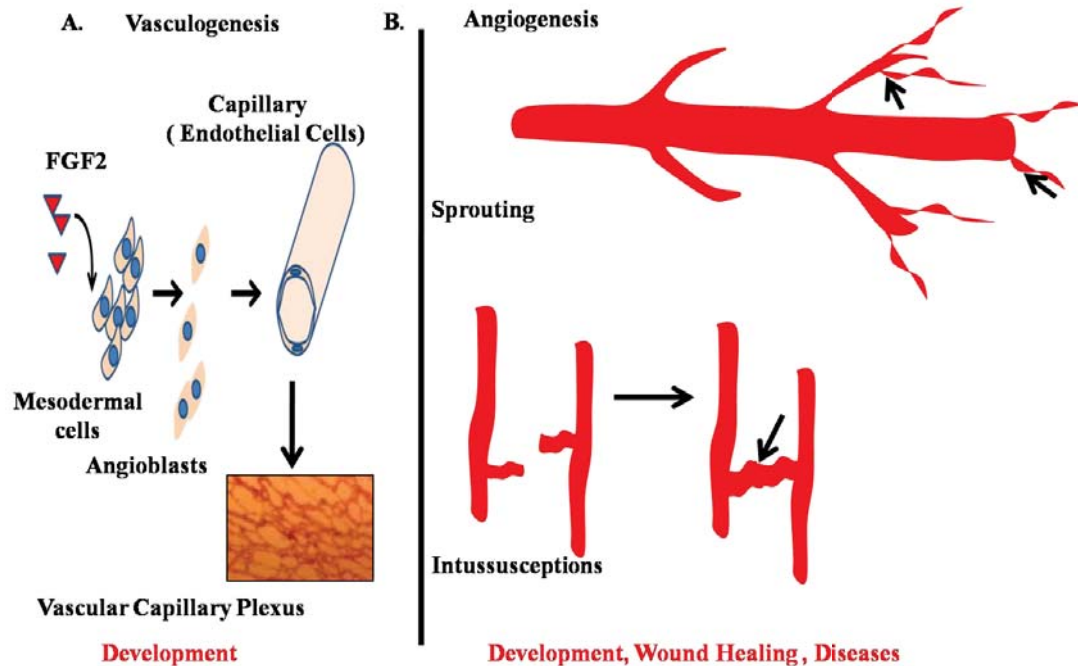


Figure (1.1): Representation of basic process of blood vessel formation. A. Blood vessel formation via vasculogenesis which occurs during development where FGF signaling triggers differentiation of mesodermal cells to angioblasts followed by endothelial cell formation which gives rise to primary capillary plexus. B. The process of angiogenesis, which uses preexisting vessels to form new vessels. Two basic forms of angiogenesis are represented by Sprouting and Intussusception. (*Recreated from Developmental Biology, Gilbert*) [4].

The importance of angiogenesis in health and disease could be highlighted by the fact that, out of ten major causes of death in 2015, five causes are directly associated with abnormal angiogenesis. One of the major diseases, where abnormal angiogenesis plays the pivotal role, is cancer. Total cancer-related death is ranked second, in factors causing death, as per WHO fact files 2015.

Angiogenesis has been long associated with cancer progression. Path-breaking finding from Sir Judah Folkman stated: “tumors are angiogenesis-dependent” [5]. Further, neoangiogenesis has the direct effect on tumor metastasis, leading to poor survival in cancer patients [6]. These findings paved the way for better understanding of molecular mechanism of angiogenesis in tumor progression and plausible ways of targeting it for therapy. Importance of angiogenesis in tumor development gave birth to the concept of ‘angiogenic switch’ [7]. Tumor progression leads to activation of various signaling pathways, among these signaling complexities the balance between

pro-angiogenic and anti-angiogenic molecules is tipped off. Activation of angiogenic switch leads to the formation of blood vessels with disrupted phenotype, promoting tumor growth and metastasis. These insights, provided by the earlier studies, led to the development of anti-angiogenic therapy [8, 9]. Anti-angiogenic therapy primarily targeted endothelial cells and endothelial cell-specific signaling molecules. The first category of drugs inhibits endothelial cell proliferation (e.g. Endostatin, Combrestatin A4, Thalidomide etc.). The second category includes monoclonal antibodies, blocking pro-angiogenic signaling (e.g. Bevacizumab, Cetuximab, Trastuzumab etc.). These monoclonal antibodies bind to VEGF and block the activation of the pathway. The third category of molecules comprises of small receptor tyrosine kinase inhibitor (e.g. Erlotinib, Sorafinib, Sunitinib, Rapamycin etc.). Receptor Tyrosine Kinases (RTKs) are the initiating point for cellular signaling. Various RTKs play the crucial role in angiogenesis and therefore are targeted for anti-angiogenic therapy (e.g. VEGFR, PDGFR, EGFR etc.) [9].

Anti-angiogenic therapy gained momentum, having an advantage of the genetic stability of endothelial cells compared to tumor cells. Tumor cells tend to acquire novel mutations during disease progression. Hence targeting tumor endothelial cells was considered a better approach. Studies have shown the presence of genetic aberrations in tumor endothelial cells also [10]. Thus, the presence of these genetic aberrations leads to one simple question, how effective can anti-angiogenic therapy be for cancer treatment? These recent turns of events pose a basic question regarding our understanding of the regulation of angiogenesis. One of the key factors responsible for the lack of success of anti-angiogenic therapy could be the poor organization of tumor vessels itself [9]. Tumor blood vessels promote irregular perfusion of oxygen, nutrients, and drugs. Growing tumor mass increases the interstitial pressure within the tumor. This enhanced interstitial pressure culminates in lower nutrient and oxygen concentration, promoting a hypoxic stromal milieu leading to increased pro-angiogenic signals [11]. The new blood vessels formed are disrupted and leaky,

leading to extravasation of tumor cells, promoting metastasis [7, 12]. Hence, the novel concept of vessel normalization is being applied alongside anti-angiogenic therapy. The concept illustrates that prior to anti-angiogenic therapy; tumor blood vessel should be normalized. Normalization of tumor blood vessel would lead to better delivery of nutrients, oxygen; drugs which could target the tumor mass and prevent the development of hypoxia within the tumor, leading to reduced tumor growth and better prognosis [9, 13]. Therefore, it is evident that for the success of anti-angiogenic therapy, more studies are required to decipher the mechanism of angiogenic regulation and identification of novel regulatory molecules.

Our search for novel regulators led to the identification of FSHD region gene 1 (FRG1) as putative angiogenesis regulator. FRG1 is the first candidate gene of Facioscapulohumeral muscular dystrophy (FSHD) [14]. FSHD is a progressive autosomal dominant genetic disorder characterized by weakness and atrophy of skeletal muscles of face, scapula and humeral. FSHD is manifested with loss of D4Z4 repeats at locus 4q35 [15]. This locus is flanked by FRG1 gene at 5' end. Apart from muscular atrophy, FSHD patients also suffer from hearing loss and retinal vasculature abnormalities. This observation posed a question; do FSHD candidate genes regulate vascular integrity? Studies associated with FRG1 had mostly focused on muscle development and function until 2009, when the study by Wuebbles et al. in *Xenopus laevis* embryo showed that FRG1 regulates angiogenesis during embryonic development [16]. Expression analysis of FSHD patients bearing retinal vasculature abnormalities (N=30), showed no significant change in FRG1 expression [17]. The interest in the role of FRG1 in tumorigenesis and the angiogenic switch was ignited by another developmental study on *Xenopus*, which showed that FRG1 regulated Epithelial-Mesenchymal Transition (EMT), during *Xenopus* muscle development. FRG1 levels dictated Vimentin expression, an EMT marker [18]. More specifically, FRG1 over-expression or knockdown led to enhanced and reduced Vimentin expression, respectively. Vimentin levels are enhanced in tumors and promote tumor

metastasis. No direct evidence has emerged that could associate FRG1 with tumor development amidst all studies involving FRG1. Few studies dropped hints, these studies provided a translucent vision of connection between FRG1 and tumorigenesis. Studies revealed functionality of FRG1 could be affected by BMP4 a tumor suppressor [19]. BMP4 levels dictated FRG1 localization, which might affect the function of FRG1. Another hint was derived from a global expression profiling study, in migratory breast cancer cells compared to average non-migratory cells. Here it was observed that FRG1 expression was reduced in migratory cells [20]. These findings make one to contemplate regarding this alliance of FRG1 and tumorigenesis.

Brief understanding of FRG1 via these studies does not provide one, with the knowledge of its clear involvement in tumor progression and tumor angiogenesis. But it undoubtedly suggests its plausible task in tumorigenesis. Thus it makes a very strong argument in favor of understanding and providing a clear picture whether FRG1 dictates angiogenesis and tumorigenesis, if so what is the probable molecular mechanism?

2. HYPOTHESIS

2. HYPOTHESIS:

Research involving FRG1 has been mostly aligned with FSHD and muscle function. Hence an association of FRG1 with tumor progression and angiogenesis was not obvious but as we introduced in the previous section, we drew parallels from referred studies, proving why it is crucial to understand the involvement of FRG1 in tumorigenesis. Moving forward, we found connections of FRG1 in angiogenesis and tumor progressions, which are still questionable. Therefore it is essential to formulate a clear idea regarding FRG1's association with tumor progression and angiogenesis. Apparently, the study would provide challenges in its own way as no organ-specific distribution, localization, and expression of FRG1 was known and this study would be first to undertake the challenge.

After presenting the arguments on FRG1 and its plausible impact on tumor development we hypothesize that “**FRG1 may be involved in tumor progression and tumor angiogenesis**”. Henceforth to validate our hypothesis we propose to undertake following objectives

Objectives:

Objective 1: To investigate effect of FRG1 expression in angiogenesis

Objective 2: To establish tumorigenic properties of FRG1 *in vivo* and *in vitro*

Objective 3: Identifying role and molecular mechanism of FRG1 in Prostate cancer

Objective 4: To determine role and molecular mechanism of FRG1 in Breast cancer

3. REVIEW OF LITERATURE

3. REVIEW OF LITERATURE:

3.1. Angiogenesis in Health and Disease:

Blood vessel development and disease association is a well-reported saga [2] . Role of angiogenesis in disease biology can be ascertained by review of major death causing factors. Looking into the WHO fact files from 2015 (Figure 3.1), we can observe that five out of top 10 factors are directly associated with abnormal angiogenesis. The significance of angiogenesis in diseases as the causative factors can be highlighted by the number of diseases caused by excessive (Table 3.1) and insufficient angiogenesis (Table 3.2). Tumor angiogenesis reflects poor prognosis that can be justified by the numbers of cancer-related deaths. We could observe that lung cancer related deaths ranks 5th with approximately around 1.8 million deaths in the year 2015 (Figure 3.1). Moving towards larger picture, overall cancer deaths were around 8.8 million in 2015 and is ever rising [21]. Thus anti-angiogenic therapy has high regards in terms of cancer cure, but in hindsight, it is important to understand key events of angiogenesis before making a discourse towards anti-angiogenic therapy.

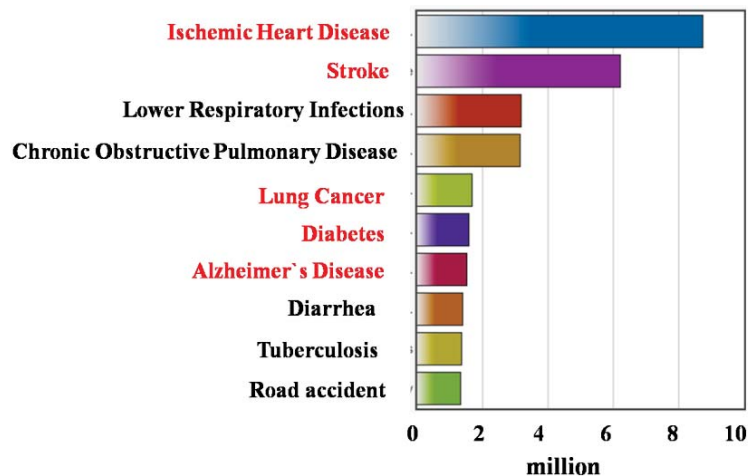


Figure (3.1): Graphical representation of top 10 causes of death in the year 2015 obtained from WHO Fact files. The causes denoted in red are associated with angiogenesis implying the significance of angiogenesis in health.

Table (3.1): Diseases associated with abnormal or excessive angiogenesis
(Source: Adopted from Carmeliet et al. 2003) [2]

S. No.	Organ	Disease
1	Numerous organ	Cancer (activation of oncogenes; loss of tumor suppressors), infectious diseases (pathogens express angiogenic genes, express angiogenic programs and transform endothelial cells), autoimmune disorders (activation of mast cells and leukocytes)
2	Blood vessels	Vascular malformations (Tie2 mutations), DiGeorge syndrome (low VEGF and neuropilin-1 expression), Hereditary hemorrhagic telangiectasia (mutations and endoglin or ALK1), cavernous hemangioma (loss of Cx37 and Cx40), atherosclerosis, transplant arteriopathy
3	Adipose tissue	Obesity (angiogenesis induced by fatty diet; weight loss by angiogenesis inhibitors)
4	Skin	Psoriasis, warts, allergic dermatitis, scar keloids, pyogenic granulomas, blistering disease, Kaposi sarcoma in AIDS patient
5	Eye	Persistent hyperplastic vitreous syndrome (loss of Ang2 or VEGF164), retinopathy, retinopathy of prematurity, choroidal neovascularization (TIMP3 mutation)
6	Lung	Primary pulmonary hypertension (germline BMPR2 mutation, somatic EC mutations), asthma, nasal polyps
7	Intestines	Inflammatory bowel and preodontol disease, ascites, peritoneal adhesions
8	Reproductive system	Endometriosis, uterine bleeding, ovarian cysts, ovarian hyperstimulation
9	Bones, Joints	Arthritis, synovitis, osteomyelitis, osteophyte formation

Table (3.2): Disease caused by insufficient angiogenesis or vessel regression
 (Source: Table adopted from Carmeliet et al. 2003) [2]

S. No.	Organ	Disease	Angiogenic mechanism
1	Nervous System	Alzheimer's Disease	Vasoconstriction, microvascular degeneration and cerebral angiopathy due to EC toxicity by amyloid β
		Amyotrophic lateral sclerosis, diabetic neuropathy	Impaired perfusion and neuroprotection, causing motor neuron or axon degeneration due to insufficient VEGF production
		Stroke	Correlation of survival with angiogenesis in brain stroke due to arteriopathy (Notch 3 mutations)
2	Blood vessels	Atherosclerosis	Characterized by impaired collateral vessel development
		Hypertension	Micro vessel refraction due to impaired vasodilation and angiogenesis
		Diabetes	Characterized by impaired collateral growth and angiogenesis in ischemic limb, but enhanced retinal neovascularization secondary to pericytes dropout
		Restenosis	Impaired re-endothelialization after arterial injury at old age
3	Gastrointestinal	Gastric and oral ulcerations	Delayed healing due to production of angiogenesis inhibitors of pathogens
		Crohn's disease	Characterized by mucosal ischemia

4	Skin	Hair loss	Retarded hair growth by angiogenesis inhibitor
		Skin purpura, telangiectesia and venous lake formation	Age dependent reduction of vessel number and maturation (SMC dropout) due to EC telomere shortening
5	Reproductive system	Pre eclampsia	EC dysfunction resulting in organ failure thrombosis and hypertension due to deprivation of VEGF by soluble Flt-1
		Menorrhagia	Fragility of SMC-poor vessels due to low Ang1 production
6	Lung	Neonatal respiratory distress	Insufficient lung maturation and surfactant production in premature mice due to reduced HIF2 α and VEGF production
		Pulmonary fibrosis, emphysema	Alveolar EC apoptosis upon VEGF inhibition
7	Kidney	Nephropathy	Age related vessel loss due to TSP1 production
8	Bone	Osteoporosis impaired bone fracture healing	Impaired bone formation due to age dependent decline of VEGF-driven angiogenesis, angiogenesis inhibitors prevent fracture healing

Blood vessel formation is guided by vasculogenesis and angiogenesis. Blood vessel formation begins from differentiation of mesoderm cells to angioblasts, via FGF signaling, the process called ‘vasculogenesis’ [3]. Differentiation of angioblasts to endothelial cells is triggered by activation of VEGF pathway leading to the formation

of primary vascular plexus. The process of angiogenesis employs these capillary plexus to form large blood vessels [2]. VEGF signaling forms the heart of angiogenesis and is mediated through two receptors, VEGFR1 (flt1) and VEGFR2 (flk1) [8]. The significance of flk1 and flt1 based signaling can be estimated by the effect of flk1 and flt1 gene knockout in mice embryos, being lethal [22, 23]. Similar effects were observed in vegf knockout mice, with the death of embryo reported at 8.5-9 days after gestation, attributed to delayed differentiation of endothelial cells [24, 25]. Henceforth, it was clear that VEGF signaling was central to angiogenesis. The discovery of other regulators, mediating angiogenesis functioning as a promoter or inhibitor, were made later with more research [26, 27]. Therapeutic and prognostic importance of angiogenesis in cancer was realized and rightly quoted by Judah Folkman “Tumors are angiogenesis dependent”. Hence, from this point onward we will be discussing angiogenesis in terms of tumor development.

3.2. Angiogenesis and Cancer:

During early 2000, Douglas Hanahan and R A Weinberg described six hallmarks of cancer. Sustained angiogenesis was described as one of the six hallmarks [28]. Requirements of oxygen and nutrients supply along with the necessity to evacuate metabolic wastes and carbon dioxide is important for sustenance of normal tissue. Similar are the needs of the tumor, which are fulfilled by tumor associated neovascularization by angiogenesis [29]. Blood vessel network traverses throughout the human body and remains quiescent ones it is fully developed. Various physiological processes, such as wound healing and female reproductive cycle, trigger angiogenic stimulus and process is turned on but, transiently [29]. Tumor progression also involves similar signals but with one difference, the angiogenic switch remains

activated, leading to continuous differentiation of quiescent vasculature into new blood vessels, sustaining the growth of neoplastic tissue [30] (Figure 3.2, Figure 3.3).

Plausible evidence has been provided that angiogenesis is regulated by the balance between activators and inhibitors of angiogenesis [7, 31]. Most of these pro-angiogenic and anti-angiogenic molecules work through surface receptors, exerting effect on vascular endothelial cells; some common examples are VEGFA and TSP1 respectively [25, 32].

VEGFA stimulates angiogenesis by activation of downstream signaling via receptor tyrosine kinases VEGFR1, VEGFR2 and VEGFR3. One of the significant findings is, VEGFA levels are enhanced in tumors via hypoxia and cancer signaling [33-35]. VEGF family of ligand is known to activate and release extracellular matrix degrading protease (e.g. MMP9, MMP1) [36]. Upregulation of various pro-angiogenic factors (viz. PLGF, PFGFA, PDGFB, EGF) in tumor microenvironment promote sustained angiogenesis. TSP1 is one key molecule that helps to keep the check on angiogenic switch. TSP1 binds to cell surface receptor, invoking and suppressive response via downstream signaling leading to suppression of EC survival and promotion of apoptosis [37].

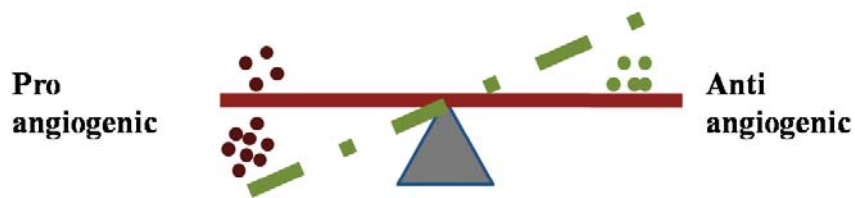


Figure (3.2): Representation of effect of angiogenic factors leading to angiogenic switch. In this picture, we can see that the balance between pro-angiogenic and anti-angiogenic factors is tipped off by enhanced level of pro-angiogenic factor. (*Recreated from Bergers et al. 2003*) [7].

Tumor induced blood vessels are the result of persistent angiogenesis due to the skewed presence of pro-angiogenic factors in the tumor milieu. These vessels are

characterized by impaired vessel sprouting, leakiness, distorted and enlarged blood vessels, micro-hemorrhaging, abnormal endothelial cell proliferation and apoptosis [38, 39]. Pictorial depiction of some of these features can be seen in figure 3.3.

According to earlier hypothesis, angiogenic switch was thought to be substantial only during macroscopic growth of the tumor, suggesting angiogenic switch was dependent on invasiveness of tumor. On the contrary, recent histological analyses revealed that noninvasive tumors, like *in situ* carcinomas and even dysplasia from various organ systems, have shown early tripping of angiogenic switch. These analyses further suggested that even in invasive tumor types angiogenic switch turns on as early as during pre-malignant growth [30, 40].

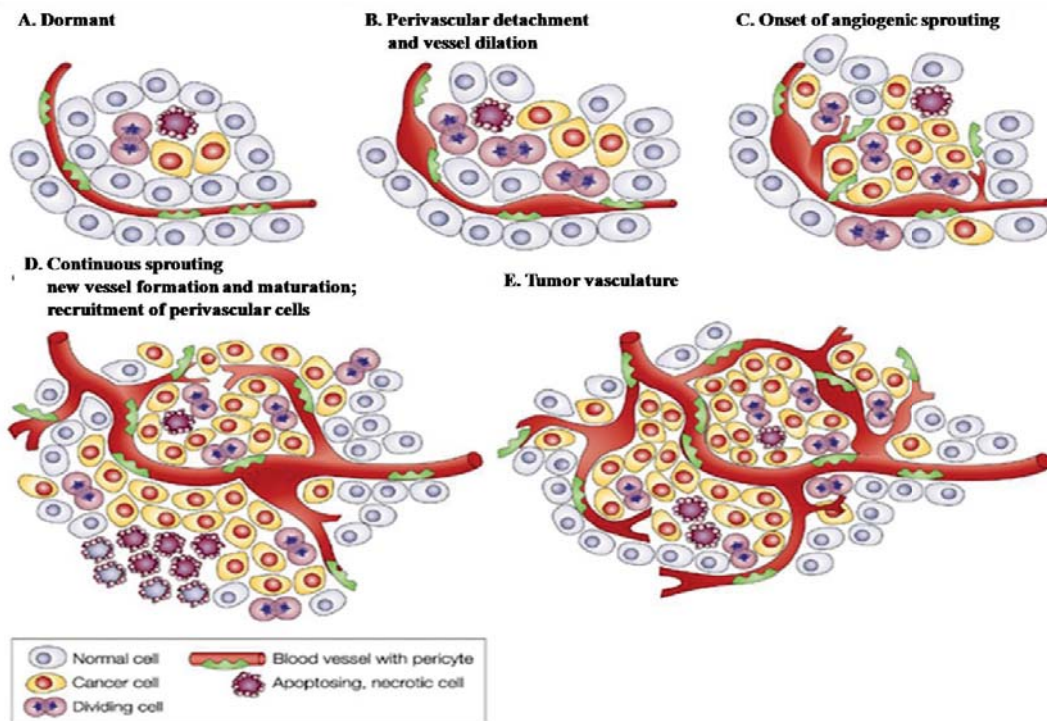


Figure (3.3): Representation of blood vessel formation during tumor progression. A. Panel shows dormant blood vessel within tumor with restricted growth size tumor size. B. Enhanced tumor growth leading to initiation of tumor angiogenesis. C- E. Represent events of formation of typical blood vessels in tumor environment with poor cell adhesion, succulent and distorted blood vessels promoting tumor growth and metastasis (Adopted from Bergers et al. 2003) [7].

In recent years, a better understanding of angiogenesis has been acquired but it has also been realized that the process is much more complex. Studies have highlighted that process of angiogenesis also depends on the stromal components. These components guide the behavior of different tumor types [7, 31]. Angiogenesis might be affected by the particular set of mutations harbored by the cancer cells during progression and its effect on the stromal microenvironment [29].

Studies focusing on inhibitors of angiogenesis have identified numerous endogenously present inhibitory molecules. Molecules like TSP1 are known inhibitors of angiogenesis. Moreover, the fragments of structural protein that are not involved in angiogenesis, obtained by proteolytic cleavage, such as plasmin (Angiostatin) and type 18 collagen (Endostatin) have shown inhibitory activity [26, 37, 41, 42]. It has been demonstrated that knockouts of these inhibitors in mice model, have no effect on body physiology but it does enhance the growth of implanted tumor, simultaneously transgenic expression of these molecules impairs the tumor growth [26, 42]. Hence, studies regarding endogenous inhibitors provide us with basic information that modulation of these molecules can act as the barrier for angiogenesis in neoplastic growth [29].

Angiogenesis research earlier had primary focus on endothelial cell differentiation and function. Recent studies have shown a shift in the trends, where the importance of endothelial cells are not undermined, but pericytes and vascular smooth muscle cells are not considered just supporting cells [29]. Studies have demonstrated that in most of the tumor neo-vasculature pericytes adherence is compromised. Mechanistically, pericyte coverage is important for tumor neo-vasculature integrity and function [12, 43]. The significance of other cell populations is not just limited to cells associated

with blood vessel formation. It has now been understood that bone marrow derived cells like macrophages, neutrophils, and myeloid progenitor cells regulate the pathological angiogenesis [44-47]. Recruitment of these cells at tumor sites promotes angiogenesis but also provides a drug evasion mechanism and protects tumor endothelial cells [48].

These findings provide us the idea of how the understanding of angiogenesis has been changed with time. Complexities of angiogenesis in tumor progression have indeed shown us where recent research stands regarding expectations and challenges of anti-angiogenic therapy in cancer.

3.3. Expectations and Challenges of Anti-angiogenic Therapy in Cancer:

The burden of 8.8 million deaths per million in 2015 and the numbers at rising, cancer therapy has always been a burning question [21]. In such circumstances, angiogenesis sparked significant therapeutic hopes for cancer treatment [5]. Anti-angiogenic therapy aimed at blocking blood vessel formation in the tumor, by targeting VEGF [49]. In the course of therapy, it has been observed that very few numbers of cancer patients got the benefit, in most of the cases tumor evolves to develop a resistance mechanism [50, 51]. In current times, it is suggested that anti-angiogenic therapy may trigger more invasive and metastatic growth of the tumor, leading to the debate regarding anti-angiogenic tumor therapy and its efficacy [52]. On the foresight, a concept has been proposed which talks about the sustained normalization of tumor vessels [9]. Normalization of these tumor blood vessels could help prevent metastasis in cancer patients [13]. Development of a sustainable anti-angiogenic therapy for

cancer requires the in-depth understanding of available therapy that would be explored in following sections.

3.4. Clinically Approved Anti-Angiogenic Therapy:

The key molecules that strike when we talk about anti-angiogenic therapy are VEGF and VEGF receptor. VEGF/ VEGF receptor form target for the majority of anti-angiogenic drugs, approved by Food and Drug Administration, USA for clinical use [49]. Anti-VEGF therapy is used in several metastatic cancers, in combination with chemotherapy and cytokine based therapy [9]. Bevacizumab (Avastin) is the anti-VEGF antibody which blocks the VEGF signaling, is used for the treatment of cancers viz. non-squamous non-small cell lung cancer, colorectal cancer, renal cell cancer, and metastatic breast cancer [9]. Based on random phase II trial, bevacizumab is used as monotherapy for recurrent glioblastoma [9]. In addition, four pan VEGF receptor tyrosine kinase inhibitors have been approved for anti-angiogenic therapy, the description of these drugs can be found in table 3.3.

Table (3.3): List of pan VEGF receptor tyrosine kinase inhibitors and concomitant cancer, being used for treatment(Source: Recreated from Potente et al. 2011) [9]

S. No.	VEGFR TKI	Tumor type
1	Sunitinib (Sutent)	Metastatic renal cell carcinoma Advanced pancreatic neuroendocrine carcinoma
2	Pazopanib (Votrient)	Metastatic renal cell carcinoma
3	Sorafenib (Nexavar)	Metastatic renal cell carcinoma Unresectable hepatocellular carcinoma
4	Vandetanib (Zactima)	Medullary thyroid cancer

The mechanisms of action of these VEGF (receptor) inhibitors are varied and affect diverse properties of tumorigenic blood vessels. VEGF (receptor) inhibitor primarily blocks vascular branching followed by the destruction of pre-existing tumor blood vessels. This approach is thought to sensitize tumor cells for chemotherapy by depriving them of survival signals from VEGF [9]. This method was thought to reduce the metastatic activity of tumor; but the development of hypoxia in the tumor tissue due to the destruction of these blood vessels might lead to recruitment of bone marrow derived cells which promotes micro metastasis leading to invasive tumor growth, as observed in figure 3.4.A. The hypothesis is yet to be verified in case of VEGF inhibitors.

An alternative approach has been suggested in recent times, which relies on maturation of tumor blood vessels. The approach suggests, pruning of tumor blood vessels which have poor association with pericytes, making them functional and continuing with conventional therapeutic options (Figure 3.4.B) [13] .

To be able to comment on the vessel normalization strategy compared to targeting tumor growth needs a great deal of molecular understanding. Anti-VEGF (receptor) therapy transiently shows vessel normalization but it later induces blood vessel regression, which may also enhance escape from VEGF blockade. Thus, normalization of these blood vessels may restore barrier functions which may be relevant in maintaining VEGF blockade [13].

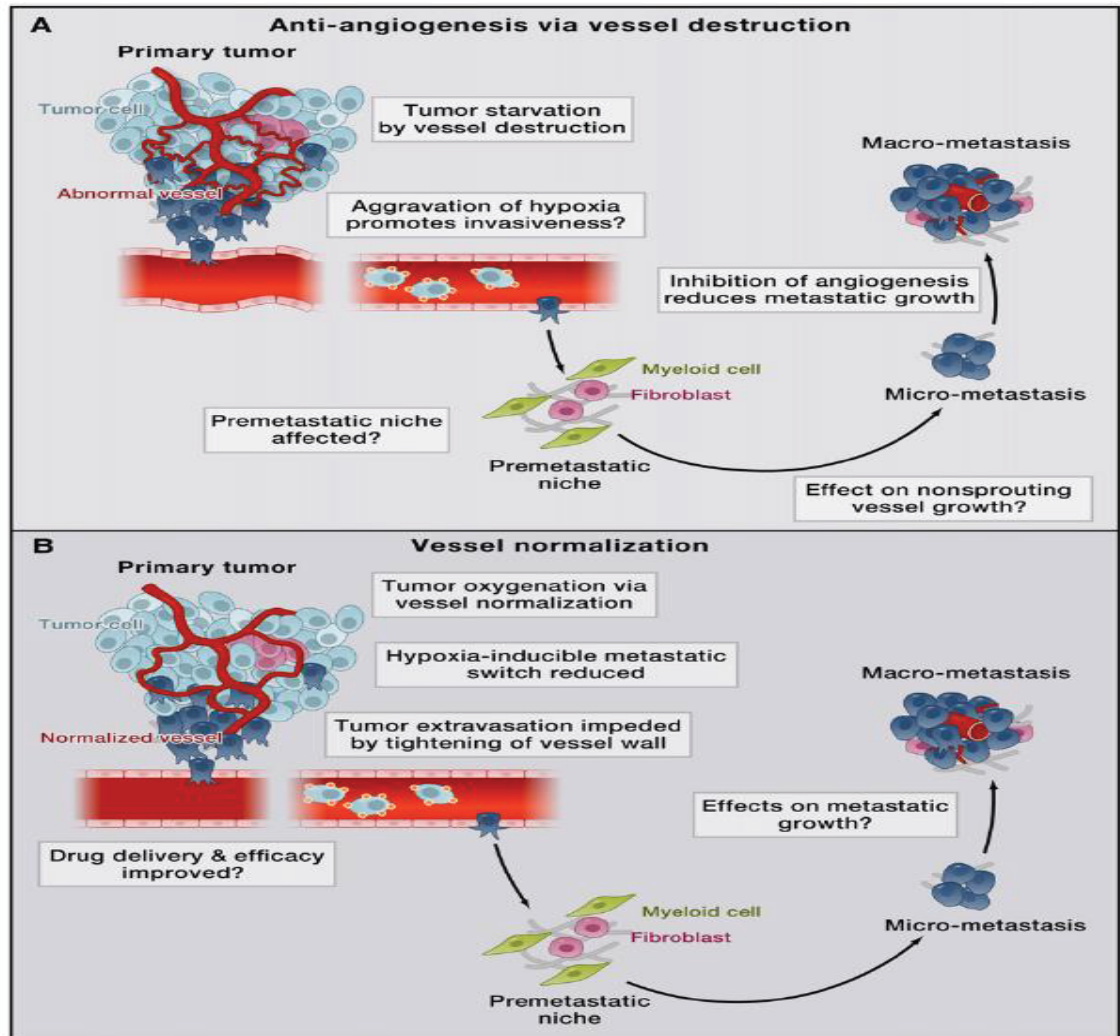


Figure (3.4): Anti-angiogenesis therapy versus vessel normalization. **A.** Anti-angiogenic agents that destroy abnormal tumor vessels and prune the tumor microvasculature can aggravate intra-tumor hypoxia, which can activate a pro-metastatic switch; the question mark reflects ongoing debate whether this metastatic switch exists in patients treated with VEGF (receptor) inhibitors. **B.** Anti-vascular targeting strategies that normalize abnormal tumor vessels are believed not to aggravate tumor hypoxia or even to improve oxygen supply, thereby impeding the hypoxia driven pro-metastatic switch. Their effect on stabilizing and tightening of the tumor vessel wall makes the vessels less penetrable for disseminating tumor cells. When improving drug delivery and tumor oxygenation, vessel normalization can also enhance the effect of conventional chemotherapy and irradiation. (*Adopted from Potente et al. 2011*) [9].

3.5. Challenges of VEGF (receptor) Based Therapies:

The major challenge for anti-VEGF (receptor) therapy was to increase survival of cancer patients, as observed in pre-clinical trials. But the failure was observed; advanced cancer cases on anti-VEGF (receptor) therapy did not prolong survival of

the patients. This failure was attributed to acquired resistance by tumor [48, 50, 52]. Clinical trials with anti-VEGF therapy showed enhancement in progression-free survival but, it was completely unsuccessful when the overall survival of patient was accounted [52]. Similar results were obtained in phase III clinical trial, VEGF inhibitor did not promote disease-free survival of the patient who had undergone tumor resection [53]. An interesting observation was made regarding monotherapy of VEGF (receptor) inhibitor which was highly effective in some cases but had side effects or was ineffective in certain tumor types [9]. Thus, identification of biomarkers associated with responsiveness of anti-VEGF (receptor) therapy needs to be done [54]. Inefficacy of anti VEGF therapy suggested requirement for better preclinical cancer models, as various studies have observed numerous factors leading to poor efficacy of anti VEGF therapy, as listed in table 3.4 [48, 50, 52, 55, 56]. Some of these factors include presence of other pro-angiogenic molecules in the tumor microenvironment, sprouting independent blood vessel formation, poor understanding of blood vessel feature in the micro-metastatic niche [9]. One of the major factors for which endothelial cells were suggested as the better target, was genomic stability but reports of genetic aberrations in tumor endothelial cells pose a significant question regarding targeting endothelial cells for cancer therapy [10]. One of the important causes of concern regarding anti-angiogenic therapy is the difference in findings concerning the efficacy of anti VEGF (receptor) therapy. Studies have demonstrated recently that VEGF blockade led to the development of aggressive tumor phenotype promoting metastasis and recruitment of inflammatory cells via enhanced hypoxia [52]. These observations have sparked debate, as malignancy was not observed during preclinical studies [57] and derives support from a large number of meta-analyses data, as they

have not reported of poor clinical outcome [52, 58]. One of the preclinical studies where VEGF blockade led to the development of aggressive phenotype was in glioblastoma, in this study the aggressive phenotype was attributed to hypoxic cancer stem cell niche [59]. These conflicting findings have definitely made it difficult to pursue with VEGF blockade therapy, but identification of proper dose and duration has become essential [9]. Amidst all these conundrums it is essential to look into other targets and approaches for cancer therapeutics via anti-angiogenic therapy.

Table (3.4): Various factors leading to evasion of VEGF (receptor) blockade (Source: Adopted from Potente et al. 2011) [9]

S. No.	Organ system	Description
1	VEGF independent vessel growth	Tumors produce additional proangiogenic molecules besides VEGF, before or after treatment with VEGF (receptor) blockers.
2	Sprouting independent vessel growth	Tumors possess/switch to modes of vessel growth (vessel co-option, vascular mimicry, intussusception etc.) that can be less sensitive to VEGF (receptor) blockade.
3	Stromal cells	Both myeloid cells and cancer-associated fibroblasts produce other proangiogenic factors besides VEGF or recruit proangiogenic bone marrow-derived cells.
4	Endothelial cell instability	Endothelial cells with cytogenetic abnormalities or tumor ECs, which differentiate from cancer stem cell-like cells (as in glioblastoma), may not be as sensitive to VEGF (receptor) blockade as sprouting Endothelial Cells (EC).
5	Vascular independence	Mutant tumor clones or inflammatory cells are able to survive in hypoxic tumors; their reduced vascular dependence impairs the antiangiogenic response. Certain

		tumors have a hypo-vascular stroma. Tumors can also metastasize via lymphatics; their growth may not be blocked by antiangiogenic therapy.
6	Mature vessels	Mature supply vessels are covered by vascular smooth muscle cells and not easily pruned by endothelial cell targeted treatment.
7	Endothelial cell radio-resistance	Hypoxic activation of HIF1 α renders ECs resistant to irradiation.
8	Organ specific differences	Tumors show opposite invasive behaviors depending on the organ of inoculation.
9	Gene variations	Gene variations in VEGF receptors determine the responsiveness to VEGF (receptor) blockade.
10	Vessel normalization	Transient vessel normalization can reduce antiangiogenic drug delivery and efficacy; alternatively, barrier tightening could impede drug penetration.
11	Primary tumor vs metastasis tumor	Distinct signals regulate angiogenesis in primary versus metastatic tumors.

3.6. Alternative Approach for Anti Angiogenic Therapy:

The above discussion suggests that available anti-angiogenic therapy is designed to starve tumor tissue and induce tumor cell death. A similar approach to various other targets, apart from VEGF, is being developed [9]. However, alternative therapies (other than vessel destruction) are also being considered [9].

VEGF inhibitors were effective in destroying vessels with poor pericytes coverage. Thus, a combinatorial therapeutic approach was applied, where PDGF (receptor) inhibitors along with VEGF (receptor) inhibitor were used for treatment. The therapeutic approach was expected to target pericytes and endothelial cells rendering

regression of tumor vasculature, but never met the expectations as no significant effect was observed in the survival of cancer patients [9, 60].

Sustained vessel normalization works by converting tumor vessel into normal, which in turn would improve perfusion and oxygenation in the tumor, counteracting the effect of hypoxia. Hypoxia driven genes regulate various tumor promoting properties viz. epithelial-mesenchymal transition, invasion and intravasation, which activate the metastatic switch [13, 61, 62]. Normalized vessel wall would prevent intravasation of tumor cells and also would improve the effect of chemotherapy or immunotherapy [13, 61, 62].

As we have discussed above, success at the clinical trial level and failure in reality, which later on was attributed to presence of previously unknown escape mechanisms, indicating towards an incomplete understanding of angiogenesis process. Therefore, identification of novel regulators of angiogenesis has become important. miRNA based regulation of angiogenesis has been reported in recent years [63]. Targeting these miRNAs might help in preventing the angiogenic switch, therefore can be considered as potential therapeutic targets [63]. Another approach is to find putative angiogenesis regulators and validate their role in angiogenesis and tumorigenesis, for which FRG1 is a candidate gene. Limited studies have reported its involvement in the development of blood vessels and muscles [16, 18]. Search for the novel therapeutic targets and regulatory mechanism has now become essential to develop a better anti-angiogenic therapy. Therefore deciphering the effect and underlying mechanism on how FRG1 affects tumor angiogenesis and tumorigenesis may prove to be a valuable step towards the development of anti-angiogenic therapy leading to enhanced survival amongst the cancer patients.

3.7. FSHD Region Gene 1 (FRG1):

FRG1 which was discovered in the year of 1996 as a primary candidate gene for FSHD, primary research focus has always been regarding muscle development and function [14]. Till date, studies have demonstrated it is essential for muscle function, but no concrete understanding has been derived how it regulates muscle development [64]. FRG1 homolog has been reported to be present from drosophila to human and is considered to affect muscle development, but the underlying conserved molecular mechanism is unclear. Here we are providing an overview of the gene, based on available literature and why we considered it to have the role in tumorigenesis and angiogenesis.

FRG1 gene is located at 4q35, around 120kb centromeric to D4Z4 repeats. FRG1 is flanked by the set of genes, which are also associated with FSHD namely, ANT1, FRG2, and DUX4. FSHD pathophysiology is associated with deletion of these D4Z4 repeats at 4q35 [65]. FRG1 gene spans at length of 22,386 bp which harbors nine exons leading to the formation of the mature transcript of 1028 bp [14]. 258 amino acid long polypeptide chain is synthesized from the open reading frame of the mature transcript, with the molecular weight of protein approximately 30 kilodalton (Figure 3.5) [66].

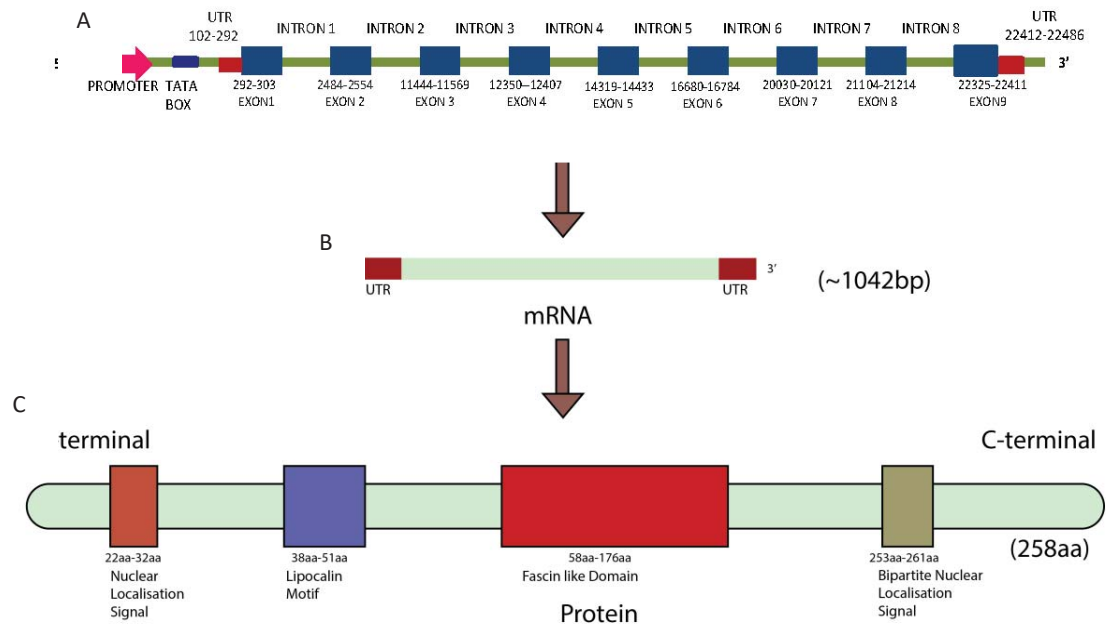


Figure (3.5): Schematic presentation for FRG1 gene, mRNA and protein. **A.** shows distribution of promoter, regulatory elements, exons and introns in FRG1 gene. Numbers show distance in base pair. **B.** Mature transcript of FRG1, its length and UTRs. **C.** shows different domains in FRG1 protein. aa depicts the amino acid positions of domains (*Adopted from Hansda et al. 2017*) [64].

Presence of FRG1 homolog in *Xenopus laevis*, *Mus musculus*, *Fugu rubireps*, *Caenorhabditis elegans*, *Brugi malayi* led us to believe that gene is highly conserved among vertebrates and invertebrates [64, 67]. The evolution of the gene in hominid could be traced back to old world monkey *Macaca mulatta*, which is known to harbor single FRG1 orthologue at 4q along with the single copy of pseudo gene. Presence of FRG1 pseudo gene has been reported in humans at chromosome 13, 14, 15, 20, 21 and 22 [66]. This finding was supported by Expressed Sequence Tag (EST) analysis, which confirmed the presence of these pseudo genes throughout the genome [67]. Sequence analysis of great apes and *Macaca mulatta* showed the conserved pattern with Alu-Sx repeat and Alu-J monomer (FRAM), both of which belong to oldest subfamilies of Alu elements in intron 7. These findings indicate common ancestry of

FRG1 gene in hominids. Initial duplication of FRG1 gene, along with D4Z4 repeats, occurred in common ancestor of hominid and *Macaca mulatta* around 33 million years ago [64, 68]. Conservation of protein sequences among invertebrates and vertebrates suggests it has certain fundamental function essential for survival (Figure 3.6). FRG1 consists of a lipocalin domain and thus was suggested to belong to this particular super family of proteins [14]. Further analysis revealed the presence of a nuclear localization signal and a conserved fascin like domain [69, 70], followed by a bipartite nuclear localization signal at carboxy-terminal (253-261 aa) (Figure 3.6) [69]. Presence of nuclear localization signal in FRG1 led to the belief that FRG1 and its homolog are localized in the nucleus, and was proven by expressing EGFP tagged FRG1 in U2OS cells [69]. Additionally, the EGFP signals were also observed in nuclear speckle [69]. *fg1*, the *Xenopus* homolog, was found to be associated with nascent mRNA chain in *Xenopus* oocytes which was verified by RNA immunoprecipitation [71].

FRG1 is also localized in the cytoplasm, particularly as an actin-bundling protein. Actin bundling functions can be imparted to fascin domain. Fascins are the family of actin-bundling protein, which are also known to regulate actin polymerization [72, 73].

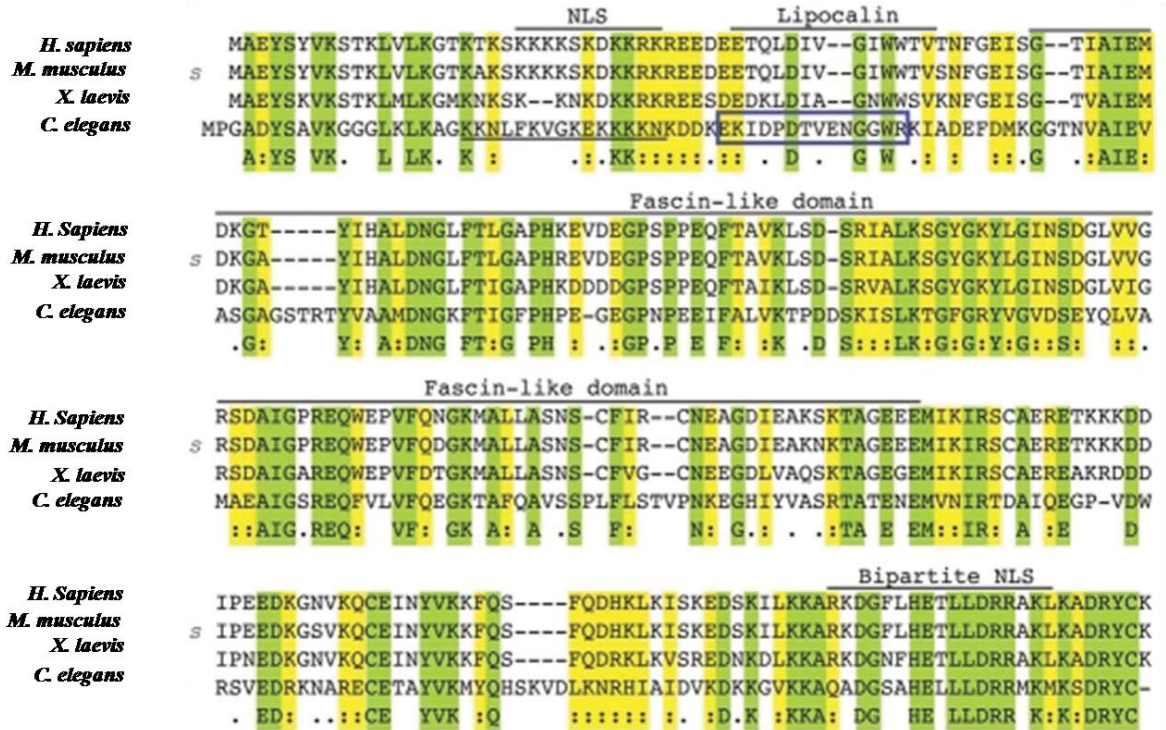


Figure (3.6): Conservation of FRG1 protein throughout various species with domain wise breakup. Green highlighted amino acids represent identical amino acids throughout the species. Yellow highlight represents similar set of amino acids throughout the species. (Adopted from Liu et al. 2010) [70].

3.8. FRG1 Associated Diseases and Molecular Function:

FRG1, the name itself suggests its association with FSHD. Most of the studies involving FRG1 have primarily focused on FSHD pathophysiology. FSHD is manifested with the loss of D4Z4 repeats which was thought to regulate FRG1 expression [64]. Loss of D4Z4 repeats results in enhanced expression of FRG1, leading to the development of FSHD [15]. To address the involvement of FRG1 in FSHD pathology, transgenic mice model was developed with high expression of FRG1 (FRG1^{high}) [74]; in this study, high FRG1 expression led to the development of FSHD like phenotype in mice [74]. Association of FRG1 with FSHD was further justified when FRG1 levels in FRG1^{high} mice was reduced by RNAi targeting, which

led to the restoration of normal muscle phenotype by reduction of the myopathic feature in mice [75]. FRG1 is one of the plausible targets regulating FSHD pathology. Therefore, various studies were performed to elucidate its significance in developmental aspect, which could also be supported by very fact that it is highly conserved among vertebrates and invertebrates. Frg1 has shown to regulate muscle development in *Xenopus* [18]. Temporal analysis of *frg1* expression showed reduction during embryonic development. Frg1 levels were altered in *Xenopus* by injecting morpholinos and rescued with Frg1 mRNA. Knockdown of Frg1 led to the development of smaller myotome [18]. Epaxial muscles altered due to the reduction in delamination, owing to reduced levels of Pax3 and MyoD [18]. Ectopic expression showed disrupted muscle physiology with enhanced delamination [18]. Hence these findings suggest that level of Frg1 expression is crucial for the development of muscle. The molecular function of FRG1 is not clearly understood till date, but two processes stand out i.e. F-actin bundling/ regulating motility and RNA biogenesis/ mRNA processing [64, 76]. We mentioned earlier that FRG1 have fascin domain and Fascins are the family of actin-bundling protein [73]. Multiple studies have demonstrated that FRG1 binds to actin. Immunocytochemistry based analysis in HeLa cells showed binding of FRG1 to F-actin [71], which was also verified by performing Gluteraldehyde cross-linking assay followed by co-sedimentation. These studies further validated interaction between F-actin and FRG1 [71]. The study in *C. elegans* has shown that *frg1* is associated with dense bodies, structural homolog to the focal adhesion point in mammalian cells. Focal adhesion points control cellular migration by regulating actin metabolism. *frg1* null mutants of *C. elegans* showed defects in

bending which could be attributed to an impaired interaction between actin and dense bodies [77].

Identification of the FRG1 protein in spliceosome C complex in human has provided evidence for its association with RNA biogenesis [78]. Further evidence could be derived from the study in *C. elegans*, where *frg1* was localized to a cluster of proteins known to regulate rRNA and mRNA biogenesis [79]. Additional shreds of evidence can be provided from studies identifying the effect of altered splice variants with FRG1 overexpression, enhancing muscular defects. One such example would be altered TNNT3 variant [80], affecting muscle strength and contractile properties, which cannot be restored even by restoration of certain positive regulators of muscle development like FHL1 [81]. Irrespective of all these understanding, key information is missing regarding the mechanism of action by FRG1. Its expression in human tissues has been determined at RNA level only, with no understanding of tissue specific localization and protein levels. Consequently, the role of FRG1 and the underlying fundamental molecular function is still a mystery.

3.9. FRG1's Association with Angiogenesis and Tumorigenesis:

It is very vital question that how the gene with the primary focus on muscular dystrophy, be associated with tumorigenesis and angiogenesis. The clear answer is yet to come, but literature provides supporting evidences. 75 % of FSHD patients have been reported to harbor retinal vasculature abnormalities [82, 83]. Moreover, the study has shown that FRG1 over expression leads to reduced proliferation of myoblasts, triggering muscular atrophy [84]. Study have shown patients with other muscular dystrophy tend to develop cancer; an example is DMD [85]. Transcription signatures of various muscular dystrophy patients were compared with tumor transcription

signatures, which revealed close resemblance between FSHD and Ewing's sarcoma [86]. This led us to hypothesize regarding the association of FRG1 with tumor angiogenesis (Figure 3.7).

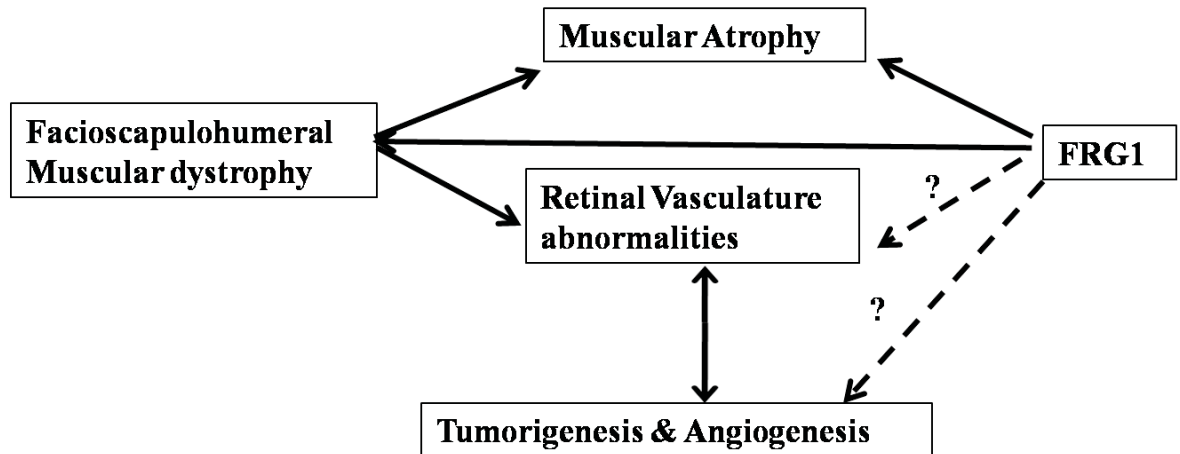


Figure (3.7): Schematic representation of our hypothesis in this study regarding involvement of FRG1 in tumorigenesis and angiogenesis.

To identify any link between FRG1 and angiogenesis comparative gene expression study of 30 FSHD patients harboring retinal vasculature abnormalities, along with healthy individuals was done. Findings of this study showed, no significant change in FRG1 expression level in patients compared to healthy individual [17].

Another study on *Xenopus* model reported that *frg1* levels dictate angiogenesis during *Xenopus* development [16]. Effect of *frg1* on angiogenesis was measured by altering *frg1* levels and looking for expression levels of angiogenesis marker *dab2*, which is homolog of DAB2 a known tumor suppressor in humans [64]. Injection of morpholino against *frg1* into *Xenopus* embryo led to reduction in *dab2* levels, which meant reduced angiogenesis [16]. Injection of *frg1* mRNA in these embryos (with *frg1* knock down) rescued *dab2* levels and restored angiogenesis (Figure 3.8.A). To confirm the effect of *frg1* on vasculogenesis, expression level of *msr* (a

vasculogenesis marker) was observed, but no reduction on *msr* was noticed [16]. Transgenic expression of *Frg1* in *Xenopus* embryos led to formation of disrupted and leaky blood vessels, leading to formation of blood islands, which represented the blood vessels phenotype similar to tumor blood vessels [16] (Figure 3.8.B).

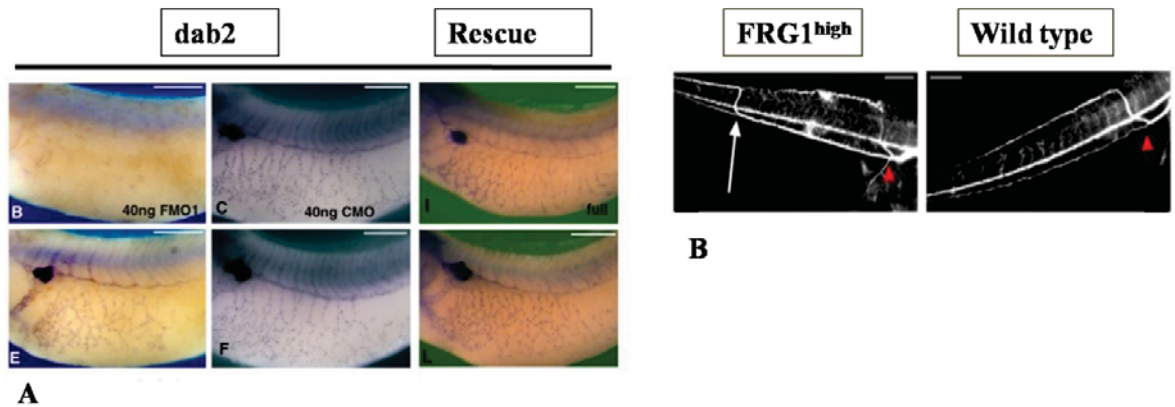


Figure (3.8): Effect of *Frg1* expression on angiogenesis in *Xenopus* embryos. **A.** *FRG1* knockdown by injecting morpholino into *Xenopus* embryos led to reduction of *dab2* a vascular marker. *Dab2* levels were restored when *frg1* mRNA was injected into these embryos. **B.** Transgenic expression of *frg1* in *Xenopus* led to formation of abnormal blood vessel. Figure shows that the vessel branching, pattern and structure is disrupted in transgenic *frg1* embryo compared to wild type. (Adopted from *Wuebbles et al. 2009*) [16].

Findings from the study in *Xenopus laevis* provided a significant link between *FRG1* and angiogenesis but no clear idea has been published suggesting the involvement of *FRG1* in tumor progression. During our review of the literature, we found few reports, which provided us with information that could link *FRG1* to tumor progression independent of angiogenesis.

The study by Hanel et al. observed that *frg1* knockdown led to reduction in cell migration from myotome [18]. Moreover, they observed the change in Vimentin levels, which is an EMT marker. It is noteworthy that cancer cells at advanced stage undergo EMT that promotes metastasis and tend to have higher vimentin levels. In *Xenopus* embryos, *frg1* knockdown led to reduced vimentin levels suggesting *frg1* levels regulate EMT or MET (Figure 3.9) [18].

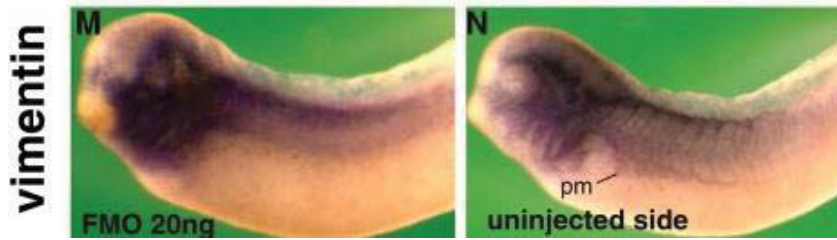


Figure (3.9): Comparison of Vimentin Expression levels in Xenopus embryos. Left panel shows embryo with FRG1 knockdown and right panel shows wild type embryo. FRG1 reduction leads to reduction in Vimentin level, left panel showing low Vimentin levels, compared to right panel. (Adopted from Hanel et al. 2010) [18].

FRG1 has been associated with other developmental processes apart for musculature and vasculature development. Role of FRG1 was implicated in odontoblasts development and its function through BMP4 [19]. BMP4 treatment affects FRG1 localization in mDEC6 cells [19]. FRG1 shuttles between nucleus and cytoplasm and have different roles in different cellular compartments. BMP4 is a known tumor suppressor and its association with FRG1 indirectly pointed out towards FRG1's potential association with tumorigenesis. One interesting case reports emerged during this period, which for the first time reported that FSHD patient developed breast cancer [87]. Another report presenting loss of FRG1 in migratory breast cancer cells, compared to non-migratory breast cancer cells, provides enough room to suspect the role of FRG1 in tumor progression [20]. These studies may not provide the distinct picture of FRG1's involvement in tumorigenesis but they definitely raise questions, is FRG1 involved in tumorigenesis, if yes how?

4. MATERIALS AND METHODS

4. MATERIALS AND METHODS:

4.1. Oncomine Analysis:

Oncomine cancer microarray database ([http:// www.oncomine.org](http://www.oncomine.org)) [88] was used to determine gene expression of FRG1 in various tumor types. For analysis, we set thresholds of p value ≤ 0.05 and fold change ≥ 1.5 and, comparisons were drawn between tumor and normal group.

4.2. Kaplan Meier Plotter Analysis:

Kaplan Meier plotter (<http://kmplot.com/analysis>) [89] analysis was done to determine the prognostic value of FRG1 gene expression. Overall survival (OS) was analyzed in Breast (N = 4142), Ovarian (N = 1648), Lung (N = 2437) and, Gastric (N = 1065) cancer. Patients were divided into two groups, FRG1 high and FRG1 low, based on gene expression. Comparative survival analysis was done between both the groups. To ascertain the effect of FRG1 expression on survival, Hazard Ratio (HR) with 95% CI, was calculated, along with the log rank p value. p value of ≤ 0.05 , was considered to be significant.

4.3. Immunohistochemistry:

4.3.1. Reagents for Immunohistochemistry: Buffered Formalin (10 % Formalin; 0.025 M sodium dihydrogen phosphate; 0.046 M disodium hydrogen phosphate in distilled water), Poly-L-Lysine (Sigma), Acetone (Merck), Xylene (Merck), Ethanol (Merck), Fibrinogen (Instrumentation laboratory), Paraffin (Fischer scientific), Haematoxylin (HiMedia), Eosin (HiMedia), Tris Buffered Saline pH 7.2 (0.05 M Tris, 0.8 % NaCl), Tris-EDTA buffer pH 9 (10 mM Tris, 1 mM EDTA), EnVision Flex HRP (Dako), EnVision Flex DAB + Chromogen (Dako), EnVision Flex Peroxidase

Blocking Reagent (Dako), EnVision Flex Substrate Buffer (Dako), DPX mountant (Fisher scientific).

4.3.2. Poly-L-Lysine Coating of Slides: Glass slides were washed with detergent followed by 1 % acetic acid ethanol solution. Slides are dried completely prior to Poly-L Lysine coating using hot air oven until all traces of liquid disappears. Washed slides are immersed into 0.01 % Poly-L-Lysine solution for 20 minutes followed by two dips of distilled water. Slides were dried at 37⁰ Celsius overnight prior to use, for immunohistochemistry.

4.3.3. Preparation of Control Cell Block: HeLa cells were harvested from a T25 flask. Harvested cells were mixed with fibrinogen at 1:2 ratios and incubated at 37⁰ Celsius for 1 minute. Cell coagulant was fixed in 10 % buffered formalin followed by dehydration using alcohol gradient from 50 % - 100 %. Dehydrated cell coagulant was washed with acetone for 30 minutes followed by two rounds of incubation in xylene for 1 hour each. Cell coagulant was incubated in paraffin at 36⁰ Celsius for 1 hour and paraffin embedding was done.

4.3.4. Immunohistochemistry Protocol: FFPE blocks of various tumor types were identified from tissue archives of SRL Diagnostics Bhubaneswar. Ethical clearance for the study was taken from Institutional Ethics Committee (BioEthics # MD-1), NISER, Bhubaneswar. Information regarding list of antibodies used for immunohistochemistry along with protocols and clones is given in the (Table 4.1). 4 µm thick sections of FFPE blocks were cut and placed on Poly-L-Lysine coated slides. Sections were deparaffinized and rehydrated using alcohol gradient from 100 % to 50 %. Endogenous Peroxidase activity of the rehydrated sections was blocked using EnVision Flex Peroxidase Blocking Reagent by incubating at room temperature for 10

minutes. Primary antibody incubation was done as per the conditions given in table 4.1, followed by incubation with EnVision Flex HRP secondary antibody for 30 minutes. EnVision Flex DAB + Chromogen and EnVision Flex Substrate Buffer was applied for 5 minutes for development of color, proceeded by counter stain with haematoxylin HeLa cell block was used as positive control for anti-FRG1 antibody and mouse IgG isotype was used as negative control.

4.3.5. Immunohistochemistry Scoring: Immunohistochemistry (IHC) scoring was performed by two independent pathologists. FRG1 expression levels were scored in paired tumor tissue and uninvolved (normal) tissue, for intensity of staining and percent positive cells. Intensity of staining was scored in a scale of 0-3; where 0 = negative, 1 = weak, 2 = moderate and, 3 = strong. Percent positivity of cells was scored in a scale of 0-5; where 0 = negative, 1 < 1 %, 2 = 1 – 10 %, 3 = 11 – 33 %, 4 = 34 – 66 % and, 5 ≥ 67 %. To calculate FRG1 expression levels, Allred scores were derived, using the following formula; **Allred score = Staining intensity + Percent positive cells**. Allred scores were categorized in Low = 1 – 2, Moderate = 3 – 6, High = 7 – 8 [90]. Accordingly FRG1 expression levels were categorized into these three groups, in both tumor and uninvolved tissues.

4.3.6. Micro-Vessel Density Analysis: CD31 a known vascular marker was used to stain blood vessel. Micro vessel density (MVD) analysis was performed as per Weidner et al. [6]. Three highly vascularized areas were identified at low magnification (40 X) and micro vessels at these hotspots were counted at higher magnification (200 X). The hotspot with highest number of micro vessel was considered as MVD count.

Table (4.1): List of Immunohistochemical Markers and Protocols

IHC Markers	Antibody Clone	Vendor	Dilution	Antigen Retrieval Buffer	Incubation Time for the Antibody	Antigen Retrieval Instrument	Detection Kit
CD31	JC70A	Dako, USA	Prediluted	High pH	60 minutes	Microwave	Envision+ System-HRP Labeled Polymer-Anti-mouse
FRG1	N/A	Biorbyt, UK	1:100	High pH	60 minutes	Microwave	Envision+ System-HRP Labeled Polymer-Anti-mouse

4.4. Plasmid Preparation:

4.4.1. Reagents for Plasmid Preparation: LB Agar (Miller) (HiMedia), L B Broth (Miller) (HiMedia), Ampicillin (100 mg/ml in autoclaved Mili Q water) (Sigma), Kanamycin (50 mg/ml in autoclaved Mili Q water) (Sigma), Ethanol (Merck), Isopropanol (Sigma), Plasmid mini kit (Qiagen), Plasmid midi kit (Qiagen), PIPES (0.5 M in distilled water, pH 6.7) (Sigma), KOH (Sigma), MnCl₂.4H₂O (HiMedia), CaCl₂.2H₂O (HiMedia), KCl (Sigma), DMSO (MP Biomedicals), Glycerol (50 % in autoclaved Mili Q water) (HiMedia), Inoue Buffer (55 mM MnCl₂.4H₂O, 15 mM CaCl₂.2H₂O, 250 mM KCl, 10 mM PIPES in autoclaved Mili Q water).

4.4.2. Plasmids: FRG1 coding sequence, cloned into pCMV6.XL5 mammalian expression vector, was procured from Origene, along with pCMV6.XL5 empty vector. We procured FRG1 shRNA- pLKO.1 vector from Sigma, along with scrambled shRNA in pLKO.1 vector.

4.4.3. Preparation of *E. coli* (DH5 α) Competent Cells: DH5 α ultra competent cells were prepared as per Inoue method [91]. Single colony of DH5 α grown in LB agar

plate for 16 hours at 37⁰ Celsius, was picked and transferred to 5 ml of Lysogeny Broth (LB) and incubated for 16 hours at 37⁰ Celsius. 0.5 ml of starter culture was transferred to 250 ml of LB Broth and incubated at 18⁰ Celsius and 125 rpm. Culture was grown until the OD reached 0.55, once the desired OD was obtained; culture flask was transferred to ice and incubated for 10 minutes. Cells were harvested by centrifugation at 2,500 g for 10 minutes at 4⁰ Celsius in a 50 ml falcon tube. Media was completely removed and cells were re-suspended gently in 80 ml Inoue buffer. Cells were further centrifuged at 2,500 g for 10 minutes at 4⁰ Celsius, supernatant was discarded and pellet was re-suspended gently in 20 ml Inoue buffer. 1.5 ml of DMSO was added to the bacterial cell suspension followed by 10 minutes incubation in ice. To make aliquots for future use, 50 µl of suspension was added to chilled 1.5 ml micro centrifuge tubes. The micro centrifuge tubes were snap chilled in liquid nitrogen and moved to -80⁰ Celsius freezer.

4.4.4. Transformation Protocol: Transformation was performed as per heat shock method [92]. DH5 α competent cells were taken out from -80⁰ Celsius freezer, kept in ice and incubated for 10 minutes after adding 50 ng of plasmid DNA. Heat shock treatment was given to the bacterial cells by incubating in a circulating water bath at 42⁰ Celsius for 45 seconds and immediately transferred on ice for 2 minutes. 1 ml of warm LB broth was added to the transformed cells and incubated for 20 minutes, at 37⁰ Celsius and 225 rpm. 100 µl of transformed cell suspension was plated to LB agar plate with respective antibiotic for positive clone selection.

4.4.5. Plasmid Purification Protocol: Plasmid purification was done at miniprep and midiprep scales. 5 ml culture was set up for miniprep plasmid preparation and plasmid purification was done using QIAprepSpin Miniprep Kit (Qiagen) as per

manufacturer's instructions (refer to appendix 8.1). 100 ml of culture was prepared for midiprep plasmid preparation; plasmid purification was done using Qiagen Plasmid Midi Kit (Qiagen) as per the maker's protocol (refer to appendix 8.2).

4.4.6. Preparation of Glycerol Stock: Confirmed positive clones were grown in 2 ml LB broth using appropriate antibiotic, for 12 hours. 2 ml of 50 % glycerol was added to the culture and an aliquot of 1 ml mix was transferred to each cryovial. The cryovials were stored at -80⁰ Celsius freezer until use.

4.5. Cell Culture:

4.5.1. Reagents for Cell Culture: DMEM (Pan Biotech), HiGlutaXL RPMI1640 (HiMedia), HiEndoXl Endothelial Cell Growth Medium (HiMedia), PBS pH 7.4 (HiMedia) DPBS pH 7.4 (Pan Biotech), Trypsin-EDTA (Pan Biotech), Fetal Bovine Serum (Pan Biotech), Penicillin Streptomycin (Pan Biotech), Amphotericin B (HiMedia), Trypan-Blue (0.4 % in PBS) (HiMedia), Puromycin (1 mg/ml in autoclaved Mili Q water) (MP Biomedicals), DMSO (MP Biomedicals), Lipofectamine 3000 (Invitrogen).

4.5.2. Preparation of Media: DMEM and RPMI1640 were supplemented with 100 units/ml of Penicillin, 50 µg/ml Streptomycin, 0.25µg/ml Amphotericin B and 10 % FBS. Complete media was filtered through 0.2 µm vacuum driven filter unit (Biofil); thereafter it was stored at 4⁰ Celsius. HiEndoXL endothelial cell growth medium was constituted by mixing part A and part B components. Complete endothelial cell growth medium was filtered through 0.2 µm vacuum driven filter unit (Biofil) and stored at 4⁰ Celsius. Freezing medium was prepared for cryopreservation of cells, by adding 10 % DMSO to FBS.

4.5.3. Cell Culture Protocol: HEK293T cell line is a derivative of Human Embryonic Kidney 293 cells with SV40 T antigen. HEK293T cell line was procured from National Centre for Cell Science (NCCS) and maintained in complete DMEM. Human Umbilical Vein Endothelial Cells, which are isolated from endothelium of veins of umbilical cord, were procured from HiMedia, Mumbai. HUVECs were maintained in complete HiEndoXL endothelial cell growth medium. DU145 cell line is derived from metastatic lesion of primary adenocarcinoma prostate, at central nervous system of 69 year old Caucasian male. DU145 was obtained from Dr. Rajeeb Swain's Lab from Institute of Life Sciences, Bhubaneswar and was maintained in complete DMEM. PC3 cell line was established from grade IV adenocarcinoma bone metastatic lesion from a 62 year old Caucasian male and was procured from NCCS, Pune. PC3 cell line was maintained in complete RPMI1640. MCF7 cell line is derived from pleural effusion of malignant adenocarcinoma of breast, from 69 year old Caucasian female. MCF7 cell line was obtained from NCCS, Pune and was maintained in complete DMEM. All cell lines were grown at 37⁰ Celsius and 5 % CO₂, for various experiments.

4.5.4. Revival of Cells: Frozen vial of cell line was retrieved from liquid nitrogen dewar and placed in water bath maintained at 37⁰ Celsius. Thawed cell suspension was transferred to pre warmed complete media in a 15 ml centrifuge tube. Cell suspension was centrifuged at 200 g for 5 minutes. Thereafter supernatant was discarded and pellet was resuspended into 6 ml pre-warmed complete media and transferred to a T-25 cm² cell culture flask and incubated, at 37⁰ Celsius and 5 % CO₂.

4.5.5. Subculture, Splitting and Trypsinization of Cells: Splitting or sub culture of cell lines/ primary cells was done once cells reached at confluency of 80 %. Cells were washed twice with DPBS, subsequently trypsin-EDTA was added to cell culture

flasks and incubated at 37⁰ Celsius until cells detach from surface. Complete medium was added to neutralize trypsin activity; acquired cell suspension was centrifuged at 200 g for 5 minutes. Supernatant was discarded and pellet was re-suspended in complete medium Total viable cell count was determined using trypan-blue stain in haemocytometer and required numbers of viable cells were seeded into culture plates. Culture plates were incubated into humidified incubator, at 37⁰ Celsius and 5 % CO₂.

4.5.6. Cell Freezing and Cryopreservation: Cells with around 70 – 80 % confluency were washed twice with PBS and trypsinized. Total cell count was determined and cells were centrifuged at 200 g for 5 minutes. Supernatant was discarded and pellet was re-suspended in freezing medium at cell concentration of 1 x 10⁶ cells per ml. One ml of suspension was dispensed into each cryovial and transferred into – 1⁰ Celsius per minute cooler and kept - 80⁰ Celsius freezer. 24 hours later vials were transferred into liquid nitrogen dewar for long term storage.

4.5.7. Transient Transfection: To identify effect of FRG1 expression on various cell lines transient transfection was performed in HEK293T, DU145, PC3 and MCF7 cell lines for FRG1-pCMV6.XL5 or its empty vector pCMV6.XL5 0.5 x 10⁶ cells were seeded in a 6 well plate; transfection was carried out after 24 hours of seeding as per the instructions provided in the product manual of Lipofecatmine 3000 (refer to appendix 8.3). Transient transfections were also performed for PC3 cell line for FRG1 knockdown using FRG1sh-pLKO.1 vector along with pLKO.1-scrambled vector control (refer to appendix 8.3).

4.5.8. Stable Transfection: Stable line was prepared to determine effect of FRG1 knockdown (FRG1sh-pLKO.1) along with scrambled vector control (pLKO.1-scrambled) in HEK293T, DU145 and MCF7 cell lines. Cells were transfected as per

the manufacturer's 3000 (refer to appendix 8.3) for all three cell lines cells were subjected to antibiotic selection by adding 0.5 µg/ml puromycin in the growth medium after 48 hours. Stable clones were selected at 2 µg/ml of puromycin and expression levels were verified by western blot.

4.6. Cell Proliferation Assay:

4.6.1. Reagents for Cell Proliferation Assay: CellTiter 96 AQueous One solution Reagent (Promega).

4.6.2. Protocol for Cell Proliferation Assay in Transiently Transfected Cells: 2×10^3 cells were seeded into individual wells of 96 well plates. Transfections were performed (refer to section 4.5.7) and transfection mix was replaced after six hours with 5 % serum containing medium. Cells were grown for 96 hours and replaced with 100 µl of fresh medium prior to addition of 20 µl CellTiter 96 AQueous One solution reagent. Cells were incubated for two hours after addition of CellTiter 96 AQueous One solution reagent and absorbance was measured at 490 nm wavelength in Bio-rad iMark Microplate absorbance reader (Bio-rad). Experiments were performed three times with nine replicates in each group.

4.6.3. Protocol for Cell Proliferation Assay in Stable Cells: 3×10^3 cells were seeded in a 96 well plate. 24 hours after seeding, the growth medium was replaced with 5 % serum containing growth medium, subsequently cells were grown for 96 hours in 5 % serum containing growth medium. 96 hours later cells were replenished with 90 µl fresh medium followed by addition of 20 µl CellTiter 96 AQueous One solution reagent. After two hours of incubation absorbance was measured at 490 nm wavelengths in Bio-rad iMark Microplate absorbance reader (Bio-rad). Experiments were performed three times with nine replicates in each group.

4.6.4. Protocol for Cell Proliferation Assay in HUVECs: 5×10^3 HUVECs were seeded in 96 well plates. 24 hours after seeding cells media was replaced with conditioned medium obtained from transfected HEK293T. HUVECs were grown for 96 hours in conditioned media and henceforth replaced with 100 μ l fresh medium along with 20 μ l CellTiter 96 AQueous One solution reagent. Plates were incubated for two hours followed by measurement of absorbance at 490 nm wavelength using Bio-Rad iMark Microplate absorbance reader (Bio-Rad). Experiments were performed three times with nine replicates in each group.

4.7. Scratch Wound Healing Assay:

4.7.1. Reagents for Scratch Wound Healing Assay: Phosphate Buffered Saline (pH 7.4) (HiMedia).

4.7.2. Protocol for Scratch Wound Healing Assay for Transiently Transfected Cells: 0.25×10^6 cells were seeded in a 6 well plate. 24 hours after seeding, cells were transfected and grown for 48 hours. Thereafter, scratch was made using a P200 tip and cells were washed with PBS. Cells were grown in reduced serum medium (2 % FBS) and images of scratch wound were taken at 0, 24 and 48 hours for each cell line, depending on the wound closure speed. Imaging was done under Primovert inverted microscope (Ziess). Cell migration was analyzed using NIH ImageJ software. The experiments were conducted in triplicates.

4.7.3. Protocol for Scratch Wound Healing Assay of Stable Cells: 0.5×10^6 cells were seeded in a 6 well plate, a scratch was made with P200 tip after cells formed a fully confluent monolayer, which was subsequently washed with PBS. Images of scratch were taken at 0, 24 and 48 hours for each cell line, grown in reduced serum

medium (2 % FBS), under Primovert inverted microscope (Zeiss). Cell migration was analyzed using NIH ImageJ software. The experiments were conducted in triplicates.

4.8. Transwell Migration Assay:

4.8.1. Reagents for Transwell Migration Assay: 8 μm pore size 12 well plate transwell growth chambers (Milipore), Methanol (Merck), Giemsa (Fisher scientific), PBS (pH-7.4) (HiMedia).

4.8.2. Transwell Migration Assay Protocol for Cell lines: 2×10^4 cells (transfected transiently or stable lines) suspended in 500 μl serum free medium, were seeded in the 8 μm pore size transwell growth chamber. Prior to addition of cells, one ml complete medium was added in the lower chambers of the well plates. The plates were incubated at 37⁰ Celsius and 5 % CO₂. After 24 hours of incubation, media was removed from transwell inserts and washed with PBS twice, afterwards cells were fixed and permeabilized by adding 200 μl of methanol and incubated at 4⁰ Celsius for 20 minutes. Following the incubation, inserts were retrieved and cells were washed with PBS twice. 300 μl of Giemsa stain was added to the washed inserts and incubated in dark for 15 minutes at room temperature. Further, cells were washed with PBS and the upper layer of cells was removed using a cotton swab. Imaging was performed using CKX41 inverted microscope and the cells were counted in five different view fields, using NIH ImageJ software. The experiment was conducted in triplicate.

4.8.3. Transwell Migration Assay Protocol for HUVECs: 0.2×10^6 HEK293T cells transfected with FRG1 over expression vector along with empty vector control was grown in a 12 well plate. 36 hours after transfection of HEK293T, 2×10^4 HUVECs were seeded in the upper chamber of the transwell growth inserts. The plates were

incubated for 24 hours at 37⁰ Celsius and 5 % CO₂. Further, media was removed from the inserts and washed with PBS, which was followed by addition of 300 µl methanol for permeabilization and fixation of the cells. Inserts were washed with PBS and incubated in 200 µl of Giemsa stain for 15 minutes. Inserts were washed with PBS and cells at the upper layer were removed by cotton swab. Imaging was performed using CKX41 inverted microscope (Olympus) and the cells were counted in five different view fields at 10 X magnification, using NIH ImageJ software. The experiment was conducted in triplicate.

4.9. Matrigel Invasion Assay:

4.9.1. Reagents for Matrigel Invasion Assay: Growth Factor Reduced Matrigel (Corning), 8 µm pore size 12 well plate transwell growth chambers (Milipore), Methanol (Merck), Giemsa (Fisher scientific), PBS (pH 7.4) (HiMedia), DMEM (Pan Biotech).

4.9.2. Matrigel Invasion Assay Protocol: Growth factor reduced matrigel was thawed and diluted in DMEM with final protein concentration of 0.5 mg/ml. 100 µl diluted matrigel was added to transwell inserts and incubated at 37⁰ Celsius for two hours. Transiently transfected and stable cells were harvested and cell count was done. 2 x 10⁴ cells suspended in 500 µl of serum free medium were seeded into the chamber of transwell growth inserts; prior to that, 1 ml of complete media was dispensed into the lower chamber. The plates were incubated for 24 hours at 37⁰ Celsius and 5 % CO₂. Media from the insert was removed and washed with PBS; cells were fixed and permeabilized by addition of 300 µl of methanol with incubation at 4⁰ Celsius for 20 minutes. Inserts were washed with PBS and stained with Giemsa for 15 minutes, in dark. Inserts were washed with PBS and cells at the upper layer were removed by

cotton swab. Imaging was performed using CKX41 inverted microscope (Olympus) and the cells were counted in five different view fields, using NIH ImageJ software. The experiments were conducted in triplicates.

4.10. Matrigel Tubule Formation Assay:

4.10.1. Reagents for Matrigel Tubule Formation Assay: Matrigel (Corning), PBS (HiMedia).

4.10.2. Matrigel Tubule Formation Assay Protocol: Matrigel was thawed overnight at 4⁰ Celsius, following which, 50 µl of matrigel was plated into individual wells of a 96 well plate. Plate was incubated for 1 hour at 37⁰ Celsius to allow the matrigel to solidify. HUVECs were harvested from T75 flask and re-suspended in conditioned media; subsequently 5 x 10³ cells in 100 µl of conditioned medium were seeded into the matrigel coated wells and incubated at 37⁰ Celsius and 5 % CO₂. Images were acquired after six hours of incubation using a CKX41 inverted microscope (Olympus) at 4X magnification. Image analysis was performed using angiogenesis analyzer plugin in NIH ImageJ software.

4.11. Preparation of Cell Lysate:

4.11.1. Reagents for Preparation of Cell Lysate: RIPA lysis buffer (25 mM Tris-HCl pH 7.6, 150 mM NaCl, 1 % NP-40, 1 % Sodium deoxycholate, 0.1 % Sodium dodecyl sulphate) (Thermo), SIGMAFAST Protease Inhibitor (AEBSF 2 mM, Aprotinin 0.3 µM, Bestatin 130 µM, EDTA 1 mM, E-64 14 µM, Leupeptin 1 µM) (Sigma), PhosSTOP phosphatase inhibitor cocktail (Roche).

4.11.2. Protocol for Preparation of Cell Lysate: Cells were grown up to 80 – 90 % confluency in cell culture dishes and well plates. Cells were washed with PBS and lysed by adding ice-cold RIPA lysis buffer followed by incubation of 20 minutes in

ice. Lysate was centrifuged at 14,000 g for 15 minutes; supernatant was collected in a fresh micro centrifuge tube and stored at -80⁰ Celsius freezer for further use.

4.12. Estimation of Protein by BCA Method:

4.12.1. Reagents for Protein Estimation by BCA Method: Pierce BCA protein assay kit (Thermo), Bovine serum albumin (MP Biomedicals).

4.12.2. Protocol for Protein Estimation by BCA Method: Bovine serum albumin standards were prepared by making serial dilutions at 1.5 fold from 2 mg/ml BSA stock to 20 µg/ml, total of 8 dilutions of standard were prepared simultaneously working reagent (WR) was prepared by mixing BCA reagent A and BCA reagent B at 50:1 ratio. 10 µl of sample and BSA standard were dispensed to individual wells of 96 well plates. BSA standard were added in triplicates and samples were added in duplicates. Following addition of samples and BSA standard, 200 µl of working reagent (WR) was added to the wells, 10 µl RIPA buffer was used as blank. Plate was covered and incubated at 37⁰ Celsius for 30 minutes. Plate was retrieved and incubated at room temperature for 10 minutes and absorbance was measured at 562 nm using in iMark Microplate absorbance reader (Bio-Rad).

4.13. SDS-PAGE Electrophoresis:

4.13.1. Reagents for SDS-PAGE Electrophoresis: 30 % Acrylamide Bisacrylamide [29 g acrylamide, (Invitrogen) and 1 g Bis acrylamide, (Sigma) dissolved in 100 ml autoclaved Mili Q water], Laemmli buffer (0.1 % 2-Mercaptoethanol, 0.0005 % Bromophenol blue, 10 % Glycerol, 2 % SDS, 63 mM Tris-HCl pH 6.8), SDS-PAGE running buffer (25 mM Tris-HCl, 250 mM Glycine, 0.1 % SDS), Tris 1.5 M (pH 8.8), Tris 1 M (pH 6.8), 10 % SDS, 10 % APS (MP Biomedicals), TEMED (Sigma).

4.13.2. Protocol for SDS-PAGE Electrophoresis: 30 µg of Protein lysates were mixed with equal volume of 2X Laemmli buffer and boiled at 95⁰ Celsius for 5 minutes. 10 % or 12 % SDS PAGE resolving gel was prepared depending on the respective protein to be analyzed. 4 % stacking gel was prepared and protein samples were loaded into the wells and ran at constant voltage of 100V for the separation of protein samples. The composition of SDS-PAGE gel is mentioned in (Table 4.2).

Table (4.2): Composition of SDS-PAGE gel

Resolving Gel Constituents	Resolving Gel		Stacking Gel Constituents	Stacking Gel 4 % (2 ml)
	10 % (5 ml)	12 % (5 ml)		
30 % Acrylamide	1.66 ml	2.08 ml	30 % Acrylamide	340 µl
Mili Q H ₂ O	1.98 ml	1.57 ml	Mili Q H ₂ O	1.36 ml
1.5 M Tris (pH 8.8)	1.25 ml	1.25 ml	1 M Tris (pH 6.8)	250 µl
10 % SDS	50 µl	50 µl	10 % SDS	20 µl
10 % APS	50 µl	50 µl	10 % APS	20 µl
TEMED	5 µl	5 µl	TEMED	2 µl

4.14. Coomassie staining:

4.14.1. Reagents for Coomassie Staining: Coomassie staining solution (0.25 % Coomassie Brilliant Blue R 250, 45 % Methanol, 10 % acetic acid in distilled water), Destaining Solution (45 % Methanol, 10 % Acetic acid in distilled water).

4.14.2. Protocol for Coomassie Staining: SDS-PAGE gel was retrieved and immersed in Coomassie staining solution for 2 - 4 hours at room temperature under constant shaking. After completion of incubation, staining solution was replaced with destainer, consequently after removal of background stain, gels were kept in distilled water and scanned for future records.

4.15. Western Blot:

4.15.1. Reagents for Western Blot: Semi-dry transfer buffer, Tris-buffered saline (150 mM NaCl, 10 mM TrisHCl pH 8.0), Methanol (Merck), Tris-buffered saline TWEEN 20 (TBS-T) (0.1 % TWEEN 20 (v/v)), 150 mM NaCl, 10 mM TrisHCl (pH 8.0), Ponceau Staining solution (0.2 % Ponceau stain in 5 % acetic acid), Blocking buffer (3 % BSA in TBS or 5 % Milk powder in TBS), Antibody dilutions were prepared in 2.5 % BSA in TBS, Super Signal West Femto Maximum Sensitivity Substrate (Thermo scientific), Restore Western Blot Stripping Buffer (Thermo scientific), Immobilon-P Membrane, PVDF, 0.45 μ m (Milipore), Ponceau (HiMedia), TWEEN 20 (Sigma), BSA (MP Biomedicals), Skimmed Milk (HiMedia).

4.15.2. Protocol for Western Blot: Protein samples were resolved in SDS-PAGE gel; followed by transfer of proteins from gel to methanol activated Immobilon PVDF membrane, using semidry transfer buffer in Bio-Rad Transblot SD Semidry Transfer Cell (Bio-Rad) at 17 V for 1 hour. Visualization of transferred protein, was done by staining membrane with Ponceau Staining solution, which was later washed with MiliQ water to remove stain. Complete removal of Ponceau staining solution, was done by washing TBS-T for two minutes. The blot was incubated in blocking buffer for one hour, followed by three times TBS-T wash for five minutes each. Blot was incubated in diluted primary antibody overnight at 4⁰ Celsius. After completion of incubation, blot was washed with TBS-T, three times for five minutes each. Thereafter blot was incubated in HRP conjugated secondary antibody with respective dilutions as mentioned in (Table 4.3) at room temperature for one hour on the rocker. Secondary antibody was removed and blot was washed with TBS-T. Blot was developed by using SuperSignal West Femto Maximum Sensitivity Substrate as per manufacturer's

instructions in Chemidoc XRS+ (Bio-Rad). Exposure time intervals were determined as per the signal strength. To characterize another protein in same blot, stripping was performed using Restore Western Blot Stripping Buffer according to manufacturer's protocols. The lists of antibodies used are mentioned in table 4.3.

Table (4.3): List of Antibodies Used in Western Blotting

Antibody	Dilution	Vendor	Catalog	Origin
FRG1	1:1000	Novus Biologicals	H00002483-2146	Mouse
GAPDH	1:20000	Sigma	G9545	Rabbit
Beta Tubulin	1:2000	Cell Signaling Technologies	2146	Rabbit
Total - p38	1:1000	Cell Signaling Technologies	9212	Rabbit
Phospho - p38	1:1000	Cell Signaling Technologies	9211	Rabbit
Total – ERK	1:1000	Cell Signaling Technologies	9120	Rabbit
Phospho - ERK	1: 1000	Sigma	9102	Rabbit
HRP tagged mouse IgG	1:10000	Thermo Scientific	31452	Rabbit
HRP tagged Rabbit IgG	1: 10000	Cell Signaling Technologies	7074	Goat

4.16. RNA Extraction and cDNA Synthesis:

4.16.1. Reagents for RNA Extraction and cDNA Synthesis: RNeasy mini kit (Qiagen), Superscript IV Reverse Transcriptase (Invitrogen), Agarose (Lonza), Tris-Acetate-EDTA buffer (40 mM Tris-acetate and 1 mM EDTA).

4.16.2. Protocol for RNA Extraction and cDNA Synthesis: Cells were grown in six well plates until a confluency of 80 – 90 % is achieved. RNA extraction was done using RNeasy mini kit as per the manufacturer's instructions (refer to appendix 8.4), once the cells reach desired confluency. RNA quality was verified by resolving samples in 1 % agarose gel using 120 V for 15 minutes, simultaneously RNA concentration was determined by using Nanodrop 2000 (Thermo). After verification of RNA quality and quantity, 5 µg of each sample was subsequently used for cDNA synthesis using one unit of Superscript IV Reverse Transcriptase. cDNA synthesis thus was followed as per manufacturer's instructions (refer to appendix 8.5). cDNA was stored at -80⁰ Celsius, until further use for expression analysis.

4.17. Quantitative –Real Time PCR:

4.17.1. Reagents for Quantitative –Real Time PCR: Nuclease Free Water (Genei), Fast SYBR GREEN (Roche), Primers (Integrated DNA Technologies) (Primer set for individual genes are provided with respective sequence in table 4.6).

4.17.2. Protocol for Quantitative – Real Time PCR: cDNA from various samples were diluted to 5 ng/µl concentration and a total of 10 ng of cDNA was used for expression analysis. Reaction was setup in an optically clear 96 well plate as mentioned in table 4.4. Each reaction was set up in triplicates, added by a no template control (NTC). Optically clear sealing film was applied to the plates; the plates were centrifuged (Eppendorf, 5810R) at 1500 rpm in a swinging rotor for two minutes.

Reaction was set in ABI7500 real time PCR machine, using parameters as mentioned in table 4.5. GAPDH was used as reference gene, to quantify the expression levels by $\Delta\Delta C_t$ methods. List of primers are provided in table 4.6.

Table (4.4): Reaction mix for q-RT-PCR

Composition	cDNA	No Template Control
Template	2 μ l	0
2X SYBR GREEN	10 μ l	10 μ l
Primer Forward (2.5 μ M)	1 μ l	1 μ l
Primer Reverse (2.5 μ M)	1 μ l	1 μ l
H ₂ O	6 μ l	8 μ l
Total	20 μ l	20 μ l

Table (4.5): ABI 7500 Run protocol

Stage	Temperature	Time
Holding	50 ⁰ C	2 minutes
Holding	95 ⁰ C	10 minutes
Melting x 40 cycles	95 ⁰ C	15 seconds
(Annealing + extension) x 40 cycles	60 ⁰ C	1 minute

Table (4.6): List of Primers

Gene	Primer 5' ---- 3'
MMP1 F	AGAGCAGATGTGGACCATGC
MMP1 R	TTGTCCCGATGATCTCCCCT
MMP2 F	CGTCGCCCATCATCAAGTTC
MMP2 R	CAGGTATTGCACTGCCAACTC
MMP3 F	CACTCACAGACCTGACTCGG
MMP3 R	AGTCAGGGGGAGGTCCATAG
MMP8 F	AAGCCAGGAGGGGTAGAGTT
MMP8 R	TTTTCCAGGTAGTCCTGAACAGT
MMP9 F	TTCAGGGAGACGCCCATTTT
MMP9 R	AACCGAGTTGGAACCACGAC
MMP10 F	AGTTTGGCTCATGCCTACCC
MMP10 R	TTGGTGCCTGATGCATCTTCT
MMP13 F	GTTTGCAGAGCGCTACCTGA
MMP13 R	GACTGCATTTCTCGGAGCCT
FGF2F	GCTGTACTGCAAAAACGGGG
FGF 2 R	TAGCTTGATGTGAGGGTCGC
PLGF F	CCATGCAGCTCCTAAAGATCC
PLGF R	TCCTCCTTCCGGCTTCA
CXCL1 F	AACCGAAGTCATAGCCACAC
CXCL1 R	GTTGGATTTGTCAGTTCAGC
CXCL8 F	ACCGGAAGGAACCATCTCAC
CXCL8 R	GGCAAAACTGCACCTTCACAC
IL 10 F	AAGACCCAGACATCAAGGCG
IL 10 R	AATCGATGACAGCGCCGTAG
PDGFA F	GCCAACCAGATGTGAGGTGA
PDGFA R	GGAGGAGAACAAGACCGCA

PDGFB F	ACCTGCGTCTGGTCAGC
PDGFB R	ATCTTCCTCTCCGGGGTCTC
GM-CSF F	CTGGAGCTGTACAAGCAGGG
GM-CSF R	ACAGGAAGTTTCCGGGGTTG
G-CSF F	AGCAAGTGAGGAAGATCCAGG
G-CSF R	TTGTAGGTGGCACACTCACTC
VEGFA-F	ATCTGCATGGTGATGTTGGA
VEGFA-R	GGGCAGAATCATCACGAAGT
TGF-beta-F	GCAACAATTCTGGCGATACC
TGF-beta-R	AAAGCCTCAATTTCCCTCC

4.18. Statistical Analysis:

Continuous data of two groups was compared by student's t-test. For correlation analysis, statistical significance was determined by Pearson Correlation coefficient. p value ≤ 0.05 was considered statistically significant. Graphpad Prism (Version 7) was used to perform statistical analysis.

5. RESULTS AND DISCUSSION

List of Abbreviations:

FGF	Fibroblast Growth Factor
WHO	World Health Organization
VEGF	Vascular Endothelial Growth Factor
RTK	Receptor Tyrosine Kinase
VEGFR	Vascular Endothelial Growth Factor Receptor
PDGFR	Platelet Derived Growth Factor Receptor
EGFR	Epidermal Growth Factor Receptor
FSHD	Facioscapulohumeral Muscular Dystrophy
FRG1	FSHD Region Gene 1
EMT	Epithelial – Mesenchymal Transition
BMP4	Bone Morphogenetic Protein 4
Tie2	Tyrosine Kinase with Immunoglobulin-like and EGF-like Domains 2
ALK1	Activin Receptor like Kinase
AIDS	Acquired Immune Deficiency Syndrome
Ang2	Angiopoietin 2
TIMP3	Tissue Inhibitor of Metalloproteinases 3
BMPR2	Bone morphogenetic protein receptor type II
EC	Endothelial Cell
SMC	Smooth Muscle Cell
Flt1	Fms-Like Tyrosine Kinase 1
Ang1	Angiopoietin 1
HIF2 α	Hypoxia Inducible Factor 2 alpha
TSP1	Thrombospondin 1
Flk1	Fetal Liver Kinase 1
MMP	Maxtrix Metalloproteinase
PLGF	Placental Growth Factor
PDGFA	Platelet Derived Growth Factor alpha
PDGFB	Platelet Derived Growth Factor beta
EGF	Epidermal Growth Factor
HIF1 α	Hypoxia Inducible Factor 1 alpha
ANT1	Adenine Nucleotide Translocator 1
FRG2	FSHD Region Gene 2
DUX4	Double Homeobox 4
NLS	Nuclear Localization Signal
RNAi	RNA interference
TNNT3	Troponin T3
FHL1	Four And A Half LIM Domains 1
DAB2	Disabled 2
msr	methionine sulfoxide reductase
FMO	FRG1 Morpholino
CMO	Control Morpholino
MET	Mesenchymal – Epithelial Transition
HR	Hazard Ratio
CI	Confidence Interval
FFPE	Formalin Fixed Paraffin Embedded

IHC	Immunohistochemistry
MVD	Micro Vessel Density
IRS	Immuno reactive score
HRP	Horse radish peroxidase
shRNA	Short hairpin RNA
OD	Optical Density
DMSO	Dimethyl sulfoxide
PIPES	Piperazine-N,N'-bis(2-ethanesulfonic acid)
PBS	Phosphate Buffered Saline
NCCS	National Centre for Cell Science
NIH	National Institute of Health
RIPA	Radioimmunoprecipitation assay
EDTA	Ethylenediaminetetraacetic acid
BCA	Bicinchoninic acid assay
BSA	Bovine Serum Albumin
WR	Working Reagent
SDS	Sodium Dodecyl Sulphate
PAGE	Poly Acrylamide Gel Electrophoresis
APS	Ammonium per Sulphate
TEMED	Tetramethylethylenediamine
TBS	Tris Buffered Saline
TBS – T	Tris Buffered Saline – Tween 20
NTC	No Template Control
CXCL1	C-X-C Ligand 1
CXCL8	C-X-C Ligand 8
IL10	Interleukin 10
GM – CSF	Granulocyte-macrophage colony-stimulating factor
G – CSF	Granulocyte colony-stimulating factor
TGF - β	Transforming Growth Factor beta
DMD	Duchenne Muscular Dystrophy
HSMM	Human Skeletal Muscle Myoblasts
MDSC	Muscle Derived Stem Cells
HUVEC	Human Umbilical Vein Endothelial Cell
MAPK	Mitogen Associated Protein Kinase
ERK	Extracellular Receptor Kinase
GAPDH	Glyceraldehyde 3-phosphate dehydrogenase
TNF - α	Tumor Necrosis Factor alpha
IL 6	Interleukin 6
HER2	Human Epidermal Growth Factor Receptor 2
TNBC	Triple Negative breast cancer
ER	Estrogen Receptor
PR	Progesterone Receptor
IgG	Immunoglobulin Gamma
FRG1 KD	FRG1 knockdown

List of Figures:

S. No.	Figures	Page No.
1.	Figure (1.1): Representation of basic process of blood vessel formation	3
2.	Figure (3.1): Graphical representation of top 10 causes of death in the year 2015 obtained from WHO Fact files	10
3.	Figure (3.2): Representation of effect of angiogenic factors leading to angiogenic switch	15
4.	Figure (3.3): Representation of effect of angiogenic factors leading to angiogenic switch	16
5.	Figure (3.4): Anti-angiogenesis therapy versus vessel normalization	21
6.	Figure (3.5): Schematic presentation for FRG1 gene, mRNA and protein	27
7.	Figure (3.6): Representing conservation of FRG1 protein throughout various species with domain wise breakup	29
8.	Figure (3.7): Schematic representation of our hypothesis in this study regarding involvement of FRG1 in tumorigenesis and angiogenesis	32
9.	Figure (3.8): Effect of Frg1 expression on angiogenesis in Xenopus embryos	33
10.	Figure (3.9): Comparison of Vimentin Expression levels in Xenopus embryos	34
11.	Figure (5.1.1): Effect of FRG1 Expression on endothelial cell function	61
12.	Figure (5.1.2): Correlation between FRG1 expression and MVD count	62
13.	Figure (5.2.1): Effect of FRG1 expression on HEK293T cell proliferation and scratch wound healing	69
14.	Figure (5.2.2): Effect of FRG1 expression on transwell migration and invasion of HEK293T	70
15.	Figure (5.2.3): Effect of FRG1 expression on cell signaling molecules in HEK293T	72
16.	Figure (5.2.4): Determination of FRG1 expression levels and prognostic value by <i>in silico</i> analysis	73
17.	Figure (5.2.5): FRG1 levels and distribution pattern in tumor tissues	75
18.	Figure (5.3.1): FRG1 expression levels in prostate tumor and cell lines	82
19.	Figure (5.3.2): Effect of FRG1 expression on cell proliferation and scratch wound healing on prostate cancer cell lines	84

20.	Figure (5.3.3): Effect of FRG1 expression on transwell migration and invasion of prostate cancer cell lines	87
21.	Figure (5.3.4): Expression analysis of listed cytokines and MMPs in prostate cancer cells during FRG1 knockdown	89
22.	Figure (5.3.5): Expression analysis of listed cytokines and MMPs in prostate cancer cells during ectopic expression of FRG1	90
23.	Figure (5.3.6): Reduced FRG1 expression enhances p38 MAPK phosphorylation	91
24.	Figure (5.3.7): Model for possible molecular interaction during FRG1 knockdown in prostate cancer cells.	93
25.	Figure (5.4.1): Effect of FRG1 expression on cell proliferation of MCF7	99
26.	Figure (5.4.2): Effect of FRG1 expression on scratch wound healing in MCF7	101
27.	Figure (5.4.3): Effect of FRG1 expression on transwell migration of MCF7	102
28.	Figure (5.4.4): Effect of FRG1 expression on matrigel invasion assay of MCF7	103
29.	Figure (5.4.5): Expression analysis of cytokines and MMPs in MCF7 with altered FRG1 expression	104
30.	Figure (5.4.6): Reduced FRG1 expression enhances ERK phosphorylation in MCF7	105
31.	Figure (5.4.7): FRG1 expression levels in breast tumor compared to uninvolved breast tissue	106
32.	Figure (8.1): Immunohistochemistry of HeLa cell block for FRG1	131

List of Tables:

S. No.	Tables	Page No.
1.	Table (3.1): Diseases associated with abnormal or excessive angiogenesis	11
2.	Table (3.2): Disease caused by insufficient angiogenesis or vessel regression	12
3.	Table (3.3): List of pan VEGF receptor tyrosine kinase inhibitors and concomitant cancer, being used for treatment	19
4.	Table (3.4): Various factors leading to evasion of VEGF (receptor) blockade	23
5.	Table (4.1): List of Immunohistochemical Markers and Protocols	39
6.	Table (4.2): Composition of SDS-PAGE gel	50
7.	Table (4.3): List of Antibody Used in Western Blotting	52
8.	Table (4.4): Reaction mix for q-RT-PCR	54
9.	Table (4.5): ABI 7500 Run protocol	54
10.	Table (4.6): List of Primers	55
11.	Table (5.1.1): Data from tubule formation assay showing change in various parameters of angiogenesis.	60
12.	Table (8.1): Details of reagents for preparation of transfection mix for single well	128
13.	Table (8.2): RNA primer mix for cDNA synthesis	130
14.	Table (8.3): Reverse transcriptase mix for cDNA synthesis	130